



UNIVERSIDADE ESTADUAL DE CAMPINAS
Faculdade de Odontologia de Piracicaba

Thamara Beline

**Deposição por pulverização catódica de filmes de
óxido de tântalo (Ta_2O_5) na superfície de titânio para
aplicações biomédicas: comportamento eletroquímico,
biocompatibilidade e análise microbiológica**

**Magnetron sputtering deposition of tantalum oxide
(Ta_2O_5) films onto titanium surface for biomedical
applications: electrochemical behavior, biocompatibility
and microbiologic analysis**

Piracicaba/SP

2020

Thamara Beline

Deposição por pulverização catódica de filmes de óxido de tântalo (Ta_2O_5) na superfície de titânio para aplicações biomédicas: comportamento eletroquímico, biocompatibilidade e análise microbiológica

Magnetron sputtering deposition of tantalum oxide (Ta_2O_5) films onto titanium surface for biomedical applications: electrochemical behavior, biocompatibility and microbiologic analysis

Tese apresentada à Faculdade de Odontologia de Piracicaba da Universidade Estadual de Campinas como parte dos requisitos exigidos para a obtenção do título de Doutora em Clínica Odontológica, na Área de Prótese Dental.

Thesis presented to the Piracicaba Dental School of the University of Campinas in partial fulfillment of the requirements for the degree of Doctor in Clinical Dentistry, in Dental Prosthesis area.

Orientador: Prof. Dr. Valentim Adelino Ricardo Barão

Este exemplar corresponde à versão final da tese defendida pela aluna Thamara Beline e orientada pelo Prof. Dr. Valentim Adelino Ricardo Barão.

Piracicaba/SP

2020

Agência(s) de fomento e nº(s) de processo(s): FAPESP, 2016/07269-3; CAPES

Ficha catalográfica
Universidade Estadual de Campinas
Biblioteca da Faculdade de Odontologia de Piracicaba
Marilene Girello - CRB 8/6159

B412d Beline, Thamara, 1991-
Deposição por pulverização catódica de filmes de óxido de tântalo (Ta_2O_5) na superfície de titânio para aplicações biomédicas : comportamento eletroquímico, biocompatibilidade e análise microbiológica / Thamara Beline. – Piracicaba, SP : [s.n.], 2020.

Orientador: Valentim Adelino Ricardo Barão.
Tese (doutorado) – Universidade Estadual de Campinas, Faculdade de Odontologia de Piracicaba.

1. Titânio. 2. Corrosão. 3. Implantes dentários. 4. Propriedades de superfície. 5. Materiais biocompatíveis. I. Barão, Valentim Adelino Ricardo, 1983-. II. Universidade Estadual de Campinas. Faculdade de Odontologia de Piracicaba. III. Título.

Informações para Biblioteca Digital

Título em outro idioma: Magnetron sputtering deposition of tantalum oxide (Ta_2O_5) films onto titanium surface for biomedical applications : electrochemical behavior, biocompatibility and microbiologic analysis

Palavras-chave em inglês:

Titanium
Corrosion
Dental implants
Surface properties
Biocompatible materials

Área de concentração: Prótese Dental

Titulação: Doutora em Clínica Odontológica

Banca examinadora:

Valentim Adelino Ricardo Barão [Orientador]

Jose Humberto Dias da Silva

Ricardo Armini Caldas

Francisco Humberto Nociti Júnior

Marcelo Ferraz Mesquita

Data de defesa: 21-02-2020

Programa de Pós-Graduação: Clínica Odontológica

Identificação e informações acadêmicas do(a) aluno(a)

- ORCID do autor: <https://orcid.org/0000-0002-9729-1160>

- Currículo Lattes do autor: <http://lattes.cnpq.br/6458934228905272>



UNIVERSIDADE ESTADUAL DE CAMPINAS
Faculdade de Odontologia de Piracicaba

A Comissão Julgadora dos trabalhos de Defesa de Tese de Doutorado, em sessão pública realizada em 21 de fevereiro de 2020, considerou a candidata THAMARA BELINE aprovada.

PROF. DR. VALENTIM ADELINO RICARDO BARÃO

PROF. DR. JOSE HUMBERTO DIAS DA SILVA

PROF. DR. RICARDO ARMINI CALDAS

PROF. DR. FRANCISCO HUMBERTO NOCITI JÚNIOR

PROF. DR. MARCELO FERRAZ MESQUITA

A Ata da defesa, assinada pelos membros da Comissão Examinadora, consta no SIGA/Sistema de Fluxo de Dissertação/Tese e na Secretaria do Programa da Unidade.

Dedico este trabalho

Aos meus amados pais, **Eva** e **Antonio**, que são meus exemplos de caráter, força e honestidade. Muito obrigada por todo amor, carinho e apoio incondicionais e por tudo o que fizeram até hoje para que eu conseguisse alcançar os meus objetivos.

Ao meu querido esposo, **Lincoln**, que com muito amor, ajudou-me a seguir esperançosa nos momentos mais difíceis. Muito obrigada por todo carinho, compreensão e companheirismo.

À minha irmã, **Thalita**, por todo incentivo, carinho e amizade. Agradeço por sempre torcer pelas minhas conquistas.

Agradecimentos especiais

A **Deus**, por todas as bênçãos recebidas, pela proteção e por ser meu sustento diário.

Ao meu Orientador, **Prof. Dr. Valentim Adelino Ricardo Barão**, pelo exemplo de dedicação, foco, competência e seriedade. Sou imensamente grata por todo suporte fornecido para o desenvolvimento não somente desta tese, mas de todos os demais trabalhos desenvolvidos, pelos conhecimentos compartilhados, pela paciência e por todas as oportunidades que me foram dadas desde a época do curso de Mestrado. Muito obrigada por contribuir grandemente com meu crescimento pessoal e profissional.

Agradecimentos

À **Universidade Estadual de Campinas - UNICAMP**, na pessoa do Magnífico Reitor, **Prof. Dr. Marcelo Knobel** e à **Faculdade de Odontologia de Piracicaba – UNICAMP**, na pessoa do seu Diretor, **Prof. Dr. Francisco Haiter Neto** e Diretor Associado, **Prof. Dr. Flávio Henrique Baggio Aguiar**.

À **Profa. Dra. Karina Gonzales Silvério Ruiz**, coordenadora geral dos programas de Pós-graduação da Faculdade de Odontologia de Piracicaba da Universidade Estadual de Campinas.

Ao **Prof. Dr. Valentim Adelino Ricardo Barão**, coordenador do Programa de Pós Graduação em Clínica Odontológica da Faculdade de Odontologia de Piracicaba da Universidade Estadual de Campinas.

À **Fundação de Amparo a Pesquisa do Estado de São Paulo**, pela concessão de bolsa de estudo no período de outubro de 2016 a setembro de 2019, Processo nº 2016/07269-3, fundamental para o desenvolvimento deste trabalho.

À **Coordenação de Aperfeiçoamento de Pessoal de Nível Superior – CAPES**, pela concessão de bolsa de estudo no período de março de 2016 a setembro de 2016 – Código de Financiamento 001.

Ao **Prof. Dr. José Humberto Dias da Silva**, Professor Adjunto III da Universidade Estadual Paulista “Júlio de Mesquita Filho” – UNESP (Campus Bauru). Sou muito grata por todo apoio, paciência e tempo dedicados durante o desenvolvimento deste trabalho.

Ao **Prof. Dr. Nilton Francelosi Azevedo Neto**, pela solicitude e dedicação no desenvolvimento deste trabalho.

Ao **Prof. Dr. Francisco Humberto Nociti Junior** e à minha amiga **Amanda Bandeira de Almeida** por toda atenção, dedicação e apoio prestados durante o desenvolvimento deste trabalho.

Aos Professores da Banca do Exame de Qualificação, **Profa. Dra. Karina Gonzales Silvério Ruiz, Prof. Américo Bortolazzo Correr e, Prof. Dr. Antônio Pedro Ricomini Filho**, e da Banca do Exame de Defesa, **Prof. Dr. José Humberto Dias da Silva, Prof. Dr. Ricardo Armini Caldas, Prof. Dr. Francisco Humberto Nociti Júnior, Prof. Dr. Marcelo Ferraz Mesquita e Prof. Dr. Valentim Adelino Ricardo Barão**, pelas considerações e correções que foram essenciais para o aprimoramento deste trabalho.

Ao meu amigo **Adaias Oliveira Matos** pela convivência durante toda a pós-graduação e pela grande amizade que construímos. Muito obrigada por todos os momentos em que pude contar com seu apoio. Você é um exemplo de persistência e determinação.

Às minhas amigas da graduação **Anne Caroline Alves Ramos e Monique Gimenez**. Vocês são a prova de que a distância física não é capaz de superar a amizade. Muito obrigada por todo apoio e incentivo constantes que me deram durante todo esse processo.

À minha amiga e companheira de laboratório **Anna Gabriella Camacho Presotto**. Muito obrigada pela amizade, boa convivência e por todo apoio e incentivo dados durante o período de Pós-Graduação.

Ao **Laboratório de Plasmas Tecnológicos da Universidade Estadual Paulista “Júlio de Mesquita Filho” – UNESP (Campus de Sorocaba)**, representado pelo **Prof. Dr. Nilson Cristino da Cruz** e pela **Profa. Dra. Elidiane Cipriano Rangel**.

À secretária **Eliete Lima Marim**, e ao técnico de laboratório **Eduardo Pinez Campos**, pela ajuda e agradável convivência durante o curso de Pós-Graduação.

A todos os colegas do Laboratório de Prótese Total pela convivência, conhecimentos e experiências trocadas.

A todos os meus familiares, amigos e pessoas que indiretamente contribuíram para a concretização deste trabalho.

RESUMO

Este trabalho objetivou o desenvolvimento e otimização das propriedades físicas, químicas e biológicas de filmes de óxido de tântalo (Ta_xO_y) depositados por pulverização catódica sobre a superfície de titânio comercialmente puro (Ticp). Inicialmente, filmes de Ta_xO_y com diferentes estruturas (amorfa ou cristalina) foram desenvolvidos dependendo dos diferentes fluxos de oxigênio e parâmetros utilizados. As propriedades ópticas, morfologia, rugosidade, composição química e energia de superfície foram avaliadas. Além disso, o impacto dos filmes de Ta_xO_y na adesão inicial de *Streptococcus sanguinis* foi investigada. A morfologia e espalhamento de células pré-osteoblásticas da linhagem MC3T3E1 na superfície de Ta_2O_5 cristalina foram avaliados. A análise de difratografia de raios-X (DRX) revelou que o grupo depositado em 8 sccm de O_2 (600 °C/400 W) mostrou cristalização correspondente à fase β - Ta_2O_5 . As análises ópticas mostraram que o grupo depositado de 4 sccm de O_2 (200 °C/300W), 8 sccm de O_2 (200 °C/300 W), 8 sccm de O_2 (400 °C/300 W), 8 sccm de O_2 (600 °C/150 W), 8 sccm de O_2 (600 °C/300 W) e 10 sccm de O_2 (200 °C/300 W) exibiram franjas de interferência regulares, sugerindo alta homogeneidade dos filmes. A superfície cristalina β - Ta_2O_5 exibiu maior rugosidade e energia de superfície que os demais grupos ($p < 0,05$) e apresentou biocompatibilidade. Comparados ao Ticp, os filmes de Ta_xO_y não aumentaram a adesão bacteriana ($p > 0,05$). Posteriormente, foi desenvolvido um segundo estudo *in vitro* que, além de avaliar as propriedades físico-químicas, analisou as performances eletroquímicas e biológicas do filme de Ta_2O_5 cristalino. Discos de Ticp foram divididos em dois grupos: Ticp polido (controle) e Ticp tratado com filme de Ta_2O_5 (experimental). Testes de caracterização como DRX, microscopia de força atômica (MFA), energia de superfície e espectroscopia de fotoelétrons excitados por raios X (XPS) foram realizados. O ensaio eletroquímico foi conduzido em simulador de fluido corpóreo (SFC) e o potencial de circuito aberto, espectroscopia de impedância eletroquímica e testes potenciodinâmicos foram realizados. A adsorção de albumina e fibrinogênio foi investigada através da microbalança eletroquímica de cristal de quartzo (EQCM). Células da linhagem MC3T3-E1 foram cultivadas nas superfícies de Ticp e os ensaios metabólicos (MTT) e morfológicos (MEV) foram realizados após 1, 2 e 4 dias de cultura. A microscopia de fluorescência foi usada para avaliar a morfologia após 1 e 2 dias de cultura. A mineralização foi avaliada através do ensaio de Alizarina após 4, 7 e 14 dias. Os níveis de expressão do fator de transcrição 2 relacionado com Runt (RUNX2), fosfatase alcalina (ALP), osteocalcina (OC) e colágeno tipo I (Col-1) foram avaliados após 1, 2 e 3 dias. A bioatividade foi avaliada após a imersão das amostras em SFC por 14 dias. Mudanças na topografia de superfície foram notadas na análise de MFA para o grupo Ta_2O_5 . O grupo Ta_2O_5 exibiu maiores valores de rugosidade e energia de superfície ($p < 0,05$). Altos valores de resistência à corrosão foram notados para o grupo Ta_2O_5 ($p < 0,05$). O grupo Ta_2O_5 mostrou valores mais positivos de potencial de corrosão (E_{corr}) e valores reduzidos de densidade de corrente de corrosão (I_{corr}) e taxa de corrosão ($p < 0,05$). No teste de adsorção de proteínas, os grupos não mostraram diferença estatística entre si ($p > 0,05$). O filme de Ta_2O_5 impactou positivamente na morfologia e espalhamento celular. Na análise de mineralização, quando comparado ao Ticp, o grupo Ta_2O_5 mostrou maior concentração de íons de cálcio no 14º dia ($p < 0,05$). O grupo Ta_2O_5 mostrou os maiores valores de expressão de RUNX2 no 1º

dia e de OC e Col-1 no 3° dia quando comparado ao Ticp ($p < 0,05$). O grupo experimental mostrou melhor habilidade para formação de cristais de hidroxiapatita. Os filmes de óxido de tântalo foram capazes de melhorar as propriedades de superfície, estabilidade eletroquímica e biocompatibilidade do titânio.

Palavras-chave: Titânio, Corrosão, Implantes dentários, Eletroquímica, Propriedades de superfície, Materiais biocompatíveis.

ABSTRACT

This study aimed to tailor the synthesis and controlling the physical, chemical and biological properties of tantalum (Ta)-based thin films onto a commercially pure titanium (cpTi) surface by magnetron sputtering technique. Firstly, Ta_xO_y films with different structures (amorphous or crystalline) were produced depending on the various oxygen flow rates and parameters used. The structural and optical properties, morphology, roughness, chemical composition and surface energy were assessed. The impact of Ta_xO_y films on initial *Streptococcus sanguinis* adhesion was investigated. The morphology and spreading of pre-osteoblastic (MC3T3-E1) cells on a crystalline tantalum oxide film were evaluated. X-ray diffraction (XRD) analysis revealed that the 8 O₂ sccm (600 °C/400 W) group showed crystallization corresponding to the β-Ta₂O₅ phase. Optical analysis showed that the 4 O₂ sccm (200 °C/300 W), 8 O₂ sccm (200 °C/300 W), 8 O₂ sccm (400 °C/300 W), 8 O₂ sccm (600 °C/150 W), 8 O₂ sccm (600 °C/300 W) and 10 O₂ sccm (200 °C/300 W) groups presented regular interference oscillations, suggesting high homogeneity of the films. The crystalline β-Ta₂O₅ coating showed higher roughness and surface energy values than the other groups (p<.05) and was biocompatible. Compared with cpTi, the amorphous and crystalline tantalum oxide films did not increase bacterial adhesion (p>.05). Subsequently, a second *in vitro* study was developed which, in addition to evaluating the physical and chemical properties, analyzed the electrochemical and biological performances of the crystalline Ta₂O₅ film. CpTi disks were randomly divided into two groups: polished cpTi (control) and cpTi treated with Ta₂O₅ film (experimental). Surfaces were characterized by XRD, atomic force microscopy (AFM), surface energy and x-ray photoelectron spectroscopy (XPS). The electrochemical tests were conducted in simulated body fluid (SBF) and the open circuit potential, electrochemical impedance spectroscopy and potentiodynamic tests were performed according to the standardized method of three-cell electrodes. For biological assay, the protein adsorption of albumin and fibrinogen were investigated by electrochemical quartz crystal microbalance (EQCM). MC3T3-E1 cells were cultured on the cpTi surfaces and the metabolic analysis (MTT) and the morphology (SEM) were evaluated after 1, 2 and 4 days. Also, fluorescence microscopy was used to evaluate the morphology after 1 and 2 days of cell culturing. The mineralization was determined via staining with Alizarin Red-S after 4, 7 and 14 days. The expression levels of runt-related transcription factor 2 (*Runx-2*), alkaline phosphatase (*Alpl*), osteocalcin (*Ocn*), Collagen-1 (*Col-1*) were analyzed after 1, 2 and 3 days. The bioactivity was evaluated by immersion of the coating in SBF for 14 days. Changes in surface topography were noted in AFM analysis for Ta₂O₅ group. Higher values of surface roughness and surface energy were found for Ta₂O₅ group (p<.05). Higher values of corrosion resistance were noted for Ta₂O₅ group (p<.05). More positive values of corrosion potential (E_{corr}) and lower values of corrosion current density (I_{corr}) and corrosion rate were found for Ta₂O₅ group (p<.05). No statistically significant differences were found between the groups for protein adsorption (p>.05). Morphology analysis revealed that Ta₂O₅-treated surface positively impacted the cell morphology and spreading. In the mineralization test, Ta₂O₅ group showed the highest calcium ion concentration values when compared with cpTi surface on day 14 (p<.05). Ta₂O₅ group showed higher *Runx-2* expression values on day 1 and higher *Ocn* and *Col-1* expression on day 3 when compared with cpTi (p<.05). Tantalum oxide films were able

to improve the surface properties, the electrochemical stability and the biocompatibility of cpTi.

Key-words: Titanium, Corrosion, Dental implants, Electrochemistry, Surface Properties, Biocompatible materials

SUMÁRIO

1 INTRODUÇÃO.....	14
2 ARTIGOS.....	17
2.1 ARTIGO: Tailoring the synthesis of tantalum-based thin films for biomedical application: Characterization and biological response	17
2.2 ARTIGO: β -Ta ₂ O ₅ thin film for implant surface modification triggers superior anti-corrosion performance and cytocompatibility of titanium.....	47
3 DISCUSSÃO.....	82
4 CONCLUSÃO.....	84
REFERÊNCIAS	85
ANEXOS.....	90
Anexo 1 – Comprovante de que não é necessária licença para uso do Artigo 1 na tese	90
Anexo 2 – Licença para uso do Artigo 2 na tese	91
Anexo 3 – Certificado de aprovação do Comitê de Ética	93
Anexo 4 – Relatório de verificação de originalidade e prevenção de plágio	95

1 INTRODUÇÃO

O titânio (Ti) é um dos materiais mais amplamente utilizados para fabricação de implantes dentários devido a sua estabilidade química, biocompatibilidade e resistência à corrosão (Prasad et al., 2015). A formação de uma fina camada de óxido que ocorre na superfície do Ti quando exposto ao ar ou água, que consiste em dióxido de titânio (TiO_2), reduz sua reatividade no ambiente biológico (Olmedo et al., 2008) ao prover resistência à corrosão e biocompatibilidade (Strnad e Chirila, 2015). No entanto, a natureza, espessura e composição da camada de óxido do Ti podem ser afetadas pelas condições do ambiente biológico (Bhola et al., 2011). Estudos prévios mostraram que o comportamento eletroquímico do Ti é negativamente influenciado quando exposto à saliva, fluoretos, ácido, lipopolissacarídeos (LPS), nicotina e metabólitos provenientes de bactérias (Nakagawa et al., 1999; Barão et al., 2011; Mathew et al., 2012; Zhang et al., 2013; Royhman et al., 2015; Sridhar et al., 2015; Beline et al., 2016; 2016).

O processo de corrosão, definido como a deterioração de um material devido ao ataque eletroquímico, pode resultar na liberação de íons no microambiente ao redor dos implantes (Cohen, 1998). Ainda, a liberação de íons metálicos advindos do processo de corrosão pode estar associada a sítios acometidos por periimplantite (Safioti et al., 2016). Foram encontradas altas concentrações de íons de Ti ao redor de implantes acometidos por periimplantite quando comparados a implantes saudáveis (Safioti et al., 2016), revelando que a liberação de íons de Ti da superfície do implante durante o evento de corrosão está associada à periimplantite. Dessa forma, os fatores citados previamente impõem a necessidade de se buscar alternativas para aumentar a biocompatibilidade, bioatividade e auxiliar na prevenção da degradação dos implantes no ambiente oral, objetivando-se a redução das taxas de falhas dos implantes dentários.

Dentro desse contexto, o tântalo (Ta) tem recebido atenção como biomaterial alternativo ao Ti e suas ligas por apresentar superior biocompatibilidade, bioatividade e resistência à corrosão quando comparado ao Ti (Bermúdez et al., 2005). O Ta é um metal de transição (número atômico 73; peso atômico 180,05) que permanece inerte *in vivo* (Bencharit et al., 2015). A inércia e biocompatibilidade do Ta resultam das camadas de óxido de tântalo formadas na superfície do Ta (Bencharit et al., 2015). O Ta possui duas formas de óxidos: o dióxido de tântalo (TaO_2) e o pentóxido de tântalo (Ta_2O_5), sendo este último, o óxido de maior estabilidade (Fairbrother, 1967; Bencharit et al., 2015). Estudos prévios confirmaram as excelentes propriedades Ta ao favorecer a osteogênese *in vivo* (Wauthle et al., 2015) e *in vitro* (Welldon et al., 2008; Sagomonyants et al., 2011). No entanto, o uso do Ta para a fabricação

de implantes é considerado limitado uma vez que possui elevada temperatura de fusão ($\sim 3017^\circ\text{C}$) (Balla et al., 2010). Tal característica dificulta o seu processo de fabricação e o torna oneroso. Levando esses fatores em consideração, a combinação das boas propriedades do Ti e do Ta através da aplicação de filmes de óxido de Ta, como tratamento de superfície para o Ti, poderia ser considerada uma alternativa viável para superar as limitações relatadas acima e alcançar a combinação desejada de propriedades para produzir implantes de Ti com excelente qualidade.

Várias técnicas têm sido utilizadas para depositar filmes de Ta e Ta_xO_y sobre diferentes substratos, incluindo a deposição eletroquímica, implantação iônica por imersão em plasma, sol-gel, deposição de vapor químico e pulverização catódica (Pelletier et al., 2002; Zein El Abedin et al., 2005; Balla et al., 2010; Bouchet-Fabre et al., 2011; Sun et al., 2013). A técnica de sol-gel, por exemplo, é considerada simples de executar, no entanto, seus precursores organometálicos (butóxido de Ta e o etóxido de Ti) possuem alto custo e são instáveis (Kim et al., 2011; Sun et al., 2013). A técnica da pulverização catódica é capaz de produzir filmes uniformes (Baía et al., 1999) e de alta qualidade em termos de adesão ao substrato, o que torna esse método de deposição atrativo para diversas aplicações tecnológicas (Alami et al., 2009; Sarakinos et al. 2010; He et al., 2013; He et al., 2013; He et al., 2014; He et al., 2014; Zhang et al., 2014). Além disso, os filmes podem ser produzidos em larga escala e baixo custo (Alami et al., 2009).

Através da técnica de deposição por pulverização catódica, óxidos metálicos de diferentes composições podem ser sintetizados. Por meio do controle dos parâmetros de deposição como, por exemplo, composição da atmosfera reativa (fluxos de argônio (Ar) e oxigênio (O_2)), pressão de trabalho, potência e temperatura, é possível otimizar as propriedades do filme, como rugosidade, composição química e morfologia (Kester et al., 1993). Uma das fases cristalinas do óxido de Ta é o $\beta\text{-Ta}_2\text{O}_5$, que tem mostrado boas propriedades biológicas. Pham et al. (2013) mostraram que a biocompatibilidade da liga de Co-Cr foi significativamente aumentada após o recobrimento com filme cristalino de óxido de Ta. No estudo desenvolvido por Chang et al. (2014), foram encontrados resultados similares, onde o filme de $\beta\text{-Ta}_2\text{O}_5$ cristalino mostrou alta biocompatibilidade quando testado em fibroblastos humanos e o filme de óxido de Ta amorfo reduziu a adesão de *Streptococcus aureus* e *Actinobacillus actinomycetemcomitans*. No entanto, estudos sobre a obtenção da fase $\beta\text{-Ta}_2\text{O}_5$ e sua cristalização e a cinética eletroquímica de filmes finos de Ta_2O_5 , pela técnica da pulverização catódica tem sido pouco explorados. Assim, estudos que elucidem como

modular a formação dessa fase, bem como controlar as propriedades dos filmes de óxido de Ta e seu comportamento eletroquímico sem afetar a performance biológica são necessários.

Dessa forma, este estudo objetivou o desenvolvimento e análise do controle das propriedades dos filmes de óxido de tântalo (Ta_xO_y) depositados por pulverização catódica sobre a superfície de titânio comercialmente puro (Ticp). Os objetivos específicos foram (1) controlar a síntese de filmes de óxido de Ta sobre a superfície do Ticp através da pulverização catódica por meio da modulação dos parâmetros de deposição, (2) caracterizar suas propriedades físicas e químicas, (3) investigar o impacto dos filmes na adesão inicial de *Streptococcus sanguinis*; (4) avaliar a influência do tratamento de superfície com Ta_2O_5 no comportamento eletroquímico do Ticp e (5) investigar a resposta de células pré osteoblásticas MC3T3-E1 frente ao tratamento de superfície com Ta_2O_5 .

2 ARTIGOS

2.1 ARTIGO: Tailoring the synthesis of tantalum-based thin films for biomedical application: Characterization and biological response#

Thamara Beline^{a,b}, José H. D. da Silva^c, Adaias O. Matos^{a,b}, Nilton F. Azevedo Neto^c, Amanda B. de Almeida^a, Francisco H. Nociti Júnior^a, Douglas M. G. Leite^d, Elidiane Cipriano Rangel^e, Valentim A. R. Barão^{a,b}

^a*University of Campinas (UNICAMP), Piracicaba Dental School, Department of Prosthodontics and Periodontology, Av. Limeira, 901, Piracicaba, São Paulo, Brazil, 13414-903.*

^b*Institute of Biomaterials, Tribocorrosion and Nanomedicine (IBTN), Brazil.*

^c*São Paulo State University (UNESP), School of Sciences, Department of Physics, Av. Eng. Luís Edmundo C. Coube, 14-01, Bauru, São Paulo, Brazil, 17033-360.*

^d*Plasma and Processes Laboratory, Technological Institute of Aeronautics (ITA), Pça. Marechal Eduardo Gomes, 50, São Jose dos Campos, São Paulo, Brazil, 12228-900.*

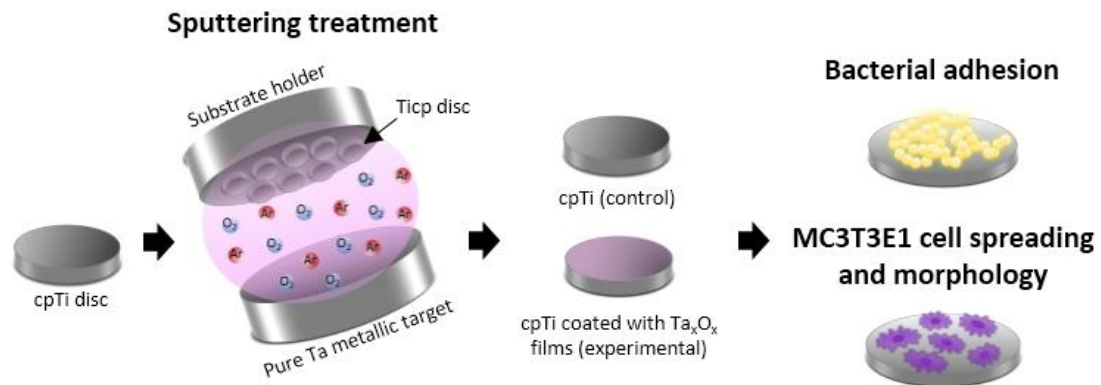
^e*São Paulo State University (UNESP), Institute of Science and Technology, Laboratory of Technological Plasmas, Av. Três de Março, 511, Sorocaba, São Paulo, Brazil, 18087-180.*

* *Corresponding author.* Tel: +55-19-2106 5218.

E-mail address: vbarao@unicamp.br (V. Barão).

Artigo publicado: Beline et al. Mater Sci Eng C Mater Biol Appl. 2019 Aug;101:111-119.
doi:10.1016/j.msec.2019.03.072

Graphical Abstract



Highlights

- Amorphous and crystalline tantalum oxide films were synthesized by sputtering
- Titanium surface properties were improved by the crystalline tantalum oxide film
- Neither the amorphous nor crystalline tantalum oxide film have contributed to the increase of bacterial adhesion
- The crystalline tantalum oxide film improved cell spreading and morphology

Abstract

The aim of this study was to tailor the deposition parameters of magnetron sputtering to synthesize tantalum oxide (Ta_xO_y) films onto commercially pure titanium (cpTi) surface. The structural and optical properties, morphology, roughness, elemental chemical composition and surface energy were assessed. The impact of Ta_xO_y films on initial *Streptococcus sanguinis* adhesion was investigated. The morphology and spreading of pre-osteoblastic (MC3T3-E1) cells on a crystalline tantalum oxide film were evaluated. Ta_xO_y films with estimated thickness of 600 nm and different structures (amorphous or crystalline) were produced depending on the various oxygen flow rates and parameters used. X-ray diffraction analysis revealed that the 8 O₂ sccm (600 °C/400 W) group showed crystallization corresponding to the β -Ta₂O₅ phase. Optical analysis showed that the 4 O₂ sccm (200 °C 300 W) to 8 O₂ sccm (600 °C 300 W) groups and 10 O₂ sccm (200 °C 300 W) group presented regular and large-amplitude interference oscillations, suggesting high optical homogeneity of the films. The crystalline β -Ta₂O₅ coating showed higher roughness and surface energy values than the other groups ($P < .05$) and was biocompatible. Compared with cpTi, the amorphous and crystalline tantalum oxide films did not increase bacterial adhesion ($P > .05$). By tailoring the deposition parameters, we synthesized a crystalline β -Ta₂O₅ coating that improved titanium surface properties and positively affected cell spreading and morphology, making it a promising surface treatment for titanium-based implants.

Key words: Dental implants, Magnetron sputtering, Tantalum oxide, Biofilms, Optical characterization.

1. Introduction

Commercially pure titanium (cpTi) is one of the most extensively used materials for manufacturing dental implants due to its chemical stability, biocompatibility, corrosion resistance, and successful integration with the surrounding bone tissue [1]. Although the treatment with Ti-based dental implants exhibits a high success rate [2], failures are prone to occur [3,4], since Ti and its alloys do not present suitable bioactive properties and exhibit mechanical bonding rather than chemical bonding with the human bone. This is evidenced by their slow ingrowth into bone and poor bone-bonding ability. Consequently, implant loosening and premature fracture are common [5].

Within this context, tantalum (Ta) has been thought of as a promising metal, and compared to Ti, Ta is highly bioactive and makes a chemical bond with bone tissue that provides better biomineralization kinetics, optimizing the osseointegration process [6]. In addition, its excellent biocompatibility, corrosion resistance, radiopacity, and hemocompatibility have contributed to Ta becoming a promising material for using in biomedical implants [7,8]. However, the bulk use of Ta implants is limited due to its high density, high melting point, and manufacturing costs [9]. Thus, combining the good properties of Ti and Ta by applying a layer of Ta oxide film as a coating onto a Ti surface would be a good alternative to overcome this drawback and to achieve a desirable combination of properties to produce a Ti-based implant with excellent quality.

Several techniques have been used to deposit Ta and Ta_xO_y thin films onto substrates, including electrochemical deposition, laser processing, liquid phase deposition, metal-organic decomposition, plasma immersion, ion implantation, chemical vapor deposition, sol-gel, and magnetron sputtering [6,10–13]. The sol-gel technique is considered easy to handle in practice, but the tantalum butoxide and titanium ethoxide - organometallic precursors – used in sol-gel technique are unstable and expensive [10,14]. Magnetron sputtering deposition can produce uniform film growth over very large areas [15] and high-quality films in terms of adhesion, making this technique attractive for several technological applications [16–22].

In the magnetron sputtering technique, metal oxide films with different compositions can be obtained. Controlling such deposition parameters as the reactive atmosphere (Ar and O_2 flows), sputter pressure, plasma power and temperature is fundamental to optimize the properties of the films, such as roughness, phase composition, chemical state, and morphology [23]. One of crystalline phases of tantalum oxide is β - Ta_2O_5 ,

which has good biological properties. Pham et al. [24] showed that the in vitro biocompatibility of Co–Cr coated by DC magnetron sputtering with crystalline tantalum oxide film was significantly improved. Chang et al. [8] observed similar results, wherein hydrophilic crystalline tantalum oxide (β -Ta₂O₅) coatings exhibited superior human skin fibroblast cellular biocompatibility, while the amorphous tantalum oxide coatings reduced *Streptococcus aureus* and *Actinobacillus actinomycetemcomitans* adhesion. However, obtaining this phase and its crystallization are challenge and have not been reported [25]. Thus, more studies are warranted to understand how to control the phase formation and properties of Ta_xO_y films deposited by magnetron sputtering.

Therefore, this study aimed (1) to tailor the synthesis of Ta-based thin films onto a cpTi surface by magnetron sputtering technique; (2) to characterize the physical and chemical properties of Ta-based films; (3) to investigate the impact of Ta-based films on initial *Streptococcus sanguinis* adhesion; and (4) to observe the morphology and spreading of pre-osteoblastic (MC3T3-E1) cells on crystalline Ta oxide film.

2. Materials and methods

2.1. Sample preparation

CpTi discs (Mac-Master Carr, Elmhurst, IL, USA) were polished with sequential SiC grinding paper (#320, #400 and #600) (Carbimet 2, Buehler, Lake Bluff, IL, USA) and polishing cloth (Satyn MB, Buehler) with a 9- μ m aqueous polycrystalline diamond suspension (MetaDi Supreme, Buehler) in an automatic polisher (EcoMet/AutoMet 250 Pro, Buehler). Afterwards, the final polishing with a colloidal silica suspension and polishing disk (Chemio MB, Buehler) was conducted to obtain a mirror-finished surface with a standardized surface roughness (Ra) of $0.02 \pm 0.008 \mu\text{m}$. Samples were cleaned in an ultrasonic bath with deionized water (10 min), acetone (10 min), and isopropyl alcohol (10 min) and air-dried at 250 °C.

2.2. Magnetron sputtering deposition

Ta_xO_y films with an estimated thickness of 600 nm were deposited by a radio frequency (RF) magnetron sputtering system (Kurt J. Lesker Company, PA, USA) using a 3"-diameter metallic Ta target (99.95% of purity) (Kurt J. Lesker Company, PA, USA) in an Ar+O₂ atmosphere. To remove contaminants from the target surface, prior to each film deposition process, cleaning plasma was applied to the Ta target surface with a pure Ar atmosphere at 7.5 mTorr using 100 W RF power for 5 minutes [26].

The initial choice of the film deposition parameters was based on the deposition rates obtained from a quartz crystal microbalance (FTM-2400, Inficon, Bad Ragaz, Switzerland). For this, the sensor head with a quartz crystal (Gamry Instruments, Warminster, PA, USA) was positioned inside the chamber at the same distance at which the substrate holder (70 mm) remained during the further depositions. During these tests, the film deposition rates were measured while O₂ flow was varied, and the working pressure, power, and Ar flow were kept constant at 4.0 mTorr, 300 W and 20 sccm, respectively.

After defining the deposition rates of the films in the various oxygen flows, different substrate temperatures were used to investigate possible structural changes in the films. The chamber base pressure was maintained lower than 5.0×10^{-3} mTorr while the working pressure was varied from 7.5 mTorr to 20 mTorr to develop a suitable reactive environment to deposit the Ta_xO_y films. Six samples were produced in each deposition process. The tailoring deposition parameters of each group are listed in Table 1.

Table 1. Tailored deposition parameters of Ta-based films.

	#1	#2	#3	#4	#5	#6	#7	#8
Group code	1 O ₂ sccm 200 °C 300 W	4 O ₂ sccm 200 °C 300 W	8 O ₂ sccm 200 °C 300 W	8 O ₂ sccm 400 °C 300 W	8 O ₂ sccm 600 °C 150 W	8 O ₂ sccm 600 °C 300 W	8 O ₂ sccm 600 °C 400 W	10 O ₂ sccm 200 °C 300 W
RF power (W)	300	300	300	300	150	300	400	300
DC Bias (V)	-148	-158	-157	-155	-122	-155	-164	-154
Ar flow (sccm)	20	20	20	20	20	20	20	20
O₂ flow (sccm)	1	4	8	8	8	8	8	10
Pressure (mTorr)	7.5	7.5	7.5	7.5	2.0	7.5	6.0	7.5
T_{heater} (°C)	200	200	200	400	600	600	600	200
Total time deposition (min)	10	74	72	72	75	72	67	77

*Depending on the deposition conditions, the reflected RF power varied from 1 to 4 W.

2.3. Surface Characterization

2.3.1. X-ray diffraction analysis (XDR) analysis

Structural properties of the films were investigated by XRD (X'Pert³ Powder, PANalytical) with a CuK α ($\lambda = 1.54056 \text{ \AA}$) radiation, using θ - 2θ configuration in the 20° to 80° range with 0.01° step size.

2.3.2. Optical characterization – reflectance and transmittance

Optical characterizations of the films were performed using reflectance measurements. The reflectance at nearly normal (8°) and the transmittance at normal incidence were performed from 250 to 1800 nm in a Perkin Elmer Lambda 1050 spectrophotometer, with a 150 mm integrating sphere apparatus.

The transmittances were used to determine the thickness (h), refractive index dispersion ($n(\hbar\omega)$), and the absorption coefficient ($\alpha(\hbar\omega)$) as a function of the photon energy ($\hbar\omega$) of the films by using the Cisneros's method [27]. In this method, the refractive index dispersion is modeled by the Wemple and DiDomenico dispersion relation [28], which is characterized by the oscillator energy E_M and the dispersion energy E_d . The explicit relationship [28] of n the photon energy is:

$$n(\hbar\omega) = 1 + \frac{E_M E_d}{E_M^2 - (\hbar\omega)^2}$$

Another useful parameter that can be derived from this equation is the static refractive index (n_o), which corresponds to the value of $n(\hbar\omega)$ in the limit $\hbar\omega \rightarrow 0$.

2.3.4. Scanning electron microscopy (SEM) and energy-dispersive spectroscopy (EDS) analyses

To characterize the film morphologies and the elemental composition (% atomic), SEM and EDS (Philips XL-30 FEG) analyses were conducted.

2.3.5. Profilometry (surface roughness)

A profilometer (Dektak 150-d; Veeco, Plainview, NY, USA) with a 500- μm cutoff, at a constant time of 12 s was used for the measurement of the surface roughness (Ra – arithmetic mean). Three measurements were obtained for each disc, and a mean value was obtained ($n = 5$).

2.3.6. Surface Energy

The surface energy analysis was performed according to the protocol suggested by Combe et al. [29] through a goniometer (ramé-hart Instrument Co., Succasunna, NJ, USA). For the determination of surface energy, the measurement of the contact angle between the disc surface and a sessile drop (2 μ L) of deionized water (polar component) and diiodomethane (dispersive component) was conducted. Three drops of each liquid were used to perform the measurement at room temperature (21 ± 1 °C) and controlled humidity. The image obtained was immediately captured by the computer, and the contact angle formed by the drop on the substrate surface was automatically measured by the Drop Image Standard software (ramé-hart Instrument Co.). The surface energy and the polar and dispersive components were obtained [29] ($n = 5$).

2.4. Microbiologic assay

2.4.1. Bacterial growth condition

For the bacterial growth condition, a total of 100 μ L of *S. sanguinis* IAL 1832 were grown in 5 mL of brain heart infusion (BHI) broth (Difco Laboratories, France) supplemented with 1% of glucose under 10% CO₂ incubation at 37 °C overnight. Afterwards, 1 mL of the mixture of the inoculum and BHI was extracted and transferred to a tube containing 9 mL of BHI supplemented with 1% of glucose, and the bacteria grew for 6 h (exponential growth phase) under the same conditions aforementioned. Then, the tubes were subjected to centrifugation (6000 *g* for 5 min at 4 °C) and washed twice with 0.9% NaCl, and the precipitate was resuspended in BHI broth. A spectrophotometer (DU800 Beckman Coulter, Brea, CA, USA) was used to adjust the optical density at 600 nm ($OD = 1.0 \pm 0.02$) of the final suspension of 10^7 cells/mL [30].

2.4.2. Bacterial adhesion assay

Discs were sterilized by gamma radiation (0.87 ± 0.05 kGy) (Cobalt-60, Gammacell 220, Atomic Energy of Canada Ltd., Ottawa, ON, Canada) prior to being tested [31]. To simulate the oral cavity, discs were coated with a human saliva pellicle prior to the bacterial adhesion assay. Three healthy volunteers provided stimulated human saliva. This study was approved by the Local Ethics Committee in Research (registration number: 57496116.5.0000.5418). Volunteers delivered written formal consent according to the rules of the aforementioned ethics committee.

After collecting saliva, the pool was centrifuged under 10,000 *g* for 10 min at 4 °C. The supernatant was filter-sterilized and immediately used. The discs were individually

and horizontally immersed in 1 mL of saliva in a 24-well culture plate and incubated under agitation for 2 h at 37 °C to form the salivary pellicle. Saliva-coated discs were transferred to another 24-well culture plate containing 100 µL of *S. sanguinis* cell suspension (10^7 cells/mL) and 900 µL of BHI broth supplemented with 1% glucose. Discs were incubated under microaerophilic (10% CO₂) conditions at 37 °C. After 4 h of incubation, to remove loosely attached cells, the discs with bacterial adhesion were washed with 2 mL of 0.9% NaCl and transferred to another 24-well plate containing the previously described fresh media and incubated for 4 h. All assays were performed twice independently, in triplicate ($2 \times 3 = 6 - n$ value).

2.4.3. Number of viable cells

To detach bacterial cells, the discs containing adhered bacteria were washed twice with 0.9% NaCl and then transferred to cryogenic tubes containing 3 mL of 0.9% NaCl and sonicated (7 W during 30 s). The sonicated suspensions were serially diluted in 0.9% NaCl, and 20 µL samples were plated in triplicate onto Trypticase Soy Broth (TSB) (Difco Laboratories) with agar. The TSB plates were incubated at 37 °C in 10% CO₂, and after 48 h, the colony-forming units (CFUs) were counted and expressed as CFU/mL.

2.5. Biological assay

2.5.1. Cell culture

MC3T3-E1 cells were cultured in Minimum Essential Medium Eagle – Alpha Modification (Alpha MEM: Gibco, Life Technologies, Gaithersburg, MD, USA) supplemented with 10% fetal bovine serum (FBS) (Gibco, Life Technologies), streptomycin (100 mg/mL: Gibco, Life Technologies) and penicillin (100 U/mL) in a humidified incubator at 5% CO₂ atmosphere at 37 °C. To determine the effect of the experimental surface on cell morphology, MC3T3-E1 cells were plated in duplicate at 2×10^4 cells/mL in 24-well culture plates in Alpha MEM supplemented with 10% FBS and antibiotics for 24 h to allow cell adhesion on the discs. Then, medium was replaced with Alpha MEM supplemented with 2% FBS plus antibiotics (day 0), which was replaced every other day until the end of the experimental period. Cell morphology was verified by SEM analysis at day 4. Briefly, culture medium was aspirated, and the cells were fixed with Karnovsky's solution (pH 7.4) overnight at 4 °C and post-fixed in 1% osmium tetroxide in distilled water for 1 h at room temperature. Then, they were dehydrated through a graded ethanol series (35%, 50%, 70%, 90%, and 100%) at room temperature for 10 min each. Finally, samples were critical-point dried (mod.

DCP-1, Denton Vacuum, Moorestown, NJ, USA) and gold sputtered (mod. SCD 050, Bal-Tec.) [32].

2.6. Statistical analysis

Statistical analyses were performed with statistical software (SPSS v.20.0, SPSS Inc., IBM Corp, Armonk, NY, USA). The Shapiro-Wilk method was performed to verify the normality of all response variables. One-way ANOVA was used to evaluate the effect of surface type on the film thickness, roughness, surface energy and CFU data. Tukey's HSD test was used as a post hoc technique for multiple comparisons ($\alpha = .05$).

3. Results and Discussion

Starting the analysis of the results with the characterization of the growth rates and film thicknesses, Fig. 1 shows the representative graph of deposition rate as a function of oxygen flow. At low oxygen flow, the deposition rate measured was approximately 4.0 $\mu\text{m/h}$. When the O_2 flow increased, the deposition rate decreased significantly (approximately 0.60 $\mu\text{m/h}$). Such a drop of the deposition rate values is due to the transition from metal mode to poisoned mode, caused by the oxygen on the target surface. In this condition, the difference between the metal sputtering yield (0.40 atoms/ Ar^+ ion) and the oxide sputtering yield (~ 0.10 atoms/ Ar^+ ion), as estimated by TRIM calculations when considering Ar^+ ions accelerated by the target voltage bias, may explain the reduction of the deposition rate in higher oxygen flow conditions.

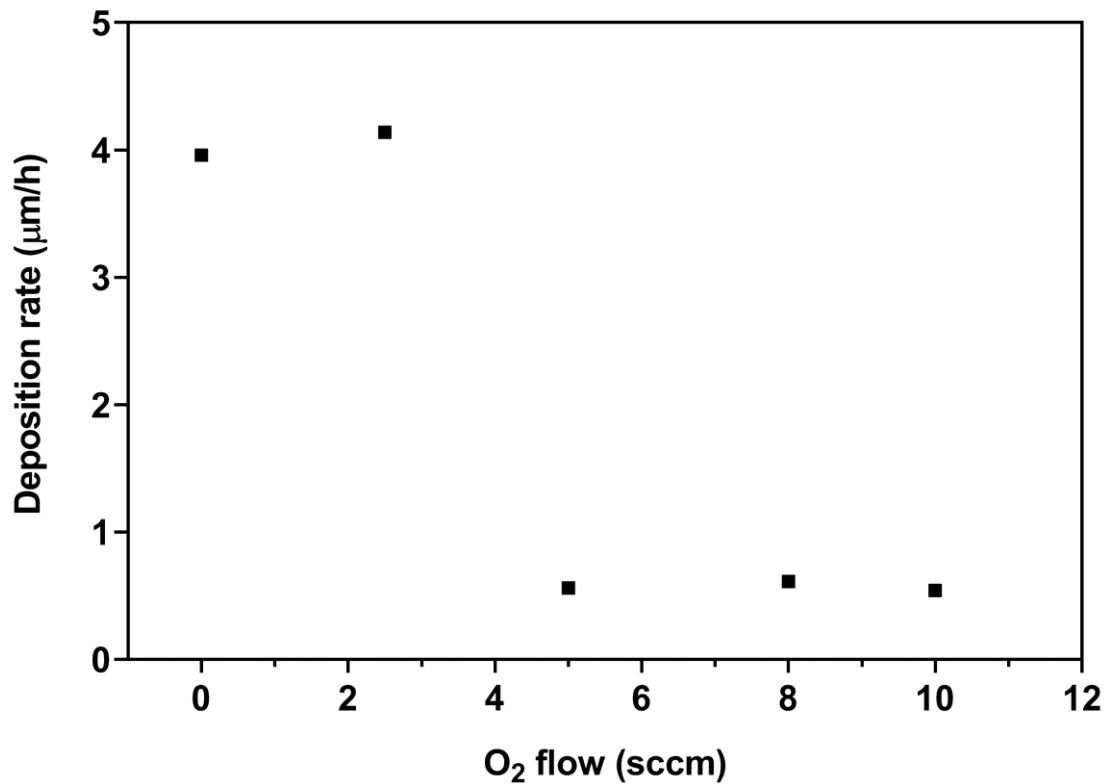


Fig. 1. Deposition rates measured with a quartz crystal microbalance under constant Ar flow (20 sccm) and RF power (300W) as a function of different O₂ flow.

The X-ray diffraction analysis of the as-grown tantalum oxide films deposited onto cpTi are shown in Fig. 2. All the diffraction patterns showed the presence of metallic titanium. Since the penetration depth of CuK α radiation into tantalum oxide is approximately 10 μm and the measured thickness of the films was approximately 0.6 μm , the presence of metallic titanium peaks in all diffraction patterns is expected [33]. Only the 1 O₂ sccm and 8 O₂ sccm (600 °C/400 W) groups showed crystallization of the deposited films. The analysis revealed that the diffraction peaks found in the 1 O₂ sccm group corresponded to TaO₂ (tetragonal body centered cubic structure) (ICDD PDF no. 77-2305). Schonberg et al. [34] reported that this phase, also named δ -TaO₂, has a rutile structure, with $a= 4.702 \text{ \AA}$ and $c= 3.065 \text{ \AA}$. However, such a structure has not received much attention, and the optimal values are not well known [25]. The 8 O₂ sccm (600 °C/400 W) group showed crystallization, as indicated by some small peaks at 27.5°, 49.0°, 53.2° and 70.6°, which corresponded to the orthorhombic phase of Ta₂O₅ film [35]. Lehovc [36] has attributed an orthorhombic structure to tantalum pentoxide, which is known as β -Ta₂O₅. The crystal structure of β -Ta₂O₅ phase

consists of 2D layers of Ta_2O_3 that are connected to each other by twofold-coordinated O atoms between Ta atoms in adjacent layers [36–38].

The different tantalum oxide phases found in this study may be related to the deposition regime. The deposition regime in the metallic mode (i.e., low oxygen flow), wherein the deposition rates measured were approximately $4 \mu\text{m/h}$, favored the TaO_2 amorphous phase growth. On the other hand, the increased oxygen flow contributed to the poisoned mode, resulting in a decrease of the deposition rate (approximately $0.6 \mu\text{m/h}$), favoring the crystalline Ta_2O_5 phase development. Almeida Alves et al. [39] reported phase changes of tantalum oxide films grown by sputtering using different values of oxygen flow, which were assigned due to the deposition regime.

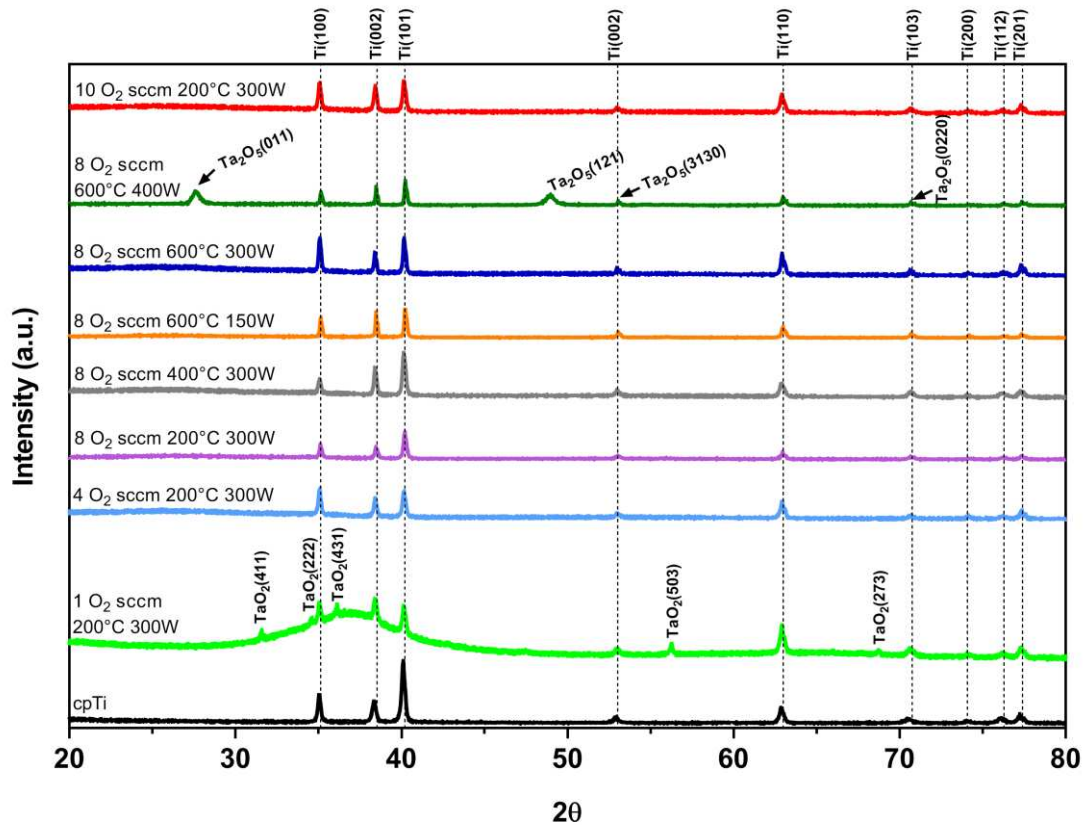


Fig. 2. X-ray diffraction pattern obtained from cpTi substrate and Ta_xO_y films deposited onto cpTi substrate. The diffraction pattern of the bare substrate (cpTi) was included for comparison, and the position of the corresponding peaks was marked using dashed lines. The peaks corresponding to the Ta_2O_5 planes were labeled.

The reflectance of Ta_xO_y films deposited onto cpTi is displayed in Fig. 3(a). The samples of the $1 \text{ O}_2 \text{ sccm}$ group presented metallic behavior with optical reflectance characteristics similar to the polished cpTi substrate and transmittances very close to zero for

samples deposited onto silica glass substrate (as shown in Fig. 3(b)). The other groups characterized by O₂ flows of 4 sccm or higher, clearly exhibited large interference fringe amplitudes, compatible with transparent low absorption and uniform thickness, indicating the formation of the Ta₂O₅ films [40]. In the 400–700 nm ranges, the interference oscillations were mostly below the reflectance of the substrates, so the films acted as anti-reflective layers for Ti.

The regularity and large amplitude of the interference oscillations in samples of groups 4 O₂ sccm to 8 O₂ sccm (600 °C 300 W) and 10 O₂ sccm evidenced a high optical homogeneity of the films, indicating that both their thickness and refractive index were homogeneous inside the optical probe area (10 mm × 4 mm). The exception was the film of group 8 O₂ sccm (600 °C 400 W), in which the amplitude of the oscillations was attenuated and the regularity was clearly hindered in the 300–400 nm range. This attenuation was attributed to scattering due to a surface roughness higher than the one observed on the other samples and to the presence of crystallites embedded in the amorphous tissue of the oxide films. The X-ray diffraction experiments of Fig. 2 clearly support the last proposition since group 8 O₂ sccm (600 °C 400 W) was the only one to show peaks related to Ta₂O₅ crystallites.

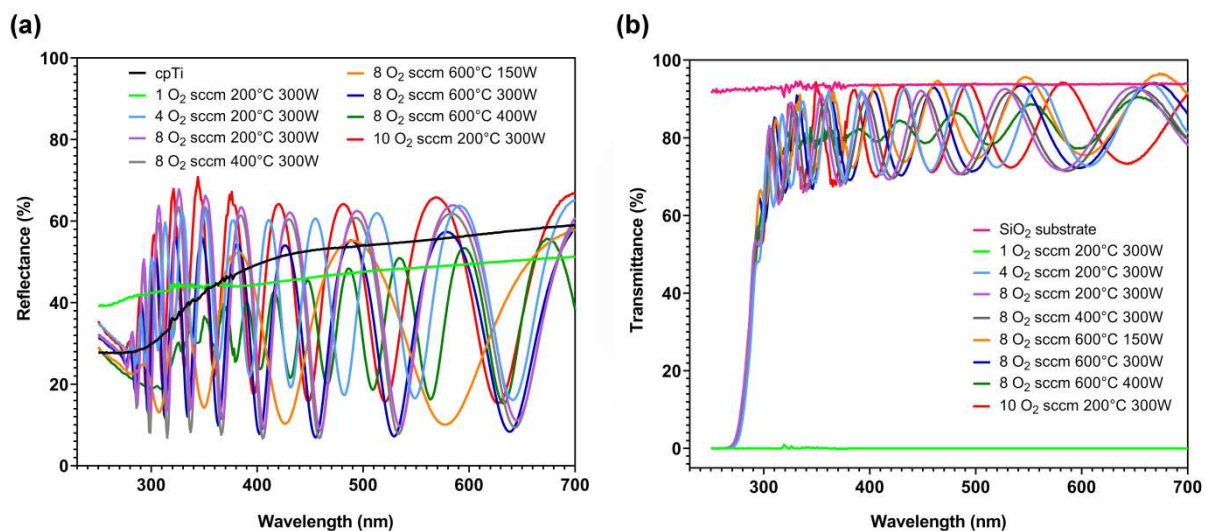


Fig. 3. Representative graphs of (a) reflectance spectra of the films deposited onto cpTi substrates and (b) transmittance spectra of the films deposited onto silica glass substrates. The spectra of a bare cpTi and silica glass substrates were included for comparison.

The transmittance data of films deposited onto silica glass on the same deposition processes as those plotted in Fig. 3(a) are depicted in Fig. 3(b). These were used to determine

the thickness (h), refractive index dispersion ($n(\hbar\omega)$) and absorption coefficient ($\alpha(\hbar\omega)$) as a function of the photon energy ($\hbar\omega$) of the films. As mentioned in Section 2, these determinations were made using Cisneros's method [27] and the Wemple and DiDomenico dispersion relation [28] for the refractive index. The absorption coefficients were employed to determine the optical bandgap using Tauc's procedure [41,42] and to estimate the minimum energy for direct transitions by the use of the α^2 plot as a function of the photon energy [43]. The resulting optical parameters are shown in Table 2. The corresponding refractive index dispersion curves and α^2 plots are shown in Figs. 4(a) and 4(b), respectively. The results obtained for Ta_2O_5 by Rodriguez-de-Marcos et al. [44] were included in the figures for comparison. Table 2 shows the numerical proximity and Fig. 4 illustrates the similarity of the optical behavior of the films. The only difference was in the behavior of the crystallized sample (8 O_2 sccm (600 °C 400 W)). It displayed a slightly smaller set of refractive indices and a slight shift of the α^2 edge to higher energies. As the sample presented a morphology that could be understood as a mix of crystallized and amorphous regions, the results for this particular sample shall be understood as an average. The optical differences noted in the group of samples were not strong, but the difference noted on samples of group 8 O_2 sccm (600 °C 400 W) was important to support, together with the X-ray diffraction, the analysis of cell growth presented later.

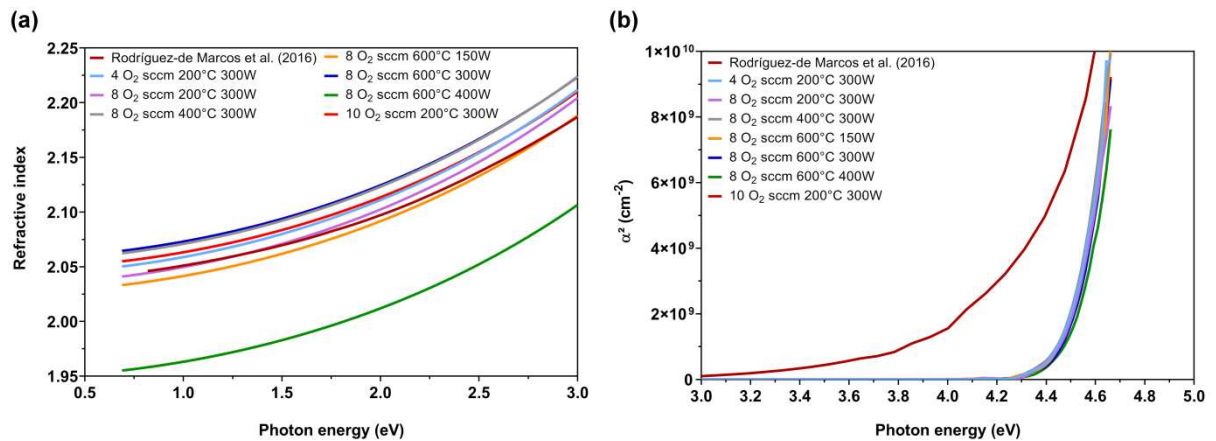


Fig. 4. (a) Refractive index dispersion curves for the different films. The plots correspond to the interpolation of the refractive index data using the Wemple and DiDomenico [28] dispersion relation, determined using the maxima and minima of the transmittance data. (b) Square of the absorption coefficient as a function of the photon energy for the different deposition conditions. The curve in dark red corresponds to data from Rodríguez-de Marcos et al. [44].

Table 2. Optical parameters determined from transmittance and reflectance measurements. The film thickness (h), the deposition rate ($\mu\text{m/h}$), refractive index dispersion data: static refractive index (n_0), Wemple and DiDomenico mean (E_m) and dispersion (E_d) energies, bandgap energies determined using the Tauc [28,45] model (E_g^{Tauc}) and the minimum energy for direct transitions (E_{dir}).

	#2	#3	#4	#5	#6	#7	#8	
Group code	4 O ₂ sccm 200 °C 300 W	8 O ₂ sccm 200 °C 300 W	8 O ₂ sccm 400 °C 300 W	8 O ₂ sccm 600 °C 150 W	8 O ₂ sccm 600 °C 300 W	8 O ₂ sccm 600 °C 400 W	10 O ₂ sccm 200 °C 300 W	Rodríguez-de Marcos et al. [44]
h (nm)	789	620	619	648	632	816	686	-
rate (mm/h)	0.64	0.52	0.52	0.52	0.53	0.73	0.61	-
n_0	2.04	2.03	2.05	2.03	2.06	1.95	2.05	2.04
E_m (eV)	6.97	6.92	7.00	7.06	7.05	6.94	7.11	7.28
E_d (eV)	22.1	21.7	22.6	21.9	22.8	19.4	22.7	22.9
E_g^{Tauc} (eV)	4.17	4.17	4.17	4.19	4.21	4.18	4.17	-
E_{dir} (eV)	4.48	4.50	4.48	4.48	4.50	4.51	4.48	4.79

To characterize the surface morphology of $Ta_xO_y/cpTi$ samples, SEM micrographs of the surfaces were taken at $\times 20,000$ magnification (Fig. 5). It is noticeable that the Ta_2O_5 film deposited using 8 sccm of O_2 , 400 W and 600 °C was the only group that presented a pronounced change in the morphology compared to the cpTi surface, exhibiting granular structure with complex geometry. On the other hand, the other groups showed very similar characteristics to the polished cpTi surface, which exhibited slightly smooth surfaces with longitudinal grooves resulting from the polishing procedure. These results remarkably match the surface roughness data (Fig. 6), wherein the Ta_2O_5 film deposited in the 8 sccm of O_2 flow, 400 W and 600 °C group presented higher surface roughness values ($0.052 \pm 0.008 \mu m$) compared with control and the other groups ($P < .05$, Tukey's HSD test). The surface roughness is one of the most important aspects that influence the implant fixation to bone. Surface roughness improves the osseointegration process compared with smooth Ti [46]. The nano-roughening (roughness between 0.01 and 1 μm) of the implant surface can significantly contribute to the protein adsorption, migration and differentiation of osteoblasts and, consequently, the osseointegration velocity [47].

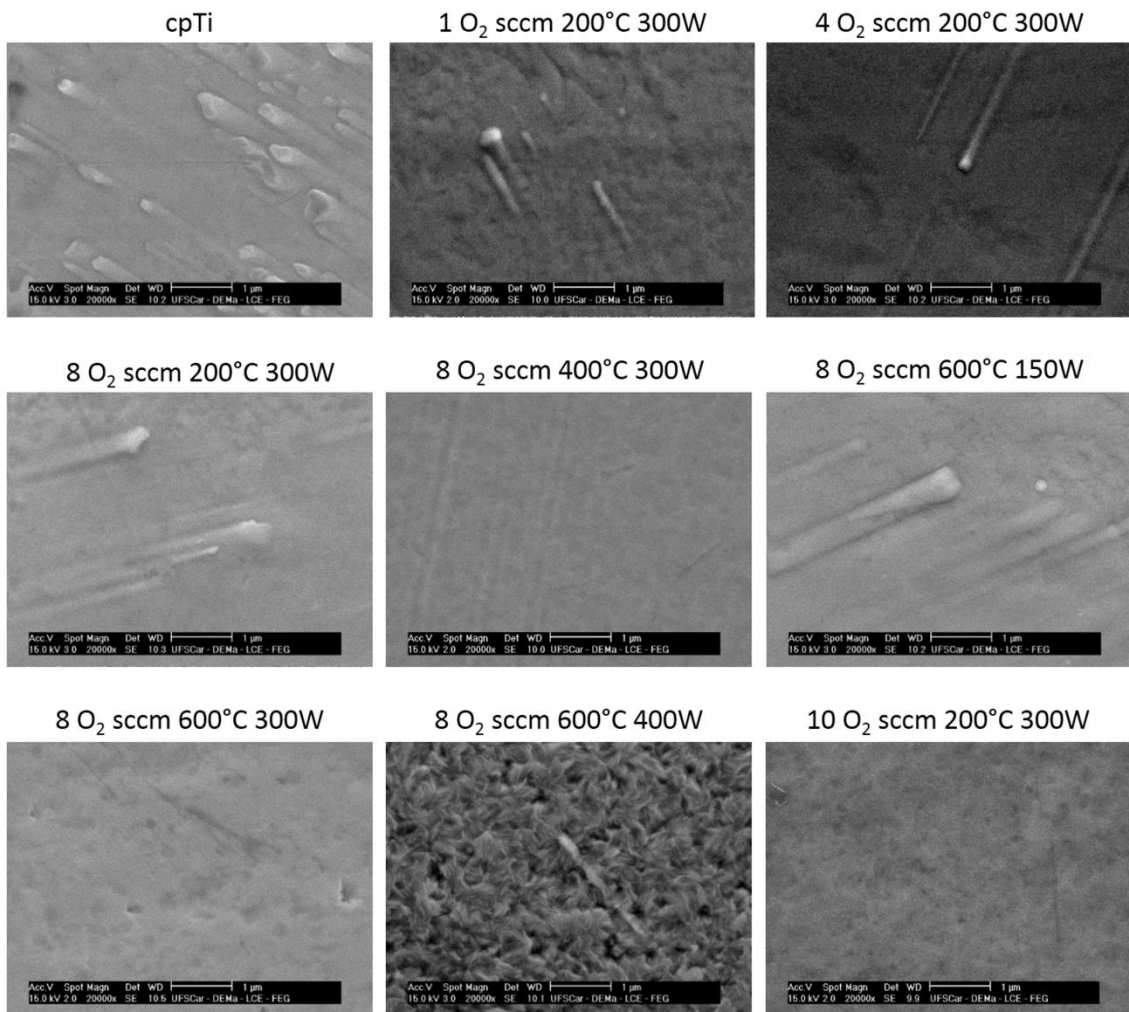


Fig. 5. SEM micrographs of Ta_xO_y coatings for different deposition parameters. The magnification ($\times 20,000$), the size of reference bar (bar = 1 μm), the electron acceleration potential (15 kV) and the working distance (10 mm) were kept constant in all measurements.

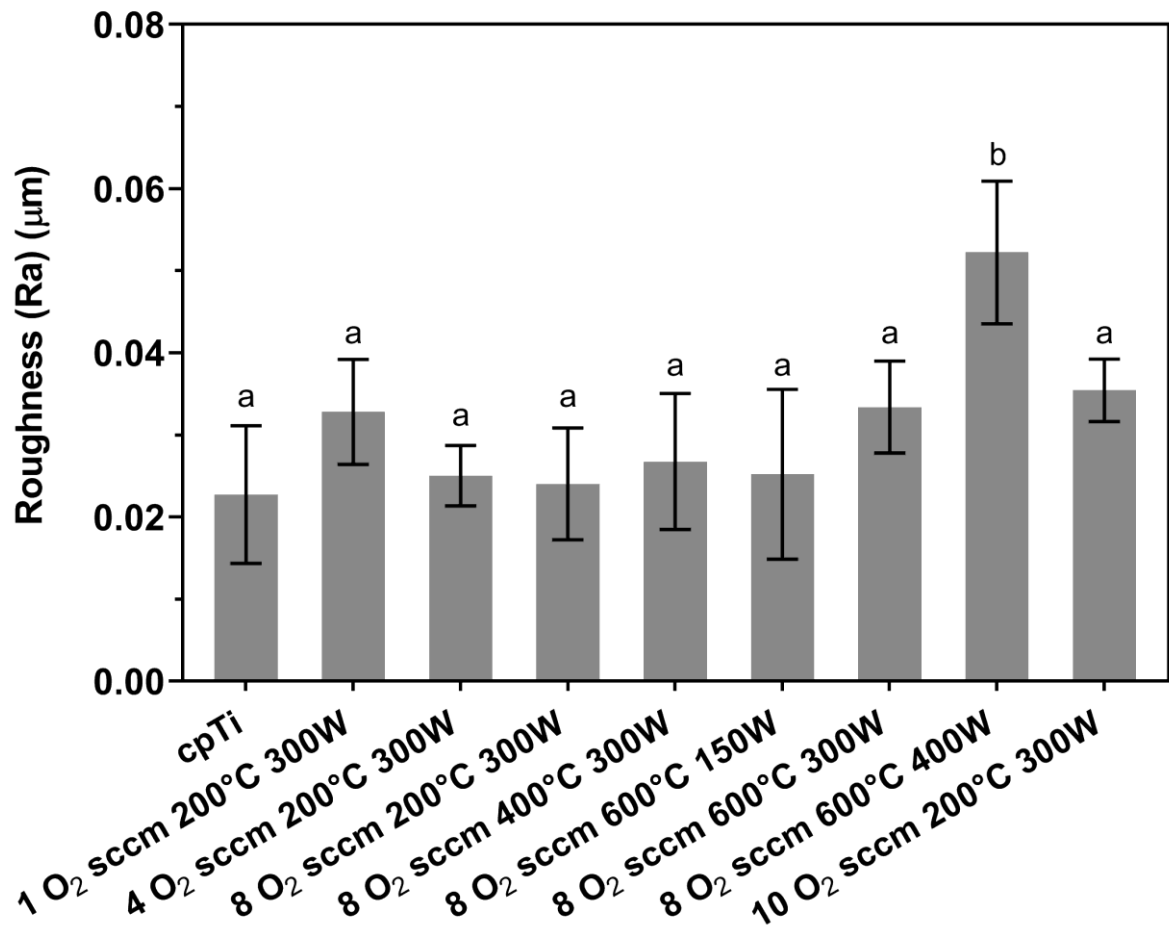


Fig. 6. Surface roughness of Ta_xO_y coatings as a function of different deposition parameters (oxygen flow, temperature and deposition power). The roughness of control (cpTi) was included for comparison. The standard deviations are represented using error bars. Different letters indicate significant differences among groups ($P < .05$, Tukey HSD test) ($n = 5$).

The semi-quantitative elemental chemical composition of the cpTi substrate and the Ta_xO_y films deposited onto the cpTi surface evaluated by EDS can be seen in Fig. 7. The control group presented a chemical composition consisting of titanium (Ti) and oxygen (O). In general, the Ta-treated groups presented tantalum (Ta), oxygen (O) and titanium (Ti) in the chemical composition. The presence of Ti may be explained due to the thin film thickness. In the graph, when the groups deposited under different oxygen flow and with the same working pressure (7.5 mTorr) and RF power (300 W) conditions were compared, the amount of Ta was inversely proportional to the oxygen content in the chamber. This event can be attributed to the oxidation of the target surface in the presence of a greater amount of oxygen, which implies a lower amount of Ta that can be removed from the target [39]. The 8 O₂ sccm group

deposited at 150 W showed the lowest Ta amount in its composition compared with the groups deposited at the same O₂ flow. In this case, the low power applied during the deposition may have hindered the exit of a greater number of atoms from the target, influencing the chemical composition of the 8 O₂ sccm (600 °C 150 W) group.

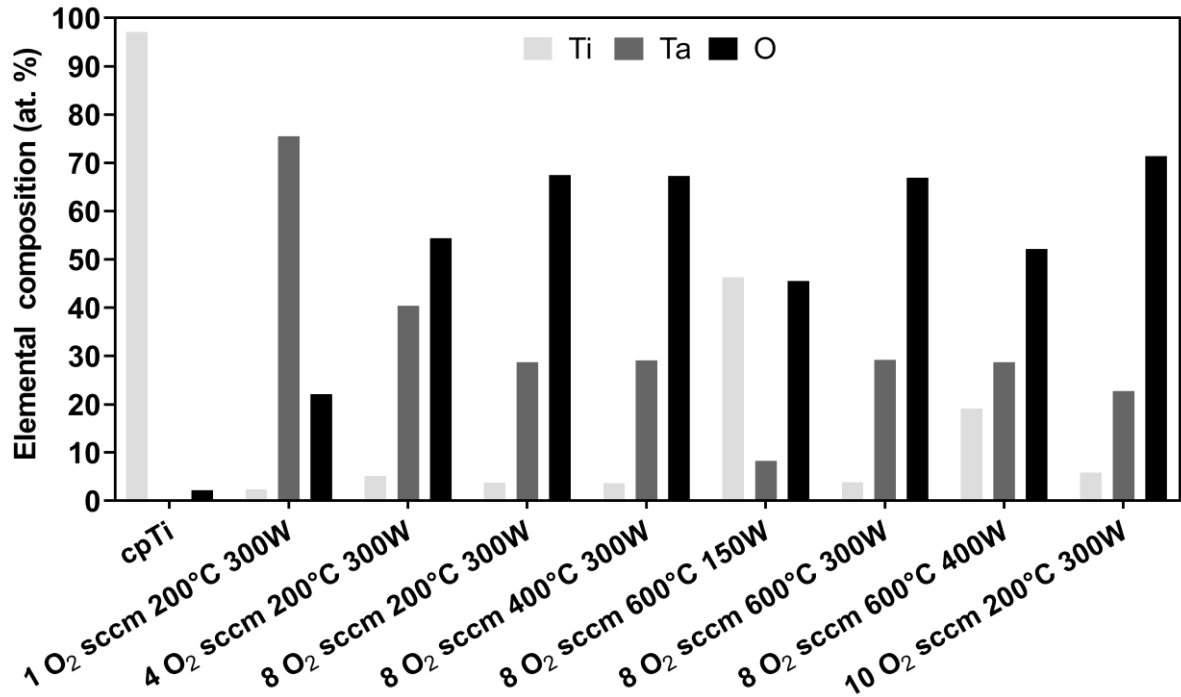


Fig. 7. Elemental chemical composition (at. %) for control (cpTi) and Ta_xO_y coatings as a function of different deposition parameters (oxygen flow, temperature and deposition power) determined by EDS.

The surface free energy is defined as a thermodynamic measurement, which contributes to the interpretation of the phenomena occurring in interfaces [48] and is one of the most crucial parameters that affect the biological response of biomaterials. In this study, the total surface free energy of the Ta_xO_y films was determined as the sum of the dispersive and polar components of the contact angle (Fig. 8). The group deposited at 8 O₂ sccm (600° C/400 W) (contact angle approximately 86°) showed a slightly higher surface energy than control and the other groups, indicating a hydrophilic tendency. The other groups had similar surface energy ($P >.05$, Tukey HSD test). Moderately hydrophilic (contact angle approximately 85–90°) and positively charged substrates can optimize cell adhesion due to the adsorption of cell adhesion-mediating proteins in an advantageous geometrical conformation, while surfaces with high hydrophilicity (contact angle <2°) prevent the adsorption of proteins [49].

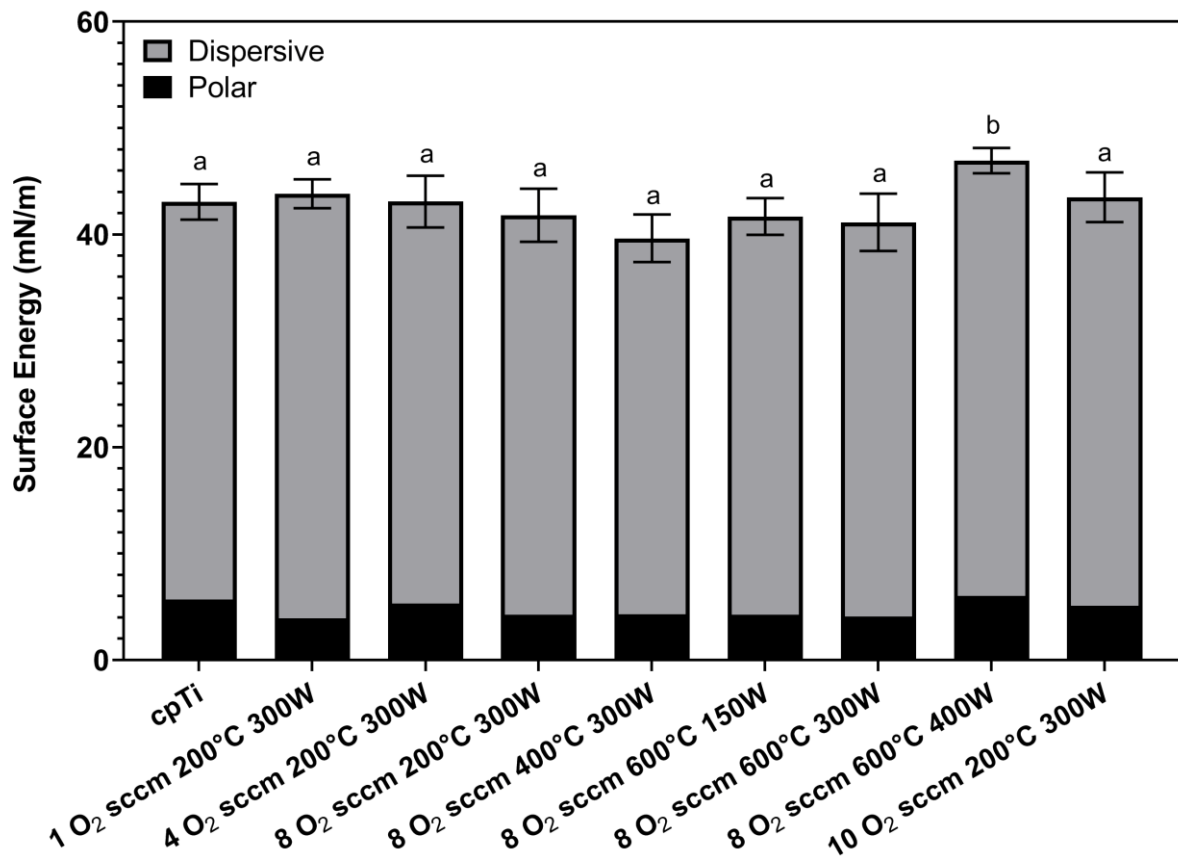


Fig. 8. Surface energy and corresponding standard deviation (error bars) for control (cpTi) and Ta_xO_y coatings as a function of different deposition parameters (oxygen flow, temperature and deposition power). Different letters indicate significant differences among groups ($P < .05$, Tukey HSD test) ($n = 5$).

The aspects affecting bacterial adhesion to a biomaterial surface are complex and depend on both surface and bacterial properties [8]. In this study, we report the interaction between *S. sanguinis* and different Ta_xO_y films deposited onto the cpTi surface. *S. sanguinis* is considered one of the first colonizers in the oral cavity [50], being the most predominant bacteria found on implant materials [51]. Therefore, it has been used by several studies on bacterial adhesion models due to its high importance in biofilm development process [30,52]. Fig. 9 shows the bacterial adhesion in colony-forming units as a function of surface type. Similar values of CFU were noted for all groups ($P = .740$, ANOVA). Although the 8 O₂ sccm (600 °C/400 W) group showed a higher roughness value and a slight tendency of hydrophilicity compared to the other groups, such surface characteristics did not affect the number of bacteria adhered on the surface. Such findings are in agreement with previous studies, which reported that the implant surface roughness does not change the initial biofilm

formation [53,54]. Thus, even with the higher roughness value, the β -Ta₂O₅ film was not able to increase bacterial adhesion, which may prevent biofilm-related diseases such as peri-implantitis and the failure of implant treatment [55].

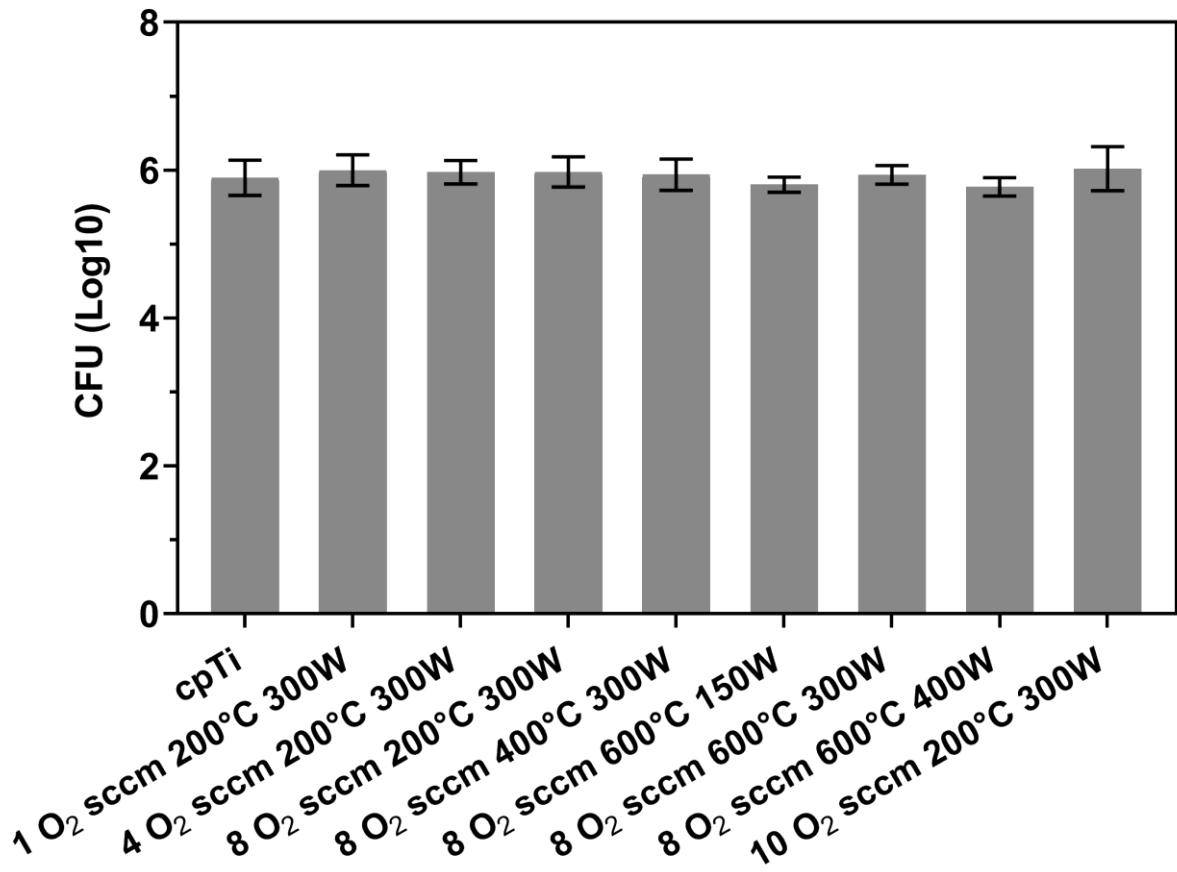


Fig. 9. Colony-forming unit (CFU) quantification and the corresponding standard deviation (error bars) for control (cpTi) and Ta_xO_y coatings as a function of different deposition parameters (oxygen flow, temperature and deposition power). The CFU data were plotted in a log₁₀ scale. No significant difference was found among groups ($P = .740$, ANOVA) ($n = 6$).

Because it presented a crystalline structure, the 8 O₂ sccm (600 °C/400 W) group was selected to analyze the morphology and spreading of MC3T3E-1 cells after 4 days of incubation since the crystalline β -Ta₂O₅ structure has better biological performance compared with amorphous Ta oxide films [8]. According to SEM observation (Fig. 10), the morphology of MC3T3-E1 cells cultured on β -Ta₂O₅ film was notably different compared to uncoated cpTi (control). On the β -Ta₂O₅ surface, adherent cells with better spreading were seen, with the presence of a great number of filopodia extensions, which are considered a crucial part of the cell cytoskeleton that is necessary for proper cell movement, attachment and morphology

[56]. This behavior suggests a better cell response on the β -Ta₂O₅ surface compared to uncoated cpTi. The crystalline β -Ta₂O₅ surface showed higher roughness values than control and the other Ta groups, presenting a greater surface area available for cell attachment and proliferation. This is in agreement with a previous study that showed that biomaterial morphological characteristics affect cell attachment and proliferation [57]. Additionally, the interaction of the underlying crystalline β -Ta₂O₅ surface and the cell membranes seemed to have been governed by the surface energy. Indeed, the results of the present study suggest that the combination of such good surface properties presented by β -Ta₂O₅ film improved the biocompatibility of Ti.

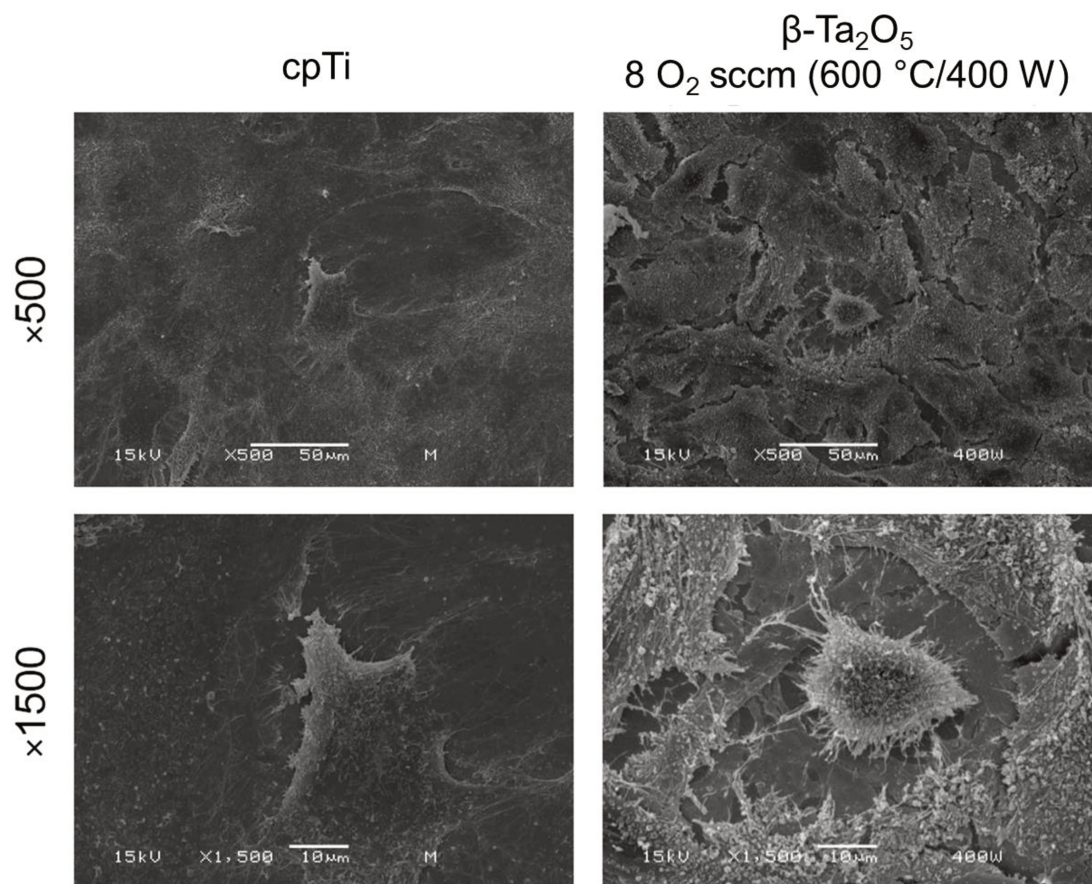


Fig. 10. SEM micrographs of MC3T3 cells morphology after 4 days of cell culture on cpTi (left column) and on β -Ta₂O₅ film surfaces (right column). The growth condition of the β -Ta₂O₅ film is indicated in the top of the right column. The figure clearly shows that the cell growth is favored when the β -Ta₂O₅ film is present.

Aiming to reduce the failure rates in implant rehabilitation treatment, surface treatments have been proposed to improve the biological performance of Ti-based dental

implants as well as to protect their surfaces against the chemical and microbiological degradation in the oral environment. This study showed that β -Ta₂O₅ film improved pre-osteoblastic (MC3T3-E1) cell spreading and morphology. In addition, Ta surface treatment did not affect the number of bacteria adhered on the surface. Although promising, the results obtained in this study are preliminary and therefore should not be immediately transferred to a clinical setting. This study only evaluated the impact of Ta₂O₅ thin films on the morphology and spreading of MC3T3E cells. Further *in vitro* and *in vivo* studies are necessary to investigate the bone-cellular response of the proposed surface treatment.

4. Conclusions

Ta_xO_y coatings having amorphous or crystalline atomic structures can be synthesized by pulsed magnetron sputtering deposition depending on the parameters used. Ta_xO_y films with different structures and morphologies did not favor the increase of bacterial adhesion as compared to cpTi. The film containing β -Ta₂O₅ crystals improved the Ti surface properties and positively affected the cell spreading and morphology, making it a promising surface treatment to improve the biocompatibility of titanium-based dental implants.

5. Acknowledgments

This work was supported by the Sao Paulo State Research Foundation (FAPESP), Brazil (grant numbers 2016/07269-3, 2016/11470-6 and 2017/18916-2) and in part by the Coordenação de Aperfeiçoamento de Pessoal de Nível Superior - Brasil (CAPES) - Finance code 001. The authors express their gratitude to the Structural Characterization Laboratory (DEMA/Ufscar) for the DRX, MEV/FEG and EDS facilities and to the Oral Biochemistry Laboratory at the Piracicaba Dental School - UNICAMP for the microbiology facility.

6. References

- [1] S. Prasad, M. Ehrensberger, M.P. Gibson, H. Kim, E.A. Monaco, Biomaterial properties of titanium in dentistry, *J. Oral Biosci.* 57 (2015) 192–199. doi:10.1016/j.job.2015.08.001.
- [2] F. Bassi, A.B. Carr, T.-L. Chang, E. Estafanous, N.R. Garrett, R.-P. Happonen, S. Koka, J. Laine, M. Osswald, H. Reintsema, J. Rieger, E. Roumanas, T.J. Salinas, C.M. Stanford, J. Wolfaardt, Clinical outcomes measures for assessment of longevity in the dental implant literature: ORONet approach, *Int. J. Prosthodont.* 26 (2013) 1–8. doi:10.11607/ijp.3402.
- [3] M. Esposito, M.G. Grusovin, P. Coulthard, P. Thomsen, H.V. Worthington, A 5-year follow-up comparative analysis of the efficacy of various osseointegrated dental implant systems: a systematic review of randomized controlled clinical trials, *Int. J. Oral Maxillofac. Implants.* 20 (2005) 557–568. doi:10.1103/PhysRevA.44.1644.
- [4] L. Levin, Dealing with dental implant failures, *J. Appl. Oral Sci.* 16 (2008) 171–175. doi:10.1590/S1678-77572008000300002.
- [5] A.C. Hee, H. Cao, Y. Zhao, S.S. Jamali, A. Bendavid, P.J. Martin, Cytocompatible tantalum films on Ti6Al4V substrate by filtered cathodic vacuum arc deposition, *Bioelectrochemistry.* 122 (2018) 32–39. doi:10.1016/j.bioelechem.2018.02.006.
- [6] V.K. Balla, S. Banerjee, S. Bose, A. Bandyopadhyay, Direct laser processing of a tantalum coating on titanium for bone replacement structures, *Acta Biomater.* 6 (2010) 2329–2334. doi:10.1016/j.actbio.2009.11.021.
- [7] Z. Tang, Y. Xie, F. Yang, Y. Huang, C. Wang, K. Dai, X. Zheng, X. Zhang, Porous tantalum coatings prepared by vacuum plasma spraying enhance BMSCs osteogenic differentiation and bone regeneration in vitro and in vivo, *PLoS One.* 8 (2013) e66263. doi:10.1371/journal.pone.0066263.
- [8] Y.Y. Chang, H.L. Huang, H.J. Chen, C.H. Lai, C.Y. Wen, Antibacterial properties and cytocompatibility of tantalum oxide coatings, *Surf. Coatings Technol.* 259 (2014) 193–198. doi:10.1016/j.surfcoat.2014.03.061.
- [9] C.F. Almeida Alves, A. Cavaleiro, S. Carvalho, Bioactivity response of Ta_{1-x}O_x coatings deposited by reactive DC magnetron sputtering, *Mater. Sci. Eng. C.* 58 (2016) 110–118. doi:10.1016/j.msec.2015.08.017.
- [10] Y.S. Sun, J.H. Chang, H.H. Huang, Corrosion resistance and biocompatibility of titanium surface coated with amorphous tantalum pentoxide, *Thin Solid Films.* 528 (2013) 130–135. doi:10.1016/j.tsf.2012.06.088.

- [11] S. Zein El Abedin, U. Welz-Biermann, F. Endres, A study on the electrodeposition of tantalum on NiTi alloy in an ionic liquid and corrosion behaviour of the coated alloy, *Electrochem. Commun.* 7 (2005) 941–946. doi:10.1016/j.elecom.2005.06.007.
- [12] H. Pelletier, D. Muller, P. Mille, J.J. Grob, Structural and mechanical characterisation of boron and nitrogen implanted NiTi shape memory alloy, *Surf. Coatings Technol.* 158–159 (2002) 309–317. doi:10.1016/S0257-8972(02)00188-3.
- [13] B. Bouchet-Fabre, A. Fadjié-Djomkam, R. Fernandez-Pacheco, M. Delmas, M. Pinault, P. Jegou, C. Reynaud, M. Mayne-L’Hermite, O. Stephan, T. Minéa, Effect of tantalum nitride supporting layer on growth and morphology of carbon nanotubes by thermal chemical vapor deposition, *Diam. Relat. Mater.* 20 (2011) 999–1004. doi:10.1016/j.diamond.2011.05.006.
- [14] N. Kim, J.F. Stebbins, Structure of amorphous tantalum oxide and titania-doped tantala: ^{17}O NMR results for sol-gel and ion-beam-sputtered materials, *Chem. Mater.* 23 (2011) 3460–3465. doi:10.1021/cm200630m.
- [15] I. Baía, M. Quintela, L. Mendes, P. Nunes, R. Martins, Performances exhibited by large area ITO layers produced by r.f. magnetron sputtering, *Thin Solid Films.* 337 (1999) 171–175. doi:10.1016/S0040-6090(98)01393-5.
- [16] J. Alami, S. Bolz, K. Sarakinos, High power pulsed magnetron sputtering: fundamentals and applications, *J. Alloys Compd.* 483 (2009) 530-534. doi:10.1016/j.jallcom.2008.08.104.
- [17] K. Sarakinos, J. Alami, S. Konstantinidis, High power pulsed magnetron sputtering: a review on scientific and engineering state of the art, *Surf. Coatings Technol.* 204 (2010) 1661–1684. doi:10.1016/j.surfcoat.2009.11.013.
- [18] G. He, X. Chen, Z. Sun, Interface engineering and chemistry of Hf-based high-k dielectrics on III-V substrates, *Surf. Sci. Rep.* 68 (2013) 68–107. doi:10.1016/j.surfrep.2013.01.002.
- [19] G. He, B. Deng, H. Chen, X. Chen, J. Lv, Y. Ma, Z. Sun, Effect of dimethylaluminumhydride-derived aluminum oxynitride passivation layer on the interface chemistry and band alignment of HfTiO-InGaAs gate stacks. *APL Mater.* 1 (2013) 012104. doi:10.1063/1.4808243.
- [20] G. He, J. Gao, H. Chen, J. Cui, Z. Sun, X. Chen, Modulating the interface quality and electrical properties of HfTiO/InGaAs gate stack by atomic-layer-deposition-derived Al_2O_3 passivation layer, *ACS Appl. Mater. Interfaces.* 6 (2014) 22013–22025. doi:10.1021/am506351u.

- [21] G. He, J. Liu, H. Chen, Y. Liu, Z. Sun, X. Chen, M. Liu, L. Zhang, Interface control and modification of band alignment and electrical properties of HfTiO/GaAs gate stacks by nitrogen incorporation, *J. Mater. Chem. C*. 2 (2014) 5299–5308. doi:10.1039/c4tc00572d.
- [22] J.W. Zhang, G. He, L. Zhou, H.S. Chen, X.S. Chen, X.F. Chen, B. Deng, J.G. Lv, Z.Q. Sun, Microstructure optimization and optical and interfacial properties modulation of sputtering-derived HfO₂ thin films by TiO₂ incorporation, *J. Alloys Compd.* 611 (2014) 253–259. doi:10.1016/j.jallcom.2014.05.074.
- [23] D.J. Kester, R. Messier, Macro-effects of resputtering due to negative ion bombardment of growing thin films, *J. Mater. Res.* 8 (1993) 1928–1937. doi:10.1557/JMR.1993.1928.
- [24] V.H. Pham, S.H. Lee, Y. Li, H.E. Kim, K.H. Shin, Y.H. Koh, Utility of tantalum (Ta) coating to improve surface hardness in vitro bioactivity and biocompatibility of Co-Cr, *Thin Solid Films*. 536 (2013) 269–274. doi:10.1016/j.tsf.2013.03.042.
- [25] E.A.I. Ellis, M. Chmielus, S.P. Baker, Effect of sputter pressure on Ta thin films: Beta phase formation, texture, and stresses, *Acta Mater.* 150 (2018) 317–326. doi:10.1016/j.actamat.2018.02.050.
- [26] A.L.J. Pereira, L. Gracia, A. Beltrán, P.N. Lisboa-Filho, J.H.D. Da Silva, J. Andrés, Structural and electronic effects of incorporating Mn in TiO₂ films grown by sputtering: Anatase versus Rutile, *J. Phys. Chem. C*. 116 (2012) 8753–8762. doi:10.1021/jp210682d.
- [27] J.I. Cisneros, Optical characterization of dielectric and semiconductor thin films by use of transmission data, *Appl. Opt.* 37 (1998) 5262–5270. doi:10.1364/AO.37.005262.
- [28] S.H. Wemple, M. DiDomenico, Behavior of the electronic dielectric constant in covalent and ionic materials, *Phys. Rev. B*. 3 (1971) 1338–1351. doi:10.1103/PhysRevB.3.1338.
- [29] E.C. Combe, B.A. Owen, J.S. Hodges, A protocol for determining the surface free energy of dental materials, *Dent. Mater.* 20 (2004) 262–268. doi:10.1016/S0109-5641(03)00102-7.
- [30] V.A.R. Barão, A.P. Ricomini-Filho, L.P. Faverani, A.A. Del Bel Cury, C. Sukotjo, D.R. Monteiro, J.C.C. Yuan, M.T. Mathew, R.C. Do Amaral, M.F. Mesquita, W.J. Da Silva, W.G. Assunção, The role of nicotine, cotinine and caffeine on the electrochemical behavior and bacterial colonization to cp-Ti, *Mater. Sci. Eng. C*. 56 (2015) 114–124. doi:10.1016/j.msec.2015.06.026.
- [31] T. Beline, I. da S.V. Marques, A.O. Matos, E.S. Ogawa, A.P. Ricomini-Filho, E.C. Rangel, N.C. da Cruz, C. Sukotjo, M.T. Mathew, R. Landers, R.L.X. Consani, M.F. Mesquita,

- V.A.R. Barão, Production of a biofunctional titanium surface using plasma electrolytic oxidation and glow-discharge plasma for biomedical applications. *Biointerphases*. 11 (2016) 011013. doi:10.1116/1.4944061.
- [32] A.O. Matos, A.P. Ricomini-Filho, T. Beline, E.S. Ogawa, B.E. Costa-Oliveira, A.B. de Almeida, F.H. Nociti Junior, E.C. Rangel, N.C. da Cruz, C. Sukotjo, M.T. Mathew, V.A.R. Barão, Three-species biofilm model onto plasma-treated titanium implant surface, *Colloids Surf. B Biointerfaces*. 152 (2017) 354–366. doi:10.1016/j.colsurfb.2017.01.035.
- [33] M. Birkholz, *Thin Film Analysis by X-Ray Scattering*, first ed., Wiley-VCH, Frankfurt, 2006.
- [34] N. Schonberg, An X-ray investigation of the tantalum-oxygen system, *Acta Chem. Scand.* 8 (1954) 240–245. doi:10.3891/acta.chem.scand.08-0240.
- [35] I. Perez, J.L. Enríquez Carrejo, V. Sosa, F.G. Perera, J.R. Farias Mancillas, J.T. Elizalde Galindo, C.I. Rodríguez Rodríguez, Evidence for structural transition in crystalline tantalum pentoxide films grown by RF magnetron sputtering, *J. Alloys Compd.* 712 (2017) 303–310. doi:10.1016/j.jallcom.2017.04.073.
- [36] K. Lehovc, Lattice structure of β -Ta₂O₅, *J. Less-Common Met.* 7 (1964) 397–410. doi:10.1016/0022-5088(64)90036-0.
- [37] S.H. Lee, J. Kim, S.J. Kim, S. Kim, G.S. Park, Hidden structural order in orthorhombic Ta₂O₅. *Phys. Rev. Lett.* 110 (2013) 235502. doi:10.1103/PhysRevLett.110.235502.
- [38] L.D. Calvert, P.H.G. Draper, A proposed structure for annealed anodic oxide films of tantalum, *Can. J. Chem.* 40 (1962) 1943–1950. doi:10.1139/v62-298.
- [39] C.F. Almeida Alves, C. Mansilla, L. Pereira, F. Paumier, T. Girardeau, S. Carvalho, Influence of magnetron sputtering conditions on the chemical bonding, structural, morphological and optical behavior of Ta_{1-x}O_x coatings, *Surf. Coatings Technol.* 334 (2018) 105–115. doi:10.1016/j.surfcoat.2017.11.001.
- [40] V.N. Kruchinin, V.A. Volodin, T.V. Perevalov, A.K. Gerasimova, V.S. Aliev, V.A. Gritsenko, Optical properties of nonstoichiometric tantalum oxide TaO_x ($x < 5/2$) according to spectral-ellipsometry and Raman-scattering data, *Opt. Spectrosc.* 124 (2018) 808–813. doi:10.1134/S0030400X18060140.
- [41] J. Tauc, R. Grigorovici, A. Vancu, Optical properties and electronic structure of amorphous germanium, *Phys. Status Solidi.* 15 (1966) 627–637. doi:10.1002/pssb.19660150224.
- [42] J. Tauc, *Optical Properties of Solids*, first ed., Abeles, Amsterdam, 1972.

- [43] J.I. Pankove, D.A. Kiewit, *Optical Processes in Semiconductors*, first ed., Prentice-Hall Inc., New Jersey, 1971.
- [44] L.V. Rodríguez-de Marcos, J.I. Larruquert, J.A. Méndez, J.A. Aznárez, Self-consistent optical constants of SiO₂ and Ta₂O₅ films, *Opt. Mater. Express*. 6 (2016) 3622–3637. doi:10.1364/OME.6.003622.
- [45] K. Strijckmans, W.P. Leroy, R. De Gryse, D. Depla, Modeling reactive magnetron sputtering: fixing the parameter set, *Surf. Coatings Technol.* 206 (2012) 3666–3675. doi:10.1016/j.surfcoat.2012.03.019.
- [46] A. Zareidoost, M. Yousefpour, B. Ghasemi, A. Amanzadeh, The relationship of surface roughness and cell response of chemical surface modification of titanium, *J. Mater. Sci. Mater. Med.* 23 (2012) 1479–1488. doi:10.1007/s10856-012-4611-9.
- [47] A. Revathi, A.D. Borrás, A.I. Muñoz, C. Richard, G. Manivasagam, Degradation mechanisms and future challenges of titanium and its alloys for dental implant applications in oral environment, *Mater. Sci. Eng. C*. 76 (2017) 1354–1368. doi:10.1016/j.msec.2017.02.159.
- [48] M. Lotfi, M. Nejib, M. Naceur, Cell Adhesion to Biomaterials: Concept of Biocompatibility, in: R. Pignatello (Ed.), *Advances in Biomaterials Science and Biomedical Applications*, IntechOpen, Catania, 2013, pp. 207–240.
- [49] L. Bacakova, E. Filova, M. Parizek, T. Ruml, V. Svorcik, Modulation of cell adhesion, proliferation and differentiation on materials designed for body implants, *Biotechnol. Adv.* 29 (2011) 739–767. doi:10.1016/j.biotechadv.2011.06.004.
- [50] P.E. Kolenbrander, R.J. Palmer, S. Periasamy, N.S. Jakubovics, Oral multispecies biofilm development and the key role of cell-cell distance, *Nat. Rev. Microbiol.* 8 (2010) 471–480. doi:10.1038/nrmicro2381.
- [51] G. Nakazato, H. Tsuchiya, M. Sato, M. Yamauchi, In vivo plaque formation on implant materials, *Int. J. Oral Maxillofac. Implants.* 4 (1989) 321–326.
- [52] L.E. Wolinsky, P.M. de Camargo, J.C. Erard, M.G. Newman, A study of in vitro attachment of *Streptococcus sanguis* and *Actinomyces viscosus* to saliva-treated titanium., *Int. J. Oral Maxillofac. Implants.* 4 (1989) 27–31.
- [53] C.M.L. Bollen, M. Quirynen, Microbiological response to mechanical treatment in combination with adjunctive therapy. A review of the literature, *J. Periodontol.* 67 (1996) 1143–1158. doi:10.1902/jop.1996.67.11.1143.
- [54] C. Ferreira Ribeiro, K. Cogo-Müller, G.C. Franco, L.R. Silva-Concílio, M. Sampaio Campos, S. de Mello Rode, A.C. Claro Neves, Initial oral biofilm formation on titanium implants with different surface treatments: an in vivo study, *Arch. Oral Biol.* 69 (2016) 33–

39. doi:10.1016/j.archoralbio.2016.05.006.

[55] T. Albrektsson, D. Buser, S.T. Chen, D. Cochran, H. Debruyne, T. Jemt, S. Koka, M. Nevins, L. Sennerby, M. Simion, T.D. Taylor, A. Wennerberg, Statements from the Estepona Consensus Meeting on Peri-implantitis, February 2-4, 2012, *Clin. Implant. Dent. Relat. Res.* 14 (2012) 781–782. doi:10.1111/cid.12017.

[56] H.H. Huang, In situ surface electrochemical characterizations of Ti and Ti-6Al-4V alloy cultured with osteoblast-like cells, *Biochem. Biophys. Res. Commun.* 314 (2004) 787–792. doi:10.1016/j.bbrc.2003.12.173.

[57] J.I. Rosales-Leal, M.A. Rodríguez-Valverde, G. Mazzaglia, P.J. Ramón-Torregrosa, L. Díaz-Rodríguez, O. García-Martínez, M. Vallecillo-Capilla, C. Ruiz, M.A. Cabrerizo-Vílchez, Effect of roughness, wettability and morphology of engineered titanium surfaces on osteoblast-like cell adhesion, *Colloids Surf. A Physicochem. Eng. Asp.* 365 (2010) 222–229. doi:10.1016/j.colsurfa.2009.12.017.

2.2 ARTIGO: β -Ta₂O₅ thin film for implant surface modification triggers superior anti-corrosion performance and cytocompatibility of titanium[#]

Thamara Beline^{a,b}, Amanda B. de Almeida^a, Nilton F. Azevedo Neto^c, Adaias O. Matos^{a,b}, Antônio P. Ricomini-Filho^d, Cortino Sukotjo^e, Paul J. M. Smeets^{f,g}, José H. D. da Silva^c, Francisco H. Nociti Jr.^a, Valentim A. R. Barão^{a,b}

^a *University of Campinas (UNICAMP), Piracicaba Dental School, Department of Prosthodontics and Periodontics, Av. Limeira, 901, Piracicaba, São Paulo, Brazil, 13414-903*

^b *Institute of Biomaterials, Tribocorrosion and Nanomedicine (IBTN), Brazil*

^c *São Paulo State University (UNESP), School of Sciences, Department of Physics, Av. Eng. Luís Edmundo C. Coube, 14-01, Bauru, São Paulo, Brazil, 17033-360*

^d *University of Campinas (UNICAMP), Piracicaba Dental School, Department of Physiological Science, Av. Limeira, 901, Piracicaba, São Paulo, Brazil, 13414-903*

^e *University of Illinois at Chicago, College of Dentistry, Department of Restorative Dentistry, 801 S. Paulina, Chicago, Illinois, USA, 60612*

^f *Department of Materials Science and Engineering, Northwestern University, Evanston, Illinois, USA, 60208*

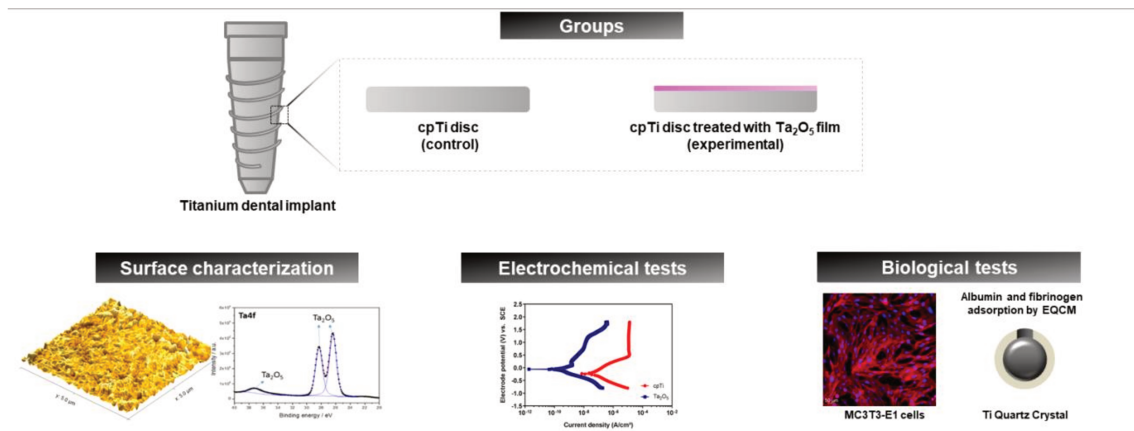
^g *NUANCE Center, Northwestern University, Evanston, Illinois, USA, 60208*

* Corresponding author.

E-mail address: vbarao@unicamp.br (V. Barão).

[#]Artigo publicado no periódico Applied Surface Science (IF = 5.155): T. Beline, A.B. de Almeida, N.F. Azevedo Neto, A.O. Matos, A.P. Ricomini-Filho, C. Sukotjo, P.J.M. Smeets, J.H.D. da Silva, F.H. Nociti Jr., V.A.R. Barão, β -Ta₂O₅ thin film for implant surface modification triggers superior anti-corrosion performance and cytocompatibility of titanium, Applied Surface Science (2020), doi: <https://doi.org/10.1016/j.apsusc.2020.146326>.

Graphical Abstract



Highlights

- Tantalum oxide film was capable to enhance the surface properties of titanium.
- The electrochemical behavior of titanium was improved by tantalum oxide film.
- Tantalum oxide film presented higher osteogenic gene expression levels showing more favorable cellular response.
- Tantalum oxide film showed greater ability to form hydroxyapatite crystals.

ABSTRACT

In this study, β -tantalum oxide (β -Ta₂O₅) thin film was synthesized via magnetron sputtering to improve the surface properties, cytocompatibility and electrochemical stability of titanium. X-ray diffraction analysis confirmed a crystalline orthorhombic phase of Ta₂O₅ film on the β -Ta₂O₅ experimental surface. A granular structure with a complex and hierarchical nature was demonstrated by atomic force microscopy. Ta₂O₅-treated surfaces exhibited greater roughness and hydrophilicity compared with untreated titanium discs (control). Enhanced electrochemical stability in simulated body fluid (pH 7.4) was noted for Ta₂O₅-treated surfaces wherein higher values of charge transfer resistance, nobler corrosion potential, and lower capacitance, corrosion current density, and corrosion rate values were observed vs untreated control. Real-time monitoring of albumin and fibrinogen protein adsorption by an electrochemical quartz crystal microbalance disclosed similar protein interactions for control and Ta₂O₅-treated discs, with higher fibrinogen adsorption rates for Ta₂O₅-treated surfaces. Cell culture assays (MC3T3-E1 cells) demonstrated that Ta₂O₅-treated discs featured greater *in vitro* mineral nodule formation, normal cell morphology and spreading, and increased mRNA levels of runt-related transcription factor 2 (*Runx-2*), osteocalcin (*Ocn*), and collagen-1 (*Col-1*). Therefore, it can be concluded that β -Ta₂O₅ thin films may be considered a promising strategy to trigger superior long-term stability and biological properties of titanium implants.

Keywords:

Dental implants

Corrosion

Magnetron sputtering

Tantalum oxide

Protein adsorption

Biomaterials

1. Introduction

Titanium (Ti) is one of the materials of choice as a permanent biomaterial, particularly for dental and orthopedic applications, due to its favorable characteristics related to mechanical strength, cytocompatibility, chemical stability, and corrosion resistance [1]. Ti is a highly reactive metal likely to undergo oxidation [1,2]. Thus, the formation, on Ti surfaces exposed to air or water, of a protective thin oxide layer consisting of titanium dioxide (TiO_2) provides corrosion resistance [3]. However, no metal or metal alloy is considered entirely inert in the biological environment [4], since the nature, thickness, and composition of the protective oxide layer on Ti surfaces may be affected by environmental conditions [5]. Previous studies have shown that the electrochemical behavior of Ti is negatively affected by exposure to saliva, fluorides, acid attack, microbial components, H_2O_2 , nicotine, and metabolites from bacteria [6–13].

The corrosion process may result in ion release into the biological environment [14]. The presence of metal ions released from corrosion events is associated with peri-implant sites [15]. High amounts of dissolved Ti around implants with peri-implantitis were found when compared with healthy implants [15], revealing that Ti ion release from implant surfaces during the corrosion process is linked to peri-implantitis. In addition, the corrosion of Ti may affect its resistance to fatigue, compromising implant mechanical stability [16] and leading to treatment failure. Such facts emphasize the need for the development of alternative materials.

In this framework, tantalum (Ta) has attracted attention as a new alternative biomaterial because of its high bioactivity and superior corrosion resistance compared with that of Ti in harsh environments [17,18]. Such good cytocompatibility and corrosion resistance of Ta can be associated with the formation of a high-stability, self-passivating tantalum pentoxide (Ta_2O_5) on the surface [19]. However, in the form of a bulk material, the high cost and density of Ta implants restrict their use. Moreover, another issue to be considered relative to its use as a biomedical device is the high melting temperature of bulk Ta (~ 3017 °C) [18]. Therefore, Ta and Ta_2O_5 coatings have been deposited on different materials to improve their surface properties. The biocompatibility, bioinertness, corrosion and abrasion resistance makes Ta_2O_5 a suitable alternative for using as a protective coating in biomedical devices [20–22]. Despite presenting the aforementioned characteristics, pure Ta coatings do not have satisfactory wear resistance [23].

Among all the methods available for the deposition of Ta_2O_5 films [18,24], magnetron sputtering is a versatile technique well-known to produce uniform film growth and

films with excellent adhesion to the substrate [25], which makes this technique interesting in terms of corrosion protection. Additionally, the films can be deposited at relatively high purity and low cost [26]. Our previous study tailored the deposition parameters of magnetron sputtering to synthesize Ta_xO_y films onto commercially pure titanium (cpTi) surfaces [27]. A crystalline β - Ta_2O_5 film appears to be more suitable for biomedical applications [27]. However, there is limited understanding of the chemical degradation of β - Ta_2O_5 films in simulated oral conditions. Additionally, no study has evaluated real-time protein/ β - Ta_2O_5 film interactions, which is crucial since protein adsorption is one of the first biological responses in the human body to trigger a manifold of biological processes [28].

Thus, to improve the electrochemical stability and cytocompatibility of cpTi, we deposited Ta_2O_5 films onto cpTi surfaces by means of a magnetron reactive sputtering deposition technique. The aims of this study were (1) to characterize the physical and chemical properties of the Ta_2O_5 film, (2) to evaluate the role of the Ta_2O_5 film in the electrochemical behavior of cpTi, (3) to investigate the real-time adsorption of albumin and fibrinogen onto the cpTi surfaces, and (4) to evaluate the cellular responses and gene expression of pre-osteoblastic cells (MC3T3-E1) cultured on modified cpTi surfaces.

2. Materials and methods

2.1. Sample preparation

CpTi grade II samples, 2 mm in thickness and 15 mm in diameter (Mac-Master Carr, USA) were ground with SiC grinding paper (#320, #400, and #600) (Carbimet 2; Buehler, USA), and polished initially using a polishing cloth (Satyn MB; Buehler) with a 9- μ m aqueous polycrystalline diamond suspension (MetaDi Supreme; Buehler) and subsequently with colloidal silica suspension and polishing disc (Chemio MB; Buehler). Finally, samples were cleaned in an ultrasonic bath with deionized water (10 min), acetone (10 min), and isopropyl alcohol (10 min) and air-dried.

2.2. Deposition of Ta_2O_5 films by magnetron sputtering

A radiofrequency (RF) magnetron sputtering system (Kurt J. Lesker Company, USA) was used for Ta_2O_5 films deposition. The deposition was conducted in an Ar + O_2 atmosphere (Ar/ O_2 ratio = 2.5). Before each deposition process, the metallic Ta target (3" in diameter and 99.95% purity) (Kurt J. Lesker Company) surface was plasma cleaned during 5 minutes in an Ar atmosphere at 7.5×10^{-3} Torr and 100 W power to eliminate contaminants

from the target surface. Base pressure lower than 5.0×10^{-6} Torr was considered appropriate to initiate the deposition in the chamber [29]. Next, the oxide films were deposited on heated cpTi discs and on quartz slabs in separate deposition cycles. While Ti substrates were heated at 600 °C, the quartz slabs used in the quartz crystal monitor were heated at 500 °C. According to the manufacturer, the quartz crystal slabs must be subjected to temperatures below 532 °C in order to prevent deterioration of the piezoelectric properties. A K-type thermocouple wire was used for substrate temperature measurements during the deposition. The deposition parameters used were based on results from our previous study [27]. The atmosphere was composed of O₂ (8 sccm) and Ar (20 sccm), the bias voltage and the process power were kept constant at -164 V and 400 W RF, while the working pressure was 6.0×10^{-3} Torr. The deposition process was conducted for 67 min.

2.3. Surface characterization

2.3.1. X-ray diffraction (XRD) analysis

X-ray diffractometry (XRD - X'Pert³ PRO MRD; PANalytical, The Netherlands) was used to investigate the structural properties of the film, with a θ -2 θ configuration in the 20° to 80° range with a step size of 0.01° and CuK α ($\lambda = 1.54056$ Å) radiation.

2.3.2. Atomic force microscopy (AFM)

AFM (Park NX10; Park System, USA) analysis was performed to evaluate the 3D surface topography of different cpTi surfaces. Images of 5 $\mu\text{m} \times 5 \mu\text{m}$ were obtained in tapping mode with a constant force and frequency of 42 N/m and 320 kHz, respectively. Two different areas were used to obtain the roughness (Ra) values, and Gwyddion software (GNU General Public License, Czech Republic) was used to calculate the estimated surface area of the samples.

2.3.3. Surface energy

Surface energy measurements were performed using a goniometer (Ramé-Hart 100-00; Ramé-Hart Instrument Co., USA) which included deionized water (polar component) and diiodomethane (dispersive component) (2 μL), following the previous protocol suggested by Combe et al. [30]. To ensure reproducibility, the test was conducted at least five times.

2.3.4. X-ray photoelectron spectroscopy (XPS)

To obtain the chemical composition of the oxide layer of cpTi and Ta₂O₅ substrates, XPS analysis was carried out. A spectrometer (K-Alpha X-ray XPS; Thermo Scientific, Finland) with a hemispheric analyzer was operated with energy step at 0.100 eV and spot size at 400 μm [6].

2.3.5. Cross-sectional analysis using a Focused Ion Beam-Scanning Electron Microscope (FIB-SEM)

A polished cpTi disc including the deposited magnetron sputtered Ta₂O₅ film was affixed onto a 45° aluminum SEM pin stub specimen mount (Ted Pella, Inc., USA) using double-sided conductive carbon tape. A dual-beam FIB-SEM (FEI Helios Nanolab 600; Thermo Fisher Scientific, USA) with a gallium liquid metal ion source (LMIS) operating at an accelerating voltage of 30 kV was used to prepare cross-sections of the Ta₂O₅ film and underlying Ti substrate. At the center of the disc, primarily a ~50 nm layer of protective platinum was deposited on a 2 μm × 20 μm (length × width) area of interest using the electron beam (5 kV, 1.4 nA) through decomposition of a (methylcyclopentadienyl)-trimethyl platinum precursor gas (FEI Helios Nanolab 600; Thermo Fisher Scientific). Directly on top of this, a ~1.0 μm thick protective platinum layer was deposited using the ion beam (30 kV, 93 pA) through decomposition of the same precursor gas. Subsequently, a several micrometer deep trench was cut directly adjacent to the area of interest using the ion beam. Next, the cross-section was cleaned up at a voltage of 30 kV and a current of 0.92 nA until approximately halfway down the length of the area of interest. The sample was then tilted to observe the cross-section using the electron beam at an incident angle of 45° using an Elstar UHR immersion lens for high resolution imaging. The final thickness assessment of the Ta₂O₅ layer was performed using line profiles (taking into account the appropriate tilt correction) using the xT microscope Control software (FEI Helios Nanolab 600; Thermo Fisher Scientific).

2.4. Electrochemical assay

A potentiostat (Interface 1000; Gamry Instruments, USA) was used for the corrosion assessment. A three-electrode cell standardized method was used in conformity with the American Society for Testing of Materials (G61 86 and G31 72). The exposed surface of cpTi sample was used as the working electrode, a graphite rod as the counter electrode and a saturated calomel electrode (SCE) as the reference electrode. AFM analysis was performed to estimate the exposed surface area of the two groups (cpTi = 1.77 cm²;

Ta₂O₅ = 7.06 cm²). For the simulation of the oral conditions (blood plasma), simulated body fluid (SBF) was used at 37° C and pH 7.4 as electrolyte solution [31]. Prior to the tests, a cathodic potential (-0.9 V vs SCE) was applied for 600 s. Subsequently, the Open Circuit Potential (OCP) was scanned for 3600 s followed by the electrochemical impedance spectroscopy (EIS) measurements [32]. Such data were used to estimate the real (Z_{real}) and imaginary (Z_{imag}) components of the impedance, which were presented as Nyquist plot, impedance ($|Z|$) and phase angle [6]. For quantifying the electrochemical kinetics, including corrosion resistance (R_p), charge transfer resistance (R_{ct}), and constant phase element (Q_{dl}), an equivalent electrical circuit was used. Subsequently, the polarization of the specimens were conducted from -0.8 V to 1.8 V (2 mV/s scan rate) [33,34]. A Tafel extrapolation method was used to determine the polarization curves, which provided the electrochemical variables corrosion potential (E_{corr}), corrosion current density (I_{corr}), and corrosion rate. All measurements were performed at least five times to guarantee reproducibility and reliability.

2.5. Biological assessments

2.5.1. Real-time monitoring of protein adsorption by EQCM

To understand how the proteins interacted with the modified Ti surfaces, we monitored the adsorption of albumin and fibrinogen using the EQCM device (eQCM 10M; Gamry Instruments). For this purpose, a 5 MHz quartz crystal (Gamry Instruments) covered with Ti (control) and a 5 MHz quartz crystal treated with a Ta₂O₅ film (experimental) were used. To ensure reproducibility, the tests were performed at least three times. Prior to the tests, the quartz crystal specimens were carefully cleaned with copious deionized water and propanol, and subsequently air-dried. The albumin (Sigma–Aldrich, USA) solution was prepared by dissolution in phosphate-buffered saline (PBS) (Gibco, Life Technologies, USA) (1 mg/mL). Fibrinogen (Sigma–Aldrich) solution was produced by dissolution in 0.9% NaCl (1 mg/mL). The quartz crystal sample was coupled in the EQCM device containing 6.5 mL of PBS or 0.9% NaCl, depending on the protein used in the test. After 30 min (1800 s) of system stabilization, a 500- μ L quantity of albumin or fibrinogen solution was inserted into the system, and the real-time protein adsorption kinetic was monitored for 2 h and 30 min by means of Gamry Resonator software (Gamry Instruments) at ambient temperature (25 °C). The QCM frequency shifts (Δf_s) were related to the mass change (ΔM) per unit area on the surface of the working electrode (quartz crystal) according to the Sauerbrey equation (1959) [35]:

$$\Delta f_s = \frac{-2nf_1^2 \Delta M}{Z_q}$$

Where n is the order of the measured harmonic (3), f_1 is the fundamental frequency (5 MHz) and Z_q is the theoretical acoustic impedance of quartz ($8.84 \times 10^6 \text{ kg m}^{-2} \text{ s}^{-1}$). Thus, the adsorption of protein was calculated by means of the ΔM on the quartz crystal surface as a function of time. Then, the following variables were calculated: ΔM (μg), adsorption rate (ng/s), mass loss (μg), and effective mass gain (μg). For the calculation of ΔM (μg), the maximum value of protein adsorption reached during the test was subtracted from the adsorption value obtained at 1800 s (point of final stabilization of the system, when the protein was inserted). The adsorption rate (ng/s) was determined by means of the division of ΔM by the difference between the initial time (1800 s) and the time where the maximum adsorption value was reached during the test. The mass loss was estimated by the difference between the maximum adsorption value and the adsorption value at the end of the analysis (10,800 s). Finally, the effective mass gain (μg) was determined by the difference between ΔM and mass loss values.

2.5.2. Cell culture

Pre-osteoblastic MC3T3-E1 cells were cultivated in Alpha MEM (Gibco, Life Technologies, USA) supplemented with penicillin (100 U/mL), streptomycin (100 mg/mL) and 10% fetal bovine serum (FBS) (Gibco), at 5% CO_2 atmosphere conditions and 37 °C. After reaching confluence, trypsin-ethylenediaminetetraacetic acid (Gibco) was used to detach the cells. Next, the cells were re-suspended in culture medium for seeding onto the samples.

2.5.3. MTT assay

Cellular metabolic activity on experimental and control surfaces was determined at 1, 2, and 4 days by MTT 3-(4,5-dimethylthiazol-2-yl)-2,5-diphenyltetrazolium bromide analysis. After the experimental periods, the culture medium was replaced by α -MEM with MTT (5 mg/mL) (Gibco) at 37 °C and 5% CO_2 atmosphere conditions for 4 h following the manufacturer's recommendation. Subsequently, dimethyl sulfoxide (Sigma-Aldrich) was used to dissolve the formazan crystals. Next, the optical density was verified (VersaMax; Molecular Devices, USA) at a 570 nm wavelength [36]. The tests were performed in triplicate to guarantee reproducibility.

2.5.4. Scanning electron microscopy (SEM) analysis

To analyze the effects of untreated control and experimental surfaces on cell morphology, pre-osteoblastic MC3T3-E1 cells were plated in duplicate at 1.5×10^4 cells/mL in 24-well culture plates containing α -MEM supplemented with antibiotics and 10% FBS, for 24 h in order to allow cell adhesion onto the specimen surface. Next, the medium was replaced by α -MEM supplemented with antibiotics plus 2% FBS (day 0), which was replaced daily until the end of each experimental period. Cell morphology and spreading were verified by SEM analysis after 1, 2, and 4 days. Briefly, cells were fixed with Karnovsky's solution at 4 °C for 12 h and subsequently fixed in 1% osmium tetroxide for 1 h at room temperature. Next, cells were dehydrated in ethanol (35, 50, 70, 90, and 100%) at 25 °C for 10 min, critical-point dried (mod. DCP-1; Denton Vacuum, USA) and sputtered with gold (mod. SCD 050; Bal-Tec, USA) [27,37].

2.5.5. Fluorescence analysis

The cell morphology was further determined by confocal imaging (LSM 800; Carl Zeiss, Germany) after 1 and 2 days. For confocal imaging, MC3T3-E1 cells were plated at a density of 1.5×10^4 cells/mL in 24-well cell culture plates, washed in PBS, fixed for 30 min with 4% formaldehyde, and permeabilized for 10 min in 0.01% Triton X100 in PBS. ActinRedTM 555 ReadyProbes[®] Reagent (Molecular Probes, USA) was used for the cell cytoskeleton staining (25 min), and Hoechst (Thermo Fisher Scientific, USA) for the nucleus staining (10 min). The specimens were then twice washed in PBS before undergoing confocal microscopic analysis.

2.5.6. Mineralization analysis by Alizarin Red staining

Mineral nodule formation was quantitatively assessed by the Alizarin Red assay at 4, 7, and 14 days of incubation in Alpha MEM plus antibiotics either supplemented with or without 100 nM dexamethasone, 0.05 mM L-ascorbic acid and 10 mM β -glycerophosphate disodium salt hydrate, allowing osteoblastic cell differentiation in an atmosphere of 5% CO₂ and 37 °C conditions. After the experimental periods, the fixation process of the cells in 70% ethanol was conducted for 60 min. NanoPure water (Resistivity of 18.2 M Ω .cm at 25 °C) was used to remove the ethanol and next, the cells were stained with Alizarin Red solution (AR-S) at 37 °C for 10 min. Subsequently, cells were immersed five times in NanoPure solution to remove the AR-S not bound to the cells/matrix, and a 600- μ L quantity of PBS was added to each well under stirring for 15 min to reduce non-specific staining. Next, cetylpyridinium

chloride at 10% was used to maximize the elution of AR-S staining for 30 min. Finally, a 100- μ L quantity of the solution from each sample was transferred to a 96-well plate in triplicate for the absorbance reading of the solution by spectrophotometry (562 nm) [38]. To ensure reliability, the tests were performed in triplicate.

2.5.7. Quantitative reverse transcriptase real-time polymerase chain reaction analysis (rtqPCR)

To analyze mRNA levels of osteogenic markers, we cultured pre-osteoblastic MC3T3-E1 cells onto untreated control and modified cpTi discs and analyzed qPCR reactions. Cells were cultured for 1, 2, and 3 days in an α -MEM supplemented with 100 nM dexamethasone, 0.05 mM L-ascorbic acid and 10 mM β -glycerophosphate disodium salt hydrate, allowing osteoblastic cell differentiation. Total RNA was obtained by means of RNeasy Plus Mini Kit (Qiagen Sciences, USA), a commercially available system as recommended by the manufacturer. RNA concentration and quality were assessed by spectrophotometry (Nanodrop 1000; Thermo Scientific), and cDNA was obtained by means of a RT2 First Strand Kit for reverse transcription polymerase chain reaction (Qiagen Sciences). qPCR reactions were performed by means of the FastStart Universal SYBR Green Master (Roche Diagnostics GmbH, Germany) and LightCycler[®] 480 instrument (Roche Diagnostics GmbH). Transcript levels for runt-related transcription factor 2 (*Runx-2*), alkaline phosphatase (*Alpl*), osteocalcin (*Ocn*), and Collagen-1 (*Col-1*) were obtained and normalized by β -actin mRNA levels (Table 1). All the tests were performed in triplicate.

Table 1

Primer sequences for the assessed genes.

Genes		Primer Sequences (3' to 5')
<i>Runx-2</i>	Forward	<i>cgtgtcagcaaagcttctttt</i>
	Reverse	<i>ggctcacgtcgctcatct</i>
<i>Alpl</i>	Forward	<i>ggggacatgcagtatgagtt</i>
	Reverse	<i>ggcctggtagttgttgag</i>
<i>Ocn</i>	Forward	<i>tgaacagactccggcg</i>
	Reverse	<i>gataccgtagatgcgtttg</i>
<i>Col-1</i>	Forward	<i>gaggccaagacgaagacatc</i>
	Reverse	<i>cagatcacgtcatcgcacaaac</i>
<i>β-actin</i>	Forward	<i>ctaaggccaaccgtgaaaag</i>
	Reverse	<i>accagaggcatacagggaca</i>

2.5.8. Bioactivity test

For the bioactivity test, untreated control and experimental surfaces were immersed in SBF solution at 37 °C for 14 days in a plastic tube following the protocol suggested by Kokubo *et al.* [39]. The volume of SBF was estimated in agreement with the following formula: $V_{\text{SBF}} = S_a/10$, where V_{SBF} is the volume of SBF (unit: mL) and S_a is the surface area of the specimen (unit: mm²). After 14 days, the discs were washed with distilled water and air dried. The XRD test was conducted to investigate the presence of apatite crystals on the specimen [39].

2.6. Statistical analysis

IBM SPSS Statistics for Windows (IBM SPSS Statistics for Windows, v.21.0, IBM Corp., USA) was used to evaluate the data. The comparison of surface roughness, surface energy, corrosion data (R_p/R_{ct} , Q , E_{corr} , I_{corr} , and corrosion rate), EQCM data (ΔM , adsorption rate, mass loss, and effective mass gain) between cpTi and Ta₂O₅-coated samples were conducted with an independent t-test. A 2-way ANOVA test (factor 1, surface type in 2 levels; factor 2, days in 3 levels) and the Tukey Honestly Significant Difference (HSD) test for post hoc comparisons were used to analyze the cell metabolism (MTT) data. Calcium ion concentration results were evaluated with 3-way ANOVA (factor 1, surface type in 2 levels; factor 2, days in 3 levels; factor 3, culture medium conditions in 2 levels) for investigation of the impact of surface treatment, days, and non-osteogenic (control) or osteogenic medium conditions and their interaction on calcium ion concentration levels. The Tukey HSD test was used as a post hoc technique when needed. For qRT-PCR test, data were analyzed by Kruskal-

Wallis test for investigation of the influence of the surface treatment on *Runx-2*, *Alpl*, *Ocn* and *Col-1* expression. To compare the groups in pairs, the Mann-Whitney U test was used ($r > 0.82$). The p value, which is defined as the probability of observing the given value of the statistic test, or greater, under the null hypothesis, was considered statistically significant when <0.05 . This guarantee that the probability of error is below 5%.

3. Results and discussion

3.1. Structural analysis, surface topography, and surface energy

The X-ray diffraction patterns of control (cpTi substrate) and experimental (Ta_2O_5) groups are displayed in Fig. 1. Both groups presented diffraction peaks equivalent to metallic Ti. Such behavior is explained due to the penetration depth of Cu-K_α radiation ($\sim 10 \mu\text{m}$), which is higher than the film thickness ($\sim 600 \text{ nm}$) [40]. Additionally, the diffraction peaks at 27.5° , 49.0° and 70.6° found in the Ta_2O_5 group appoint to the presence of the crystalline orthorhombic structure of the Ta_2O_5 film (ICDD cards numbers 89-2843 and 79-1375), which can also be referred to as $\beta\text{-Ta}_2\text{O}_5$ [41].

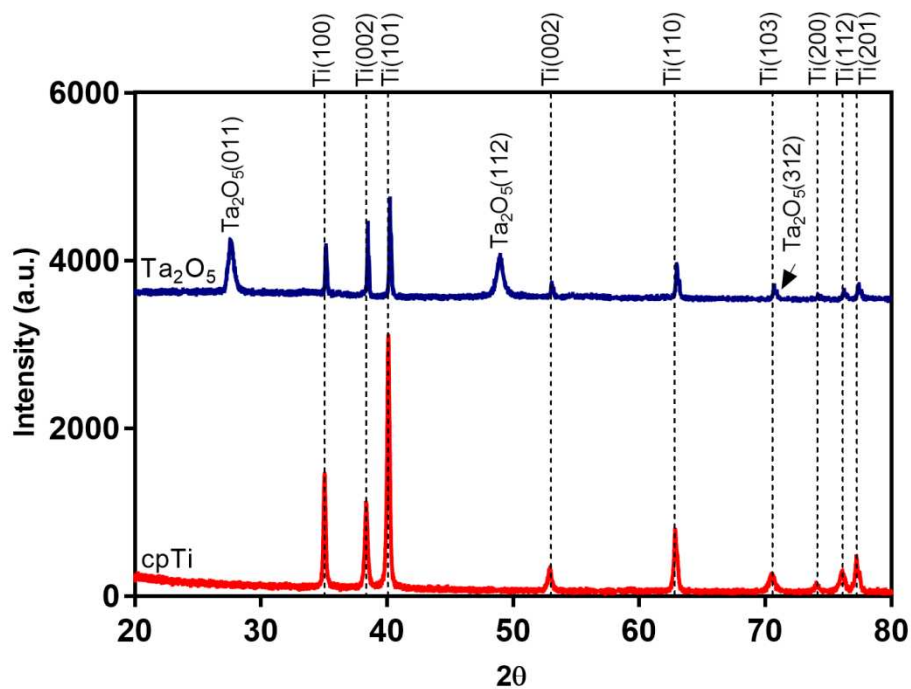


Fig. 1. X-ray diffraction patterns obtained from the cpTi substrate (red pattern) and the Ta_2O_5 film deposited on cpTi surfaces (blue pattern).

The surface topography is well known for playing an essential role in cytocompatibility, being considered crucial for biological applications [42]. The morphology and topography of the cpTi substrate and the Ta₂O₅ film deposited on cpTi surfaces obtained from AFM analysis are shown in Fig. 2. The surface treatment with Ta₂O₅ films evidently modified the surface topography of the cpTi substrates, showing a granular structure with a complex and hierarchical nature. In contrast, the polished cpTi group exhibited smooth and flat surfaces. In the 3D profile, a greater Ra value (mean \pm standard deviation) can be observed for the Ta₂O₅ group (Ra = 12.47 \pm 1.96 nm), while the control group exhibited the lowest value (Ra = 3.68 \pm 0.64 nm). It has been showed that cell adhesion was significantly improved in surfaces with nanoscale patterns when compared with cells cultivated on surfaces with microscale patterns [43].

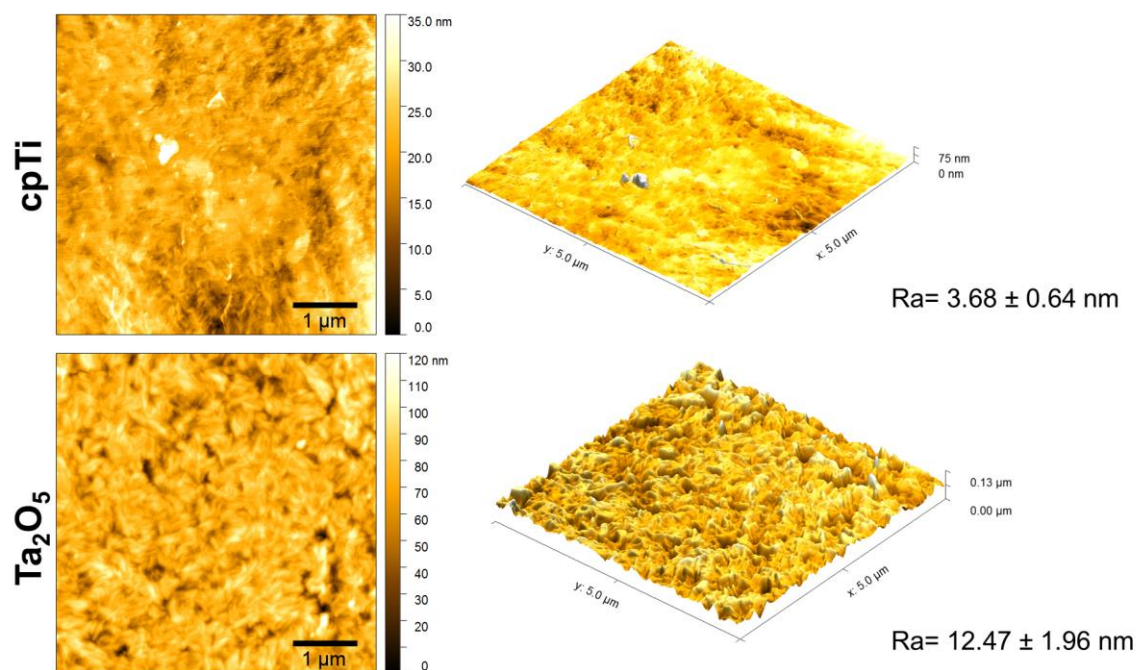


Fig. 2. AFM 2D and 3D images obtained from the cpTi substrate and Ta₂O₅ film deposited on cpTi surfaces (scale bar = 1 μ m).

In addition to surface roughness, another important factor with respect to the surface properties of a biomaterial is surface energy, which controls the contact area of the substrate with the cell membrane [44]. Fig. 3 shows the surface energy values for all groups. Higher surface energy values were found for the Ta₂O₅ group when compared with cpTi, which indicates a hydrophilic tendency of the Ta₂O₅ group. It was reported that hydrophilic surfaces positively impact on the attachment and spreading of osteoblasts [45].

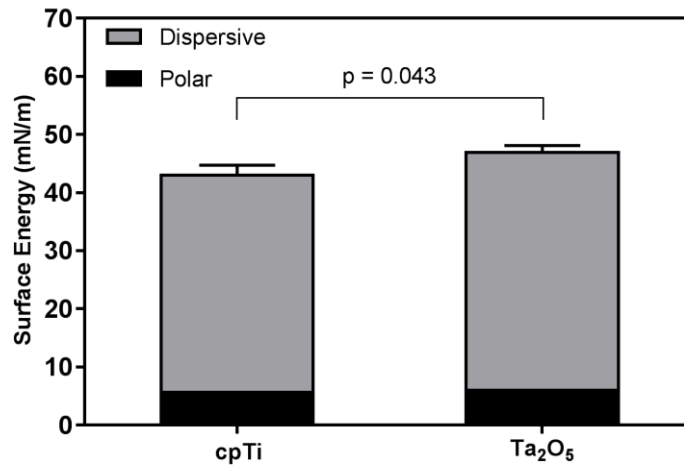


Fig. 3. Surface energy for control cpTi and Ta₂O₅ surfaces. Intergroup difference (cpTi vs Ta₂O₅) is illustrated by the p-value.

3.2. Surface chemistry characterization

Fig. 4 shows the high-resolution spectra of control and Ta₂O₅ groups obtained from XPS analysis. In the Ti 2p spectrum, doublets can be seen at 464.70 and 459.20 eV, corresponding to the Ti 2p_{1/2} and Ti 2p_{3/2} bands, respectively (Fig. 4a). These peaks values are related to TiO₂ [46,47]. The energy peaks found in the O 1s spectrum of the control group (Fig. 4b) also correspond to TiO₂. In the Ta 4f spectrum (Fig. 4c), the energy peaks found are related to the formation of Ta₂O₅, corroborating results from previous studies [48,49]. Two peaks can be observed in the O 1s spectrum of the Ta₂O₅ group (Fig. 4d), wherein the 530.00 eV energy is appointed to Ta-O binding, constituting tantalum oxides [49,50], and the binding energy of 531.90 eV is related to oxygen in the form of a hydroxide or to adsorbed oxygen species [49,51].

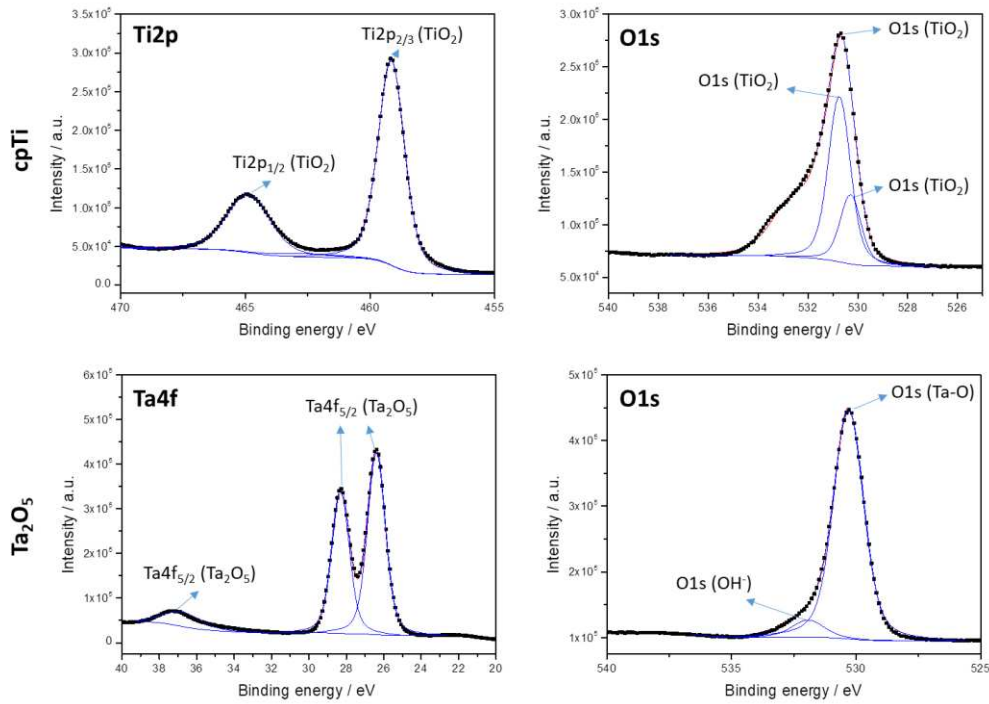


Fig. 4. X-ray photoelectron spectroscopy (XPS) spectra of (a) Ti2p and (b) O1s for the control cpTi substrate and (c) Ta4f and (d) O1s for the Ta₂O₅ film deposited on cpTi surfaces.

Cross-sectional analysis of the Ta₂O₅ thin film deposited onto the cpTi substrate by means of FIB-SEM is shown in Fig. 5. The film appears homogeneously deposited and compact (Fig. 5), with rarely displaying some pores in between the substrate and film (Fig. S1). The film thickness was measured to be approximately 600 nm.

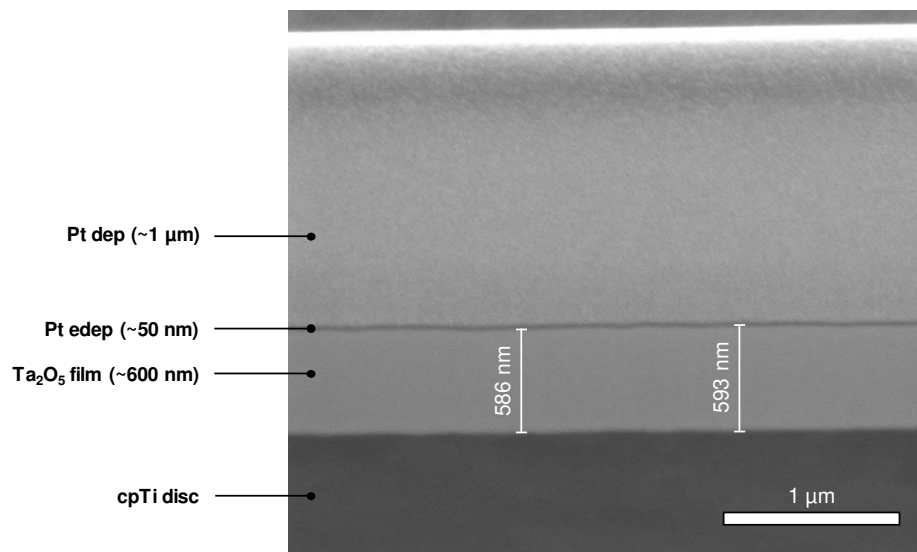


Fig. 5. Cross-sectional FIB-SEM micrograph of the Ta₂O₅ thin film deposited onto the cpTi substrate. Platinum (Pt) was deposited on the cross-section area of interest initially using the

electron beam (Pt edep) and subsequently using the ion beam (Pt dep) to protect the film from exposure to the ion beam during cross-sectional milling.

3.3. Surface electrochemistry characterization

The evolution of OCP as a function of time (s) for the cpTi substrate and the cpTi covered with the Ta₂O₅ film is shown in Fig. 6. The Ta₂O₅ group showed the most positive values of OCP compared with the control group. It is known that better corrosion behavior is associated with more positive OCP values. Considering this, these data may appoint to improvement of the electrochemical resistance of the Ta₂O₅ surface treatment.

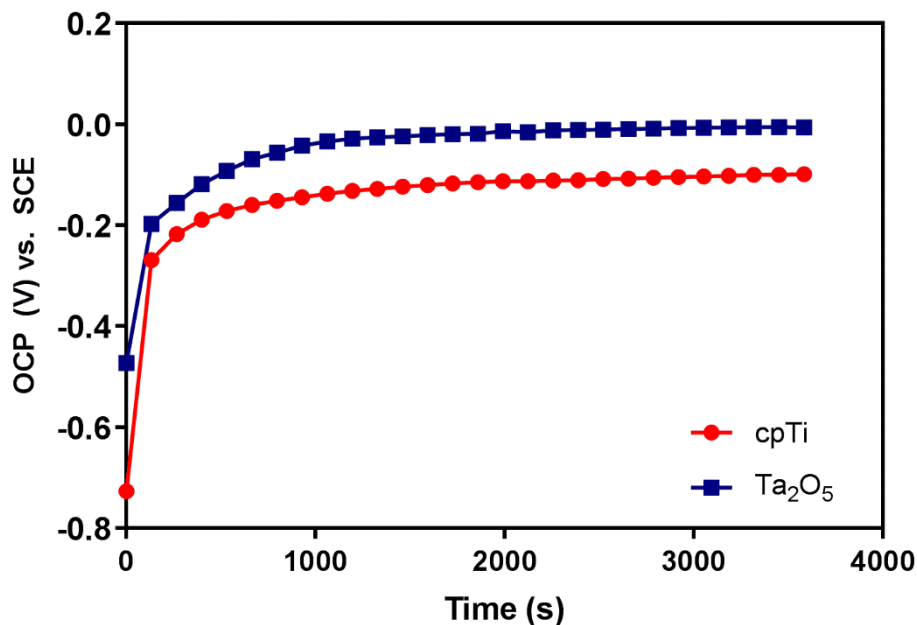


Fig. 6. Representative curve of OCP evolution (in V vs SCE) for control cpTi (red curve) and Ta₂O₅ (blue curve) surfaces exposed to SBF solution for 3600 s.

The Nyquist plot represents the evolution of resultant impedance as a function of Z_{real} and Z_{imag} components (Fig. 7a). It has been well-established that a decrease in the diameter of the semicircular loop indicates a reduction in passive film resistance [52]. The control group exhibited a decrease in the semicircular diameter (on the order of 10^5). For the Ta₂O₅ group, the semicircular diameter of the capacitance loop was on the order of 10^8 , indicating improved corrosion resistance. The variation in impedance as a function of frequency was provided by Bode plots (Fig. 7b). Greater total impedance values can be seen for Ta₂O₅-treated surfaces. Such behavior indicates that this group has superior electrochemical resistance, since high impedance values at low frequencies suggest the

formation of a highly stable oxide film on the surface. The phase angles of the Ta₂O₅-coated samples are slightly higher than those observed for cpTi samples (Fig. 7c), indicating an improvement of the electrochemical stability of cpTi when subjected to this treatment. In addition, it is possible to observe that both groups exhibited only one time constant. The equivalent electrical circuit used for the simulation of the electrical parameters of the surfaces is illustrated in Fig. 7d. The values of chi-square (χ^2) were on the order of 10^{-3} – 10^{-4} , indicating that the fitted data are in accordance with the experimental data. In the simplified circuit, R_s corresponds to the resistance of the solution between the reference and working electrodes, Q_{dl} is considered as the constant phase element (CPE) attributed to the electrical double layer, R_p is the resistance of the passive film (control group), and R_{ct} is the charge transfer resistance (experimental group). The use of this circuit was based on results from previous studies [49,53].

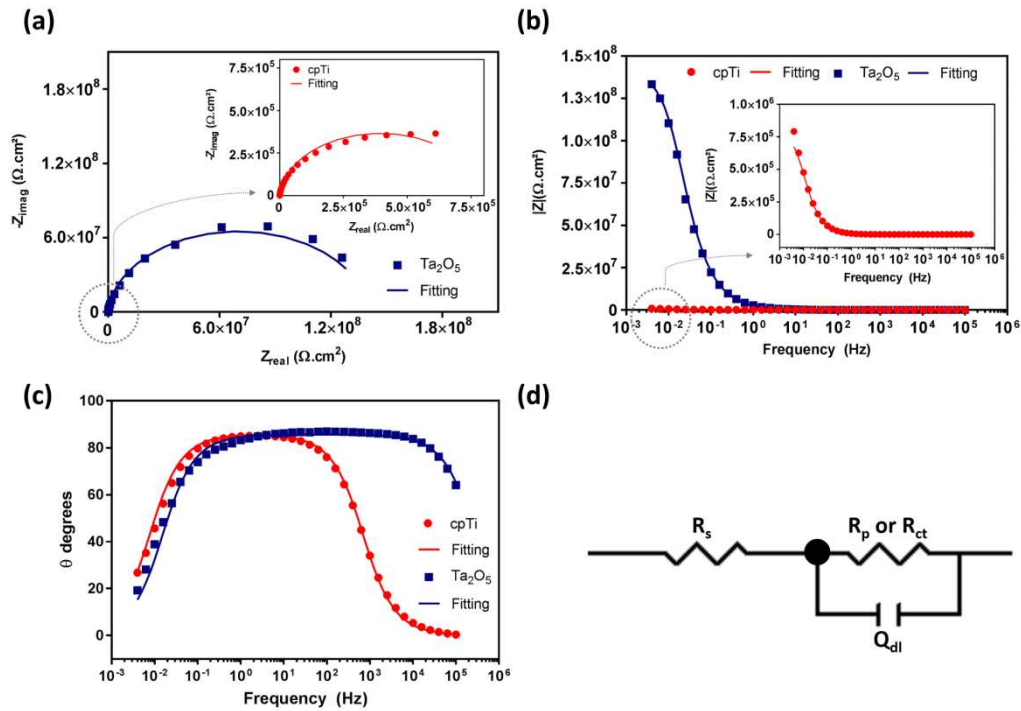


Fig. 7. Representative (a) Nyquist diagrams, (b) impedance modulus, and (c) phase angles of EIS responses for control cpTi (red curves) and Ta₂O₅ (blue curves) surfaces. Symbols represent experimental data and solid lines fitted data. Magnified graphs were plotted for better visualization. (d) Equivalent circuit used for EIS data, which shows resistance of solution (R_s) in series with a parallel combination of the constant phase element (Q_{dl}) and a charge transfer resistance (R_{ct}) or polarization resistance (R_p) of the oxide layer.

The OCP, Nyquist, and impedance data corroborates with the results of the electrochemical parameters obtained from EIS (Table 2). Higher values of resistance can be seen for the Ta₂O₅ film, while cpTi exhibited the lowest resistance values. This behavior suggests that the surface treatment is able to provide better protection against corrosion. In contrast, cpTi presented the greatest values of Q_{dl}, corroborating the corrosion resistance results. This fact supports the disadvantageous electrochemical properties of cpTi when it is exposed to SBF immersion, since higher capacitance values indicate an increase in the ionic exchange between the material and the electrolyte [6].

Table 2

Means (and standard deviations) of electrical parameters obtained from the equivalent circuit model for control cpTi and Ta₂O₅ surfaces.

Group	R _p or R _{ct} (Mohms.cm ²)	Q _{dl} (nΩ ⁻¹ S ⁿ .cm ⁻²)	n	χ ² ×10 ⁻³
cpTi	1.79 (0.35) ^a	12451.98 (1777.77) ^a	0.95 (0.01)	1.57 (1.10)
Ta ₂ O ₅	1385.34 (646.64) ^b	11.14 (3.57) ^b	0.94 (0.03)	3.38 (0.35)

Note: Intergroup difference (cpTi vs Ta₂O₅) is illustrated by the different lower-case letters. R_p is the resistance of the passive film (control cpTi group), and R_{ct} is the charge transfer resistance (Ta₂O₅ experimental group).

In the polarization curves (Fig. 8), it is possible to observe that the Ta₂O₅ group shifted the current density to lower values. When compared with the cpTi group, Ta₂O₅ shifted the curve to the upper left region of the graph, shifting the electrode potential to more positive values, which suggests a less active behavior in ion exchange of the Ta₂O₅ surface compared with cpTi.

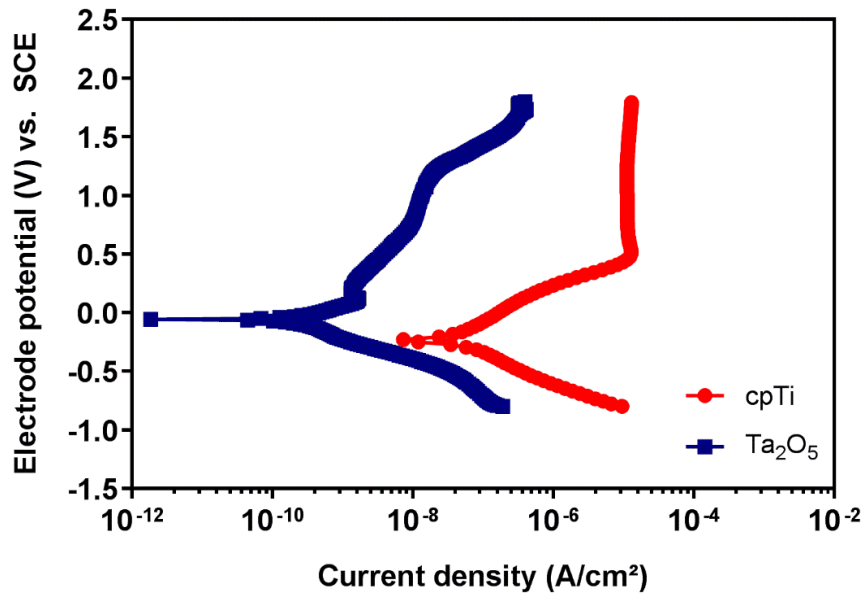


Fig. 8. Representative potentiodynamic polarization curves of control cpTi (red curve) and Ta₂O₅ (blue curve) surfaces. The electrode potential is expressed in V vs the saturated calomel electrode (SCE).

The electrochemical parameters including E_{corr} , I_{corr} , and corrosion rate are described in Table 3. I_{corr} is an electrochemical parameter that indicates the current flow at an open circuit potential as a result of oxidation or reduction reactions [54]. The results show that the Ta₂O₅ group exhibited lower I_{corr} and corrosion rate values. Such findings demonstrate that the Ta₂O₅ film deposited on cpTi surfaces provides more efficient corrosion protection for the cpTi surface, confirming its favorable electrochemical properties. Additionally, more positive/nobler E_{corr} values were observed for the Ta₂O₅ group when compared with the cpTi group.

The mechanism of the high corrosion protection of the Ta₂O₅ film may be related to its characteristics of high homogeneity and compactness as can be seen from the FIB-SEM cross-sectional analysis (Fig. 5). Such characteristics may help to reduce the penetration of ionic species through the film, leading to the mitigation of the electrochemical degradation process, explaining the excellent anti-corrosion performance of the Ta₂O₅ thin film.

Table 3

Mean (and standard deviation) values of electrochemical parameters obtained from the potentiodynamic polarization curves for control cpTi and Ta₂O₅ surfaces.

Group	E _{corr} (mV)	I _{corr} (nA/cm ²)	Corrosion rate (mpy)×10 ⁻⁴
cpTi	- 206.15 (26.21) ^a	21.93 (3.27) ^a	131.52 (63.65) ^a
Ta ₂ O ₅	- 14.01 (5.86) ^b	0.44 (0.27) ^b	2.05 (1.27) ^b

Note: Intergroup difference (cpTi vs Ta₂O₅) is illustrated by the different lower-case letters.

3.4. Real-time interplay between protein and biomaterial

The subsequent cell-biomaterial interactions are mediated by protein adsorption. The human body contains thousands of proteins, with each protein performing a set of distinct and crucial functions, essentially since they have the ability to bind to specific molecules [55]. Albumin is the most predominant protein found in blood serum (~60%) [56]. Because of its high concentration in blood plasma, albumin is extensively used in protein adsorption studies [55]. Another important protein is fibrinogen, an abundant glycoprotein in blood plasma, involved in the blood coagulation process [55,57]. The previous literature demonstrated that fibrinogen is associated to the promotion of cell adhesion *in vitro* [57,58]. It was found that the adsorption of fibrinogen can contribute to fibrin formation, enhancing platelet adhesion [57]. In this study, we investigated the adsorption kinetics of albumin and fibrinogen onto Ti and Ta₂O₅ surfaces in real time using EQCM. The quantitative EQCM results showed similar protein interactions with Ti and Ta₂O₅ surfaces (Table 4). Fig. 9 shows the changes in Δf_s and ΔM as a function of time during the adsorption processes of (a-b) albumin and (c-d) fibrinogen on quartz crystal sensors covered with Ti and treated with Ta₂O₅. When the proteins were injected into the system (1800 s), flowing through sensor surfaces, a rapid increase of ΔM and a significant decrease of Δf_s can be observed. Subsequently, for both groups and proteins, ΔM values were gradually increased over time, while Δf_s showed the opposite behavior. Interestingly, in fibrinogen adsorption tests, it was observed that the Ta₂O₅ group reached the maximum value of ΔM (as appointed by the black arrows in the graph) more quickly when compared with the Ti group, indicating that the Ta₂O₅ film may have a rapid response of fibrinogen adsorption when compared with Ti. This behavior corroborates the quantitative results shown in Table 4, wherein the Ta₂O₅ group presented a tendency to higher adsorption rate values. In addition, the effective mass gain (ΔM - mass loss) results indicate that such values would provide good biological performance for Ta₂O₅-treated surfaces, as shown in the following cellular results.

Table 4

Mean and (standard deviation) values of albumin and fibrinogen adsorption kinetics parameters obtained from EQCM analysis.

Protein	Group	Adsorption rate		Effective mass gain	
		ΔM (μg)	(ng/s)	Mass loss (μg)	(ΔM - Mass loss) (μg)
Albumin	Ti	0.12 (0.08)	0.01 (0.00)	0.01 (0.01)	0.10 (0.06)
	Ta ₂ O ₅	0.12 (0.02)	0.54 (0.72)	0.04 (0.04)	0.07 (0.05)
Fibrinogen	Ti	0.14 (0.01)	0.02 (0.01)	0.01 (0.01)	0.13 (0.02)
	Ta ₂ O ₅	0.12 (0.02)	0.03 (0.02)	0.01 (0.01)	0.11 (0.02)

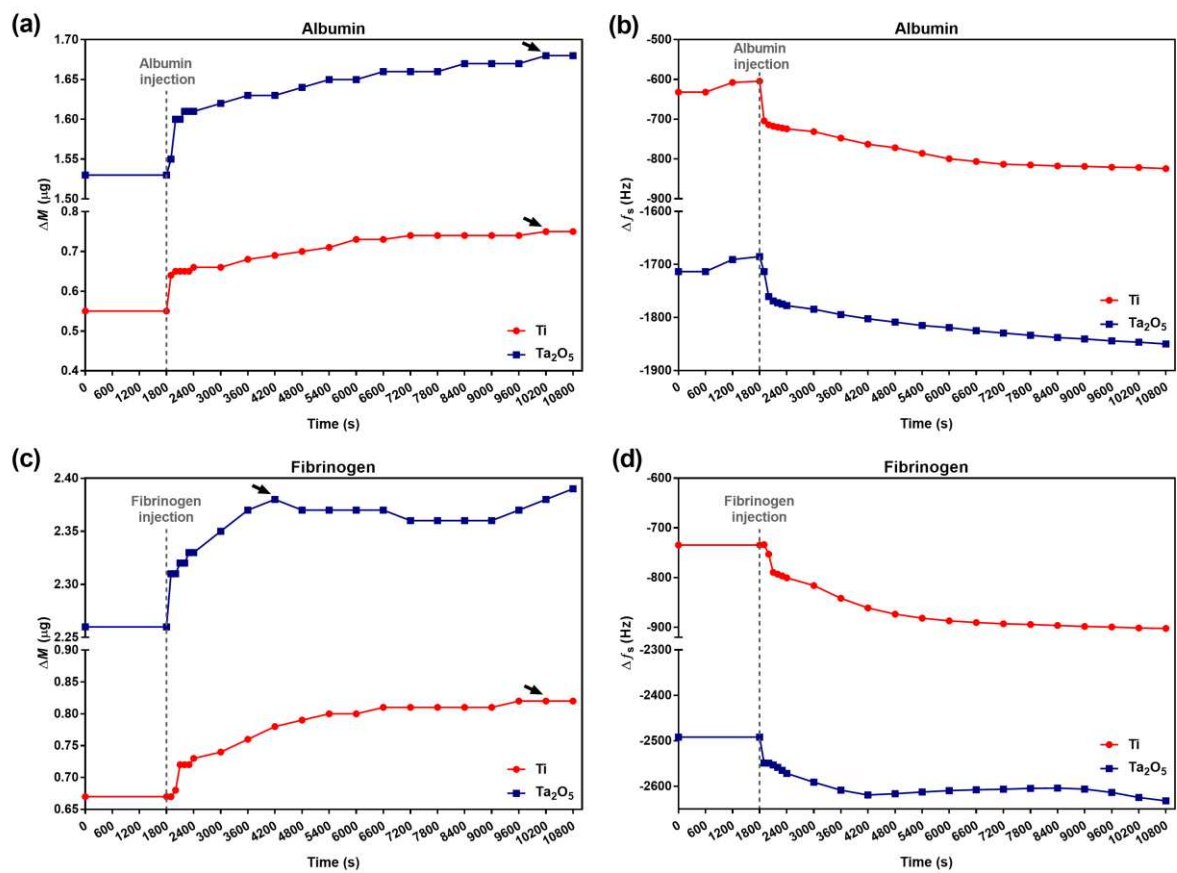


Fig. 9. Changes in Δf_s and ΔM as a function of time during the adsorption processes of (a-b) albumin and (c-d) fibrinogen on quartz crystal sensors covered with Ti (red curves) and treated with Ta₂O₅ (blue curves). Black arrows indicate the maximum ΔM value for each group.

3.5. Cell metabolism and morphology

An appropriate cellular response to implanted surfaces is crucial for tissue integration [59]. Therefore, in the current study, we carried out the MTT assay to determine

the impact of Ta₂O₅-modified cpTi surfaces on cell morphology and metabolism. The absorbance of formazan crystals produced by MC3T3-E1 cells after 1, 2, and 4 days of culturing is presented in Fig. 10. In general, data analysis showed that both groups (control and experimental) presented an increased mitochondrial metabolism over time, suggesting a non-cytotoxic effect, with the Ta₂O₅-treated group featuring an increased metabolism at day 2.

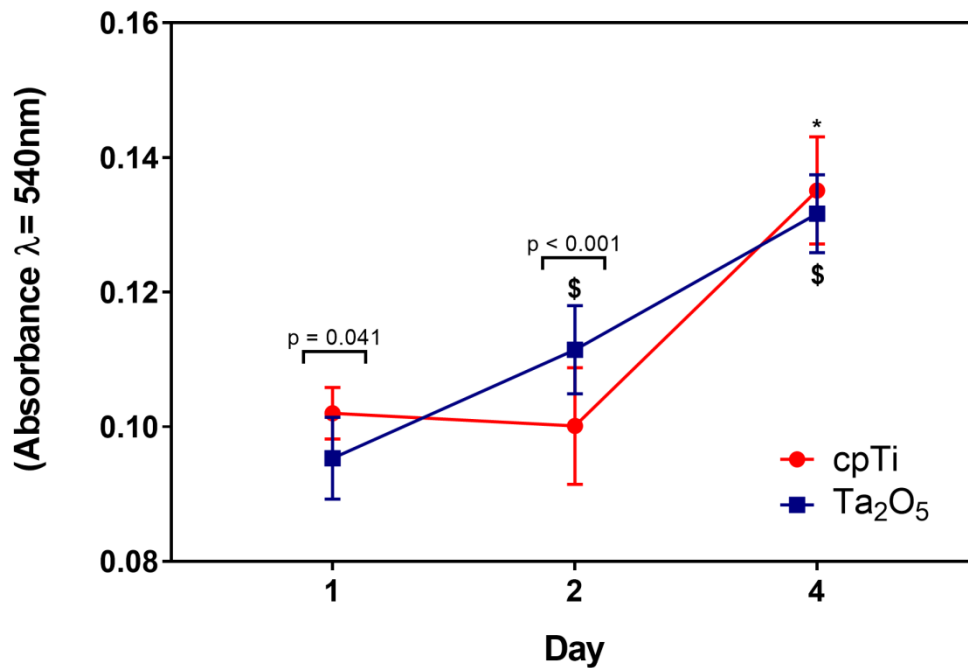


Fig. 10. MTT assay. Absorbance is expressed as a measure of cell metabolism for MC3T3-E1 cells cultured on control cpTi (untreated; red curve) and Ta₂O₅-modified surfaces (blue curve). * indicates intragroup differences (vs day 1) for cpTi, and \$ indicates intragroup differences (vs day 1) for Ta₂O₅ film. Intergroup differences (cpTi vs Ta₂O₅) within the same day are illustrated by the p-value.

If cells are to proliferate and differentiate, adhesion to surfaces is crucial [60,61]. Here, we investigated the impact of Ta₂O₅-modified cpTi surfaces on MC3T3-E1 cell adhesion and spreading after 1, 2, and 4 days, using SEM and confocal analysis (Figs. 11 and 12). According to previous literature, shapes, widths, and sizes of diverse nanoscale patterns can considerably influence cell adhesion, morphology, and differentiation [43]. In the current investigation, morphological analyses demonstrated that the Ta₂O₅-treated group displayed a well-defined and organized cytoskeleton, reflecting normal behavior [36] and well-spread

morphologies when compared with those of the cpTi substrate at all experimental periods. In addition, significantly more filopodia extensions were found for MC3T3-E1 cells cultured on Ta₂O₅ substrates, indicating that Ta₂O₅-coated samples positively affected important cellular properties *in vitro*, including adhesion, spreading, and migration.

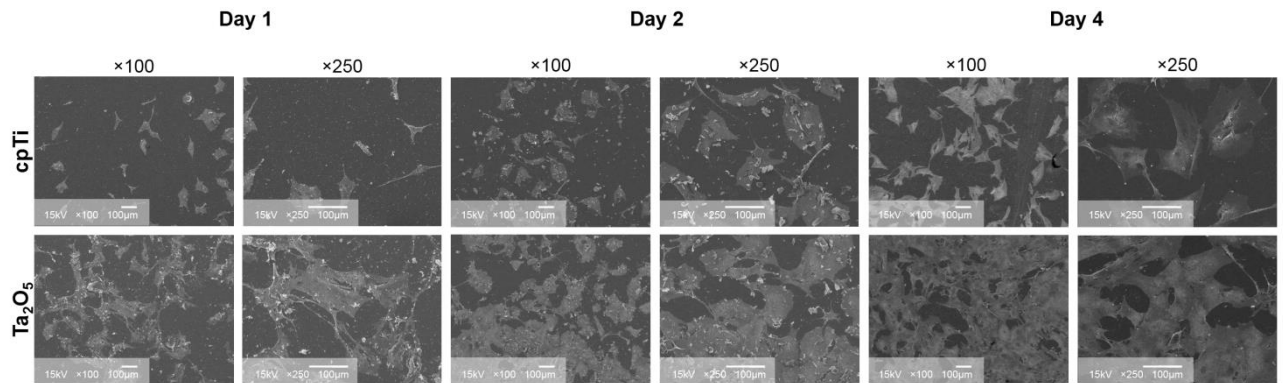


Fig. 11. Representative SEM images of MC3T3E-1 cells cultured on control cpTi and Ta₂O₅-modified surfaces after 1 day, 2 days, and 4 days. (scale bar = 100 µm).

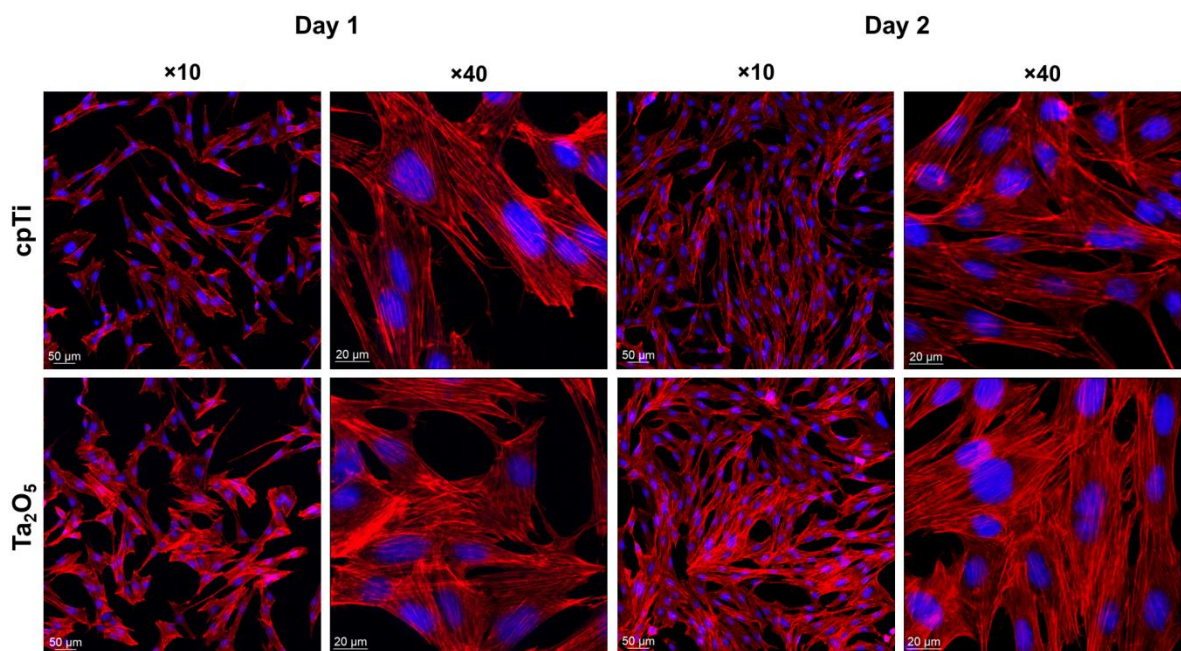


Fig. 12. Representative confocal images of MC3T3E-1 cells cultured on control cpTi and Ta₂O₅-modified surfaces after 1 and 2 days. Cell nuclei are stained in blue and the cell cytoskeleton in red.

3.6. Mineralization potential

Next, we hypothesized that Ta₂O₅-modified surfaces would affect MC3T3-E1 cell differentiation and improve mineral nodule formation *in vitro*. To test our hypothesis, we cultured cells on our control and experimental discs under osteogenic and non-osteogenic (control) conditions and carried out the AR-S assays to assess mineral nodule formation quantitatively at 4, 7, and 14 days (Fig. 13). Intragroup analysis demonstrated a significant increase in mineralization for both surfaces over time under osteogenic conditions at days 7 and 14. Intriguingly, intergroup comparisons showed that Ta₂O₅-modified surfaces displayed increased calcium levels under non-osteogenic conditions at days 7 and 14, and at day 14 under osteogenic differentiation. Altogether, these findings demonstrate that Ta₂O₅ films have the potential to enhance the differentiation of osteoblastic precursors cultured on cpTi discs.

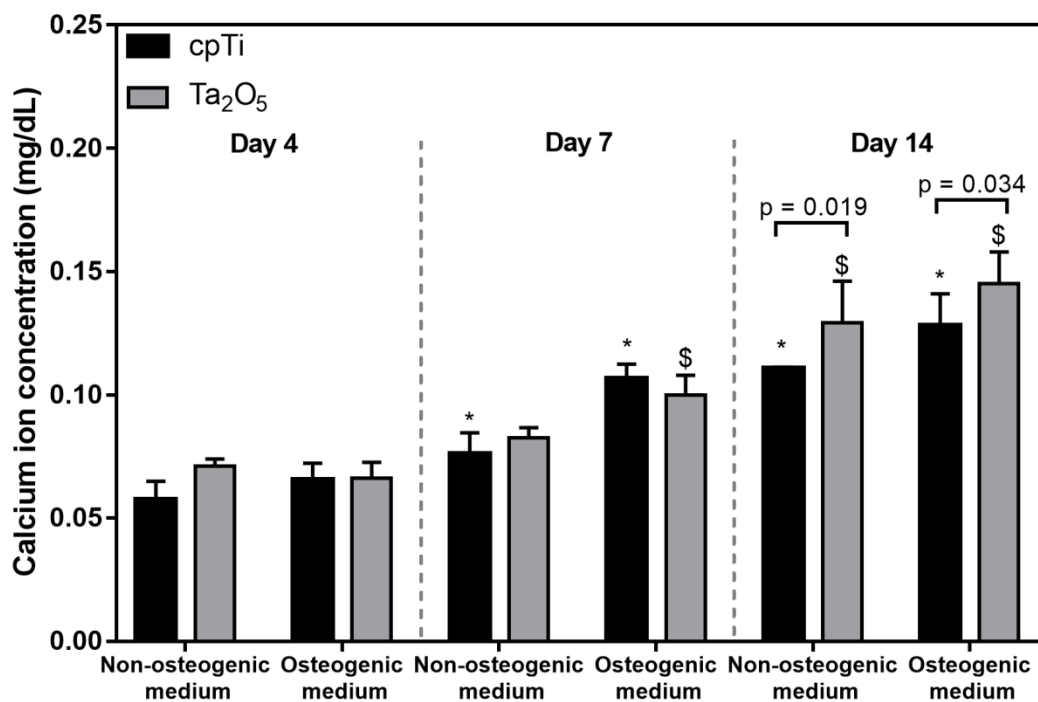


Fig. 13. Calcium ion concentrations for control and Ta₂O₅-modified surfaces. MC3T3-E1 cells were plated onto uncoated cpTi and Ta₂O₅-coated discs and cultured or not under osteogenic conditions for 4, 7, and 14 days. * indicates intragroup differences (vs day 4) for cpTi, and \$ indicates intragroup differences (vs day 4) for Ta₂O₅ film in non-osteogenic or osteogenic medium conditions separately. Intergroup differences (cpTi vs Ta₂O₅) within the same day are illustrated by the p-value.

3.7. Gene expression

For further investigation of the impact of Ta₂O₅-modified surfaces on the differentiation of osteoblastic precursor cells (MC3T3-E1), in the current study the expression of classic osteoblastic differentiation markers (including *Runx-2*, *Ocn*, *Alpl*, and *Col-1*) was quantitatively assessed (Fig. 14). Data analysis showed that transcript levels were increased by osteogenic conditions, except for *Runx-2* and *Alpl* at day 3. In addition, the findings of the current investigation demonstrated that Ta₂O₅-treated surfaces have the potential to modulate the expression of key markers of osteoblastic differentiation. Under osteogenic induction, fold change for *Runx-2* was significantly increased by Ta₂O₅-treated surfaces as early as 24 h after osteogenic induction, at days 2 and 3 for *Ocn* and at day 3 for *Col-1*, as compared with the cpTi group. In contrast to the cpTi group, at day 3, Ta₂O₅-modified surfaces resulted in decreased expression of *Runx-2* and *Alpl* in MC3T3-E1 cells under differentiation. Intergroup analysis further demonstrated that, at days 2 and 3, Ta₂O₅-modified surfaces led to increased changes for *Ocn* transcript levels as compared with cpTi under osteogenic conditions, whereas *Col-1* fold change was increased at day 3. Taken together, these findings suggest that Ta₂O₅ films have the potential to anticipate osteoblast precursor cell differentiation and, therefore, support the hypothesis that Ta₂O₅ films functionally affect markers of osteoblastic differentiation, leading to increased mineralization *in vitro*.

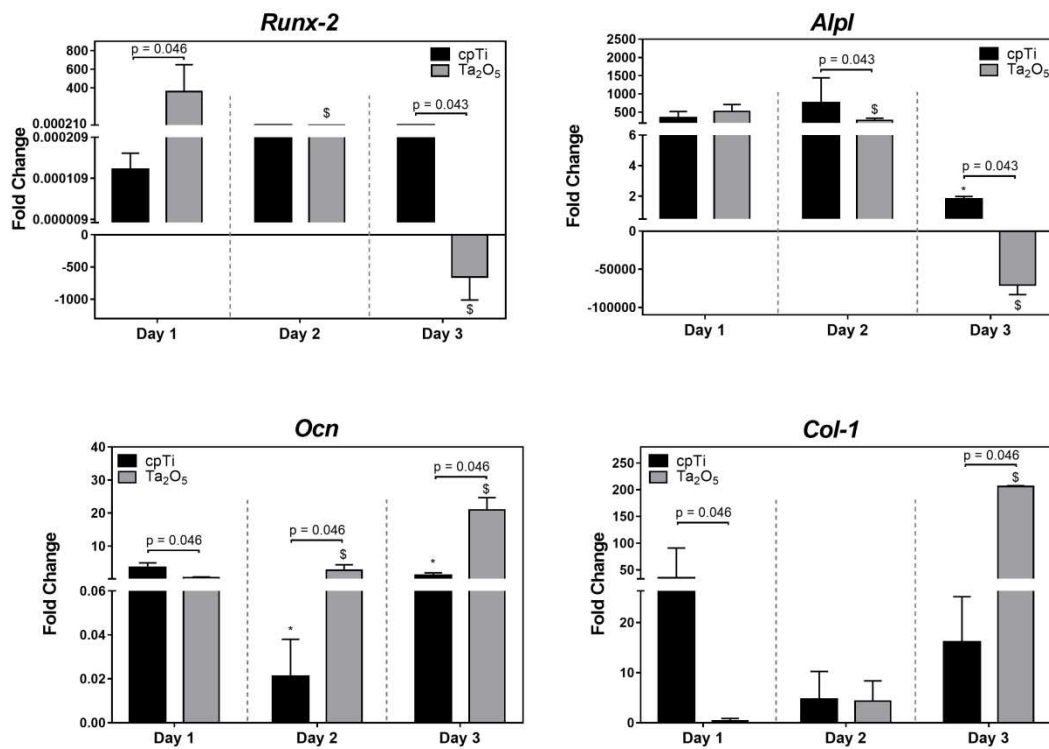


Fig. 14. Bar graphs illustrating fold change (osteogenic/non-osteogenic conditions) of osteogenic markers, including *Runx-2*, *Alpl*, *Ocn*, and *Col-1*, in MC3T3-E1 cells cultured on control cpTi and Ta₂O₅-modified surfaces. * indicates intragroup differences (vs day 1) for cpTi, and \$ indicates intragroup differences (vs day 1) for Ta₂O₅ film. Intergroup differences (cpTi vs Ta₂O₅) within the same day are illustrated by the p-value.

3.8. Surface bioactivity

To evaluate the osteoconductive response of the Ta₂O₅-treated surface and its potential for use as a biomaterial, we carried out a bioactivity test in SBF. Fig. 15 shows the XRD results of the samples immersed in SBF after 14 days. The Ta₂O₅ group presented a low-intensity diffraction peak corresponding to hydroxyapatite (HA) at 55.88° (ICDD card number 532741) and peaks related to Ta₂O₅ as mentioned previously in the characterization results. Depending on the degree of crystallinity in the tantalum oxide films, substitution of carbonate may occur within the apatite structure, in two distinct ways: in the OH-site as an “A-type” substitution or in the PO₄-site as a “B-type” substitution. Indeed, in the “B-type”, amorphous carbonate can be incorporated into the structure of the hydroxyapatite, which can reduce the degree of crystallinity of the apatite, as observed by Almeida Alves *et al.* (2016) [62]. In contrast, the cpTi group showed diffraction peaks related only to metallic Ti, implying that no calcium phosphate is detected by XRD.

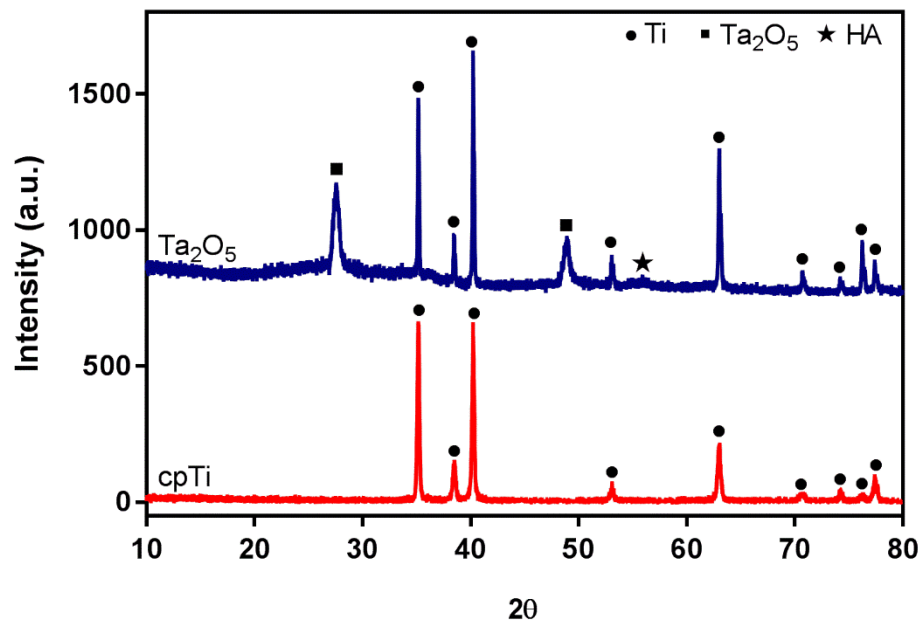


Fig. 15. XRD patterns of control cpTi (red pattern) and Ta₂O₅ (blue pattern) surfaces after 14 days of immersion in SBF at 37 °C.

3.9. Practical implications

Here, we proposed a surface modification of Ti with a β -Ta₂O₅ thin film to maintain the key physical properties of the bulk Ti material while modifying only its external surface. Such a modification controls the surface properties (such as roughness and surface energy) and, consequently, fosters the biological performance and prevents implant degradation in the biological environment. We show that the Ta₂O₅ film is able to protect cpTi against corrosion and, at the same time, enhance its cytocompatibility and bioactivity. The results obtained in this study demonstrate that the addition of a Ta₂O₅ film may be a forthcoming surface treatment feature to trigger the superior long-term stability of Ti implants. However, further studies are required to evaluate the interaction of such developed surface with living tissues.

4. Conclusions

We successfully developed a strategy to deposit a crystalline β -Ta₂O₅ thin film onto a cpTi surface by utilizing a magnetron sputtering technique. Ta₂O₅-treated surfaces exhibited greater roughness and hydrophilicity compared to untreated cpTi discs (control). Enhanced electrochemical stability in simulated body fluid was noted for Ta₂O₅-treated

surfaces wherein higher values of charge transfer resistance, nobler corrosion potential, and lower values of capacitance, corrosion current density, and corrosion rate were observed. Also, pre-osteoblastic cell culture assays (MC3T3-E1 cells) demonstrated that Ta₂O₅-treated discs featured greater *in vitro* mineral nodule formation and increased mRNA levels of runt-related transcription factor 2 (*Runx-2*), osteocalcin (*Ocn*), and collagen-1 (*Col-1*). The findings of the current investigation indicate that modification of cpTi surfaces with β-Ta₂O₅ films emerges as a viable and promising strategy to enhance dental implant electrochemical stability, improving its surface properties and biological performance.

Declarations of Competing Interest

None.

Acknowledgments

This study was supported by the São Paulo State Research Foundation (FAPESP), Brazil (grant numbers 2016/07269-3, 2016/11470-6 and 2017/18916-2), and in part by the Coordenação de Aperfeiçoamento de Pessoal de Nível Superior - Brasil (CAPES) - Finance code 001. The authors express their gratitude to the Brazilian Nanotechnology National Laboratory (LNNano) for the use of XRD, AFM, and XPS facilities and to the Microscopy Laboratory of Araraquara School of Dentistry (UNESP) for the use of Confocal Fluorescence Microscopy facilities. Additionally, this work made use of the EPIC facility of Northwestern University's NUANCE Center, which has received support from the Soft and Hybrid Nanotechnology Experimental (SHyNE) Resource (NSF ECCS-1542205); the MRSEC program (NSF DMR-1720139) at the Materials Research Center; the International Institute for Nanotechnology (IIN); the Keck Foundation; and the State of Illinois, through the IIN.

References

- [1] S. Prasad, M. Ehrensberger, M.P. Gibson, H. Kim, E.A. Monaco, Biomaterial properties of titanium in dentistry, *J. Oral Biosci.* 57 (2015) 192–199. doi:10.1016/j.job.2015.08.001.
- [2] N. Cabrera, N. Mott, Theory of the oxidation of metals, *Rep. Prog. Phys.* 12 (1949) 163–184.
- [3] L. Wang, H. Yu, K. Wang, H. Xu, S. Wang, D. Sun, Local Fine Structural Insight into Mechanism of Electrochemical Passivation of Titanium, *ACS Appl. Mater. Interfaces.* (2016). doi:10.1021/acsami.6b05080.
- [4] D. Cadosch, E. Chan, O.P. Gautschi, L. Filgueira, Metal is not inert: Role of metal ions released by biocorrosion in aseptic loosening - Current concepts, *J. Biomed. Mater. Res. A.* 91 (2009) 1252–1262. doi:10.1002/jbm.a.32625.
- [5] R. Bhola, S.M. Bhola, B. Mishra, D.L. Olson, Corrosion in titanium dental implants/prostheses - A review, *Trends Biomater. Artif. Organs.* 25 (2011) 34–46.
- [6] T. Beline, I. da S.V. Marques, A.O. Matos, E.S. Ogawa, A.P. Ricomini-Filho, E.C. Rangel, N.C. da Cruz, C. Sukotjo, M.T. Mathew, R. Landers, R.L.X. Consani, M.F. Mesquita, V.A.R. Barão, Production of a biofunctional titanium surface using plasma electrolytic oxidation and glow-discharge plasma for biomedical applications., *Biointerphases.* 11 (2016) 011013. doi:10.1116/1.4944061.
- [7] M.T. Mathew, V.A. Barão, J.C.C. Yuan, W.G. Assunção, C. Sukotjo, M.A. Wimmer, What is the role of lipopolysaccharide on the tribocorrosive behavior of titanium?, *J. Mech. Behav. Biomed. Mater.* 8 (2012) 71–85. doi:10.1016/j.jmbbm.2011.11.004.
- [8] M. Nakagawa, S. Matsuya, T. Shiraishi, M. Ohta, Effect of fluoride concentration and pH on corrosion behavior of titanium for dental use., *J. Dent. Res.* 78 (1999) 1568–1572. doi:10.1177/00220345990780091201.
- [9] T. Beline, C.S. Garcia, E.S. Ogawa, I.S.V. Marques, A.O. Matos, C. Sukotjo, M.T. Mathew, M.F. Mesquita, R.X. Consani, V.A.R. Barão, Surface treatment influences electrochemical stability of cpTi exposed to mouthwashes, *Mater. Sci. Eng. C.* 59 (2016) 1079–1088. doi:10.1016/j.msec.2015.11.045.
- [10] D. Royhman, X. Dominguez-Benetton, J.C.C. Yuan, T. Shokuhfar, C. Takoudis, M.T. Mathew, C. Sukotjo, The role of nicotine in the corrosive behavior of a Ti-6Al-4V dental implant, *Clin. Implant Dent. Relat. Res.* 17 (2015) 352–363. doi:10.1111/cid.12239.
- [11] V.A. Barao, M.T. Mathew, W.G. Assunção, J.C. Yuan, M.A. Wimmer, C. Sukotjo,

- The role of lipopolysaccharide on the electrochemical behavior of titanium, *J. Dent. Res.* 90 (2011) 613–618. doi:10.1177/0022034510396880.
- [12] S. Sridhar, T.G. Wilson, K.L. Palmer, P. Valderrama, M.T. Mathew, S. Prasad, M. Jacobs, I.M. Gindri, D.C. Rodrigues, In Vitro Investigation of the Effect of Oral Bacteria in the Surface Oxidation of Dental Implants, *Clin. Implant Dent. Relat. Res.* 17 (2015). doi:10.1111/cid.12285.
- [13] S.M. Zhang, J. Qiu, F. Tian, X.K. Guo, F.Q. Zhang, Q.F. Huang, Corrosion behavior of pure titanium in the presence of *Actinomyces naeslundii*, *J. Mater. Sci. Mater. Med.* 24 (2013) 1229–1237. doi:10.1007/s10856-013-4888-3.
- [14] J. Cohen, Current concepts review. Corrosion of metal orthopaedic implants., *J. Bone Joint Surg. Am.* 80 (1998) 1554.
- [15] L.M. Safioti, G.A. Kotsakis, A.E. Pozhitkov, W.O. Chung, D.M. Daubert, Increased levels of dissolved titanium are associated with peri-implantitis – A case-control study, *J. Periodontol.* (2016) 1–12. <http://www.joonline.org/doi/10.1902/jop.2016.160524>.
- [16] N. Tagger Green, E.E. Machtei, J. Horwitz, M. Peled, Fracture of dental implants: literature review and report of a case., *Implant Dent.* 11 (2002) 137–143. doi:10.1097/01.ID.0000015066.39485.E5.
- [17] M.D. Bermúdez, F.J. Carrión, G. Martínez-Nicolás, R. López, Erosion-corrosion of stainless steels, titanium, tantalum and zirconium, in: *Wear*, 2005. doi:10.1016/j.wear.2004.09.023.
- [18] V.K. Balla, S. Banerjee, S. Bose, A. Bandyopadhyay, Direct laser processing of a tantalum coating on titanium for bone replacement structures, *Acta Biomater.* 6 (2010) 2329–2334. doi:10.1016/j.actbio.2009.11.021.
- [19] J. Xu, X. ke Bao, T. Fu, Y. Lyu, P. Munroe, Z.-H. Xie, In vitro biocompatibility of a nanocrystalline β -Ta₂O₅ coating for orthopaedic implants, *Ceram. Int.* 44 (2018) 4660–4675. doi:10.1016/j.ceramint.2017.12.040.
- [20] P. Sochacka, A. Miklaszewski, M. Jurczyk, P. Pecyna, M. Ratajczak, M. Gajecka, M.U. Jurczyk, Effect of hydroxyapatite and Ag, Ta₂O₅ or CeO₂ addition on the properties of ultrafine-grained Ti₃₁Mo alloy, *J. Alloys Compd.* 823 (2020) 153749. doi:10.1016/j.jallcom.2020.153749.
- [21] H. Yu, S. Zhu, X. Yang, X. Wang, H. Sun, M. Huo, Synthesis of Coral-Like Tantalum Oxide Films via Anodization in Mixed Organic-Inorganic Electrolytes, *PLoS One.* 8 (2013) e66447. doi:10.1371/journal.pone.0066447.
- [22] G. Xu, X. Shen, Y. Hu, P. Ma, K. Cai, Fabrication of tantalum oxide layers onto

- titanium substrates for improved corrosion resistance and cytocompatibility, *Surf. Coatings Technol.* 272 (2015) 58–65. doi:10.1016/j.surfcoat.2015.04.024.
- [23] H. Zhang, H. Tang, T.M. Yue, Fabrication of Ta₂O₅ Reinforced Ta-based Coatings on Ta Substrates by Laser Cladding, *Int. J. Metall. Mater. Eng.* 4 (2018). doi:10.15344/2455-2372/2018/140.
- [24] Y.S. Sun, J.H. Chang, H.H. Huang, Corrosion resistance and biocompatibility of titanium surface coated with amorphous tantalum pentoxide, *Thin Solid Films.* 528 (2013) 130–135. doi:10.1016/j.tsf.2012.06.088.
- [25] I. Baía, M. Quintela, L. Mendes, P. Nunes, R. Martins, Performances exhibited by large area ITO layers produced by r.f. magnetron sputtering, *Thin Solid Films.* 337 (1999) 171–175. doi:10.1016/S0040-6090(98)01393-5.
- [26] J. Alami, S. Bolz, K. Sarakinos, High power pulsed magnetron sputtering: Fundamentals and applications, *J. Alloys Compd.* 483 (2009) 530–534. doi:10.1016/j.jallcom.2008.08.104.
- [27] T. Beline, J.H.D. da Silva, A.O. Matos, N.F. Azevedo Neto, A.B. de Almeida, F.H. Nociti Júnior, D.M.G. Leite, E.C. Rangel, V.A.R. Barão, Tailoring the synthesis of tantalum-based thin films for biomedical application: Characterization and biological response, *Mater. Sci. Eng. C.* 101 (2019) 111–119. doi:10.1016/j.msec.2019.03.072.
- [28] H.N. Pantaroto, K.P. Amorim, J. Matozinho Cordeiro, J.G.S. Souza, A.P. Ricomini-Filho, E.C. Rangel, A.L.R. Ribeiro, L.G. Vaz, V.A.R. Barão, Proteome analysis of the salivary pellicle formed on titanium alloys containing niobium and zirconium, *Biofouling.* 35 (2019) 173–186. doi:10.1080/08927014.2019.1580360.
- [29] A.L.J. Pereira, L. Gracia, A. Beltrán, P.N. Lisboa-Filho, J.H.D. Da Silva, J. Andrés, Structural and electronic effects of incorporating Mn in TiO₂films grown by sputtering: Anatase versus Rutile, *J. Phys. Chem. C.* 116 (2012) 8753–8762. doi:10.1021/jp210682d.
- [30] E.C. Combe, B.A. Owen, J.S. Hodges, A protocol for determining the surface free energy of dental materials, *Dent. Mater.* 20 (2004) 262–268. doi:10.1016/S0109-5641(03)00102-7.
- [31] L. Müller, F.A. Müller, Preparation of SBF with different HCO₃⁻ content and its influence on the composition of biomimetic apatites, *Acta Biomater.* 2 (2006) 181–189. doi:10.1016/j.actbio.2005.11.001.
- [32] X. Lou, P.M. Singh, Phase angle analysis for stress corrosion cracking of carbon steel in fuel-grade ethanol: Experiments and simulation, *Electrochim. Acta.* 56 (2011) 1835–

1847. doi:10.1016/j.electacta.2010.07.024.
- [33] V.A.R. Barao, M.T. Mathew, W.G. Assuncao, J.C.-C. Yuan, M.A. Wimmer, C. Sukotjo, Stability of cp-Ti and Ti-6Al-4V alloy for dental implants as a function of saliva pH - an electrochemical study., *Clin. Oral Implants Res.* 23 (2012) 1055–1062. doi:10.1111/j.1600-0501.2011.02265.x.
- [34] V.A.R. Barão, A.P. Ricomini-Filho, L.P. Faverani, A.A. Del Bel Cury, C. Sukotjo, D.R. Monteiro, J.C.C. Yuan, M.T. Mathew, R.C. Do Amaral, M.F. Mesquita, W.J. Da Silva, W.G. Assunção, The role of nicotine, cotinine and caffeine on the electrochemical behavior and bacterial colonization to cp-Ti, *Mater. Sci. Eng. C.* 56 (2015) 114–124. doi:10.1016/j.msec.2015.06.026.
- [35] G. Sauerbrey, The use of quartz oscillators for weighing thin layers and for microweighing, *Zeitschrift Für Phys.* 155 (1959) 206–222. doi:10.1007/BF01337937.
- [36] I. da S.V. Marques, M.F. Alfaro, M.T. Saito, N.C. da Cruz, C. Takoudis, R. Landers, M.F. Mesquita, F.H. Nociti Junior, M.T. Mathew, C. Sukotjo, V.A.R. Barão, Biomimetic coatings enhance tribocorrosion behavior and cell responses of commercially pure titanium surfaces, *Biointerphases.* 11 (2016) 031008. doi:10.1116/1.4960654.
- [37] A.O. Matos, A.P. Ricomini-Filho, T. Beline, E.S. Ogawa, B.E. Costa-Oliveira, A.B. de Almeida, F.H. Nociti Junior, E.C. Rangel, N.C. da Cruz, C. Sukotjo, M.T. Mathew, V.A.R. Barão, Three-species biofilm model onto plasma-treated titanium implant surface, *Colloids Surfaces B Biointerfaces.* 152 (2017) 354–366. doi:10.1016/j.colsurfb.2017.01.035.
- [38] T.L. Rodrigues, B.L. Foster, K.G. Silverio, L. Martins, M.Z. Casati, E.A. Sallum, M.J. Somerman, F.H. Nociti, Hypophosphatasia-associated Deficiencies in Mineralization and Gene Expression in Cultured Dental Pulp Cells Obtained from Human Teeth, *J. Endod.* 38 (2012) 907–912. doi:10.1016/j.joen.2012.02.008.
- [39] T. Kokubo, H. Takadama, How useful is SBF in predicting in vivo bone bioactivity?, *Biomaterials.* 27 (2006) 2907–2915. doi:10.1016/j.biomaterials.2006.01.017.
- [40] M. Birkholz, *Thin Film Analysis by X-Ray Scattering*, first ed., Wiley-VCH, Frankfurt, Germany, 2006.
- [41] K. Lehovc, Lattice structure of β -Ta₂O₅, *J. Less-Common Met.* 7 (1964) 397–410. doi:10.1016/0022-5088(64)90036-0.
- [42] M.H. Ding, B.L. Wang, L. Li, Y.F. Zheng, A study of TaxC1-x coatings deposited on biomedical 316L stainless steel by radio-frequency magnetron sputtering, *Appl. Surf.*

- Sci. 257 (2010) 696–703. doi:10.1016/j.apsusc.2010.07.026.
- [43] H. Jeon, C.G. Simon, G. Kim, A mini-review: Cell response to microscale, nanoscale, and hierarchical patterning of surface structure, *J. Biomed. Mater. Res. Part B Appl. Biomater.* 102 (2014) 1580–1594. doi:10.1002/jbm.b.33158.
- [44] A. Ranella, M. Barberoglou, S. Bakogianni, C. Fotakis, E. Stratakis, Tuning cell adhesion by controlling the roughness and wettability of 3D micro/nano silicon structures, *Acta Biomater.* 6 (2010) 2711–2720. doi:10.1016/j.actbio.2010.01.016.
- [45] A. Aminian, B. Shirzadi, Z. Azizi, K. Maedler, E. Volkmann, N. Hildebrand, M. Maas, L. Treccani, K. Rezwani, Enhanced cell adhesion on bioinert ceramics mediated by the osteogenic cell membrane enzyme alkaline phosphatase, *Mater. Sci. Eng. C.* 69 (2016) 184–194. doi:10.1016/j.msec.2016.06.056.
- [46] W. Ren, Z. Ai, F. Jia, L. Zhang, X. Fan, Z. Zou, Low temperature preparation and visible light photocatalytic activity of mesoporous carbon-doped crystalline TiO₂, *Appl. Catal. B Environ.* 69 (2007) 138–144. doi:10.1016/j.apcatb.2006.06.015.
- [47] J.-H. Kim, S. Lee, H.-S. Im, The effect of target density and its morphology on TiO₂ thin films grown on Si(100) by PLD, *Appl. Surf. Sci.* 151 (1999) 6–16. doi:10.1016/S0169-4332(99)00269-X.
- [48] A.C. Hee, Y. Zhao, S.S. Jamali, P.J. Martin, A. Bendavid, H. Peng, X. Cheng, Corrosion behaviour and microstructure of tantalum film on Ti6Al4V substrate by filtered cathodic vacuum arc deposition, *Thin Solid Films.* 636 (2017) 54–62. doi:10.1016/j.tsf.2017.05.030.
- [49] A.C. Hee, H. Cao, Y. Zhao, S.S. Jamali, A. Bendavid, P.J. Martin, Cytocompatible tantalum films on Ti6Al4V substrate by filtered cathodic vacuum arc deposition, *Bioelectrochemistry.* 122 (2018) 32–39. doi:10.1016/j.bioelechem.2018.02.006.
- [50] Y. Cheng, W. Cai, H.T. Li, Y.F. Zheng, L.C. Zhao, Surface characteristics and corrosion resistance properties of TiNi shape memory alloy coated with Ta, *Surf. Coatings Technol.* 186 (2004) 346–352. doi:10.1016/j.surfcoat.2004.01.012.
- [51] M. Textor, L. Ruiz, R. Hofer, A. Rossi, K. Feldman, G. Hähner, N.D. Spencer, Structural Chemistry of Self-Assembled Monolayers of Octadecylphosphoric Acid on Tantalum Oxide Surfaces, *Langmuir.* 16 (2000) 3257–3271. doi:10.1021/la990941t.
- [52] T. Fu, Z. Zhan, L. Zhang, Y. Yang, Z. Liu, J. Liu, L. Li, X. Yu, Effect of surface mechanical attrition treatment on corrosion resistance of commercial pure titanium, *Surf. Coatings Technol.* 280 (2015) 129–135. doi:10.1016/j.surfcoat.2015.08.041.
- [53] A.C. Hee, Y. Zhao, S.S. Jamali, A. Bendavid, P.J. Martin, H. Guo, Characterization of

- tantalum and tantalum nitride films on Ti6Al4V substrate prepared by filtered cathodic vacuum arc deposition for biomedical applications, *Surf. Coatings Technol.* 365 (2019) 24–32. doi:10.1016/j.surfcoat.2018.05.007.
- [54] T. Beline, A.J. Vechiato Filho, A.G. Wee, C. Sukotjo, D.M. dos Santos, T.B. Brandão, V.A.R. Barão, Initial investigation of the corrosion stability of craniofacial implants, *J. Prosthet. Dent.* 119 (2018) 185–192. doi:10.1016/j.prosdent.2017.02.015.
- [55] P. Silva-Bermudez, S.E. Rodil, An overview of protein adsorption on metal oxide coatings for biomedical implants, *Surf. Coatings Technol.* 233 (2013) 147–158. doi:10.1016/j.surfcoat.2013.04.028.
- [56] M. Talha, Y. Ma, P. Kumar, Y. Lin, A. Singh, Role of protein adsorption in the bio corrosion of metallic implants – A review, *Colloids Surfaces B Biointerfaces.* 176 (2019) 494–506. doi:10.1016/j.colsurfb.2019.01.038.
- [57] C. Sperling, M. Fischer, M.F. Maitz, C. Werner, Blood coagulation on biomaterials requires the combination of distinct activation processes, *Biomaterials.* 30 (2009) 4447–4456. doi:10.1016/j.biomaterials.2009.05.044.
- [58] C. Werner, M.F. Maitz, C. Sperling, Current strategies towards hemocompatible coatings, *J. Mater. Chem.* 17 (2007) 3376. doi:10.1039/b703416b.
- [59] C.J. Wilson, R.E. Clegg, D.I. Leavesley, M.J. Percy, Mediation of Biomaterial–Cell Interactions by Adsorbed Proteins: A Review, *Tissue Eng.* (2005). doi:10.1089/ten.2005.11.1.
- [60] J.Y. Martin, Z. Schwartz, T.W. Hummert, D.M. Schraub, J. Simpson, J. Lankford, D.D. Dean, D.L. Cochran, B.D. Boyan, Effect of titanium surface roughness on proliferation, differentiation, and protein synthesis of human osteoblast-like cells (MG63), *J. Biomed. Mater. Res.* 29 (1995) 389–401. doi:10.1002/jbm.820290314.
- [61] K.-D. Yun, Y. Yang, H.-P. Lim, G.-J. Oh, J.-T. Koh, I.-H. Bae, J. Kim, K.-M. Lee, S.-W. Park, Effect of nanotubular-micro-roughened titanium surface on cell response in vitro and osseointegration in vivo, *Mater. Sci. Eng. C.* 30 (2010) 27–33. doi:10.1016/j.msec.2009.08.004.
- [62] C.F. Almeida Alves, A. Cavaleiro, S. Carvalho, Bioactivity response of Ta1-xOx coatings deposited by reactive DC magnetron sputtering, *Mater. Sci. Eng. C.* 58 (2016) 110–118. doi:10.1016/j.msec.2015.08.017.

3 DISCUSSÃO

O uso de implantes dentários para a reabilitação oral de pacientes parcial e totalmente desdentados é amplamente relatado na literatura. Espera-se que o número de procedimentos para implantes continue aumentando ao longo do tempo devido ao aumento da expectativa de vida (Casado et al., 2018). As altas taxas de sucesso clínico apresentadas na literatura (~87%) sustentam a escolha do Ti como biomaterial para a fabricação de implantes ortopédicos e dentários (Chrcanovic et al., 2018). A biocompatibilidade, capacidade de osseointegração e resistência à corrosão são propriedades apresentadas pelo Ti são providas pela formação de uma camada de TiO_2 passiva em sua superfície, que normalmente possui menos de 10 nm (Olmedo et al., 2008). No entanto, as condições agressivas do ambiente biológico podem afetar a estabilidade da camada de óxido, levando à exposição da superfície do metal e conseqüentemente, tornando-o susceptível ao ataque corrosivo (Nakagawa et al., 1999; Barão et al., 2011; Mathew et al., 2012; Zhang et al., 2013; Royhman et al., 2015; Sridhar et al., 2015; Beline et al., 2016).

Neste cenário, o Ta tem recebido atenção como biomaterial alternativo ao Ti, por apresentar superiores propriedades de bioatividade e resistência à corrosão quando comparado ao Ti (Bermúdez et al., 2005; Balla et al., 2010). Estudos prévios confirmaram essas propriedades do Ta ao favorecer a osteogênese *in vivo* (Wauthle et al., 2015) e *in vitro* (Welldon et al., 2008; Sagomonyants et al., 2011). No entanto, o uso do Ta para a fabricação de implantes é limitado devido sua alta densidade, ponto de fusão e custos de manufatura (Balla et al., 2010). Levando-se em consideração que as respostas biológicas dos tecidos ao redor dos implantes são controladas majoritariamente pelas características de superfície do biomaterial (rugosidade, composição química, estrutura e molhabilidade) (Turzo, 2011), a combinação das boas propriedades do Ti e do Ta através da aplicação de filmes de óxido de Ta, como tratamento de superfície para o Ti, poderia ser considerada uma alternativa viável para superar as limitações relatadas acima e alcançar a combinação desejada de propriedades para produzir implantes de Ti com excelente qualidade.

Dentre as diversas técnicas utilizadas para deposição de filmes de Ta e Ta_xO_y , a técnica da pulverização catódica é conhecida por produzir filmes uniformes (Pereira et al., 2012) e de alta qualidade em termos de adesão, o que a torna atrativa para as mais variadas aplicações tecnológicas (Alami et al., 2009; Sarakinos et al., 2010; He et al., 2013; He et al., 2013; He et al., 2014; He et al., 2014; Zhang et al., 2014). Ainda, através da técnica da pulverização catódica é possível a criação de filmes de óxidos metálicos de diferentes composições por meio da modulação dos parâmetros de deposição.

No entanto, a literatura é limitada no que concerne à obtenção da fase β -Ta₂O₅ através da pulverização catódica e sua cristalização (Ellis et al., 2018). Sendo assim, o Capítulo 1 do presente trabalho forneceu subsídios para o entendimento dos efeitos da variação dos parâmetros de deposição sobre a estrutura, morfologia e composição química dos diferentes filmes de Ta_xO_y produzidos pela técnica da pulverização catódica sobre a superfície do Ticp. Os resultados mostraram que a combinação das boas propriedades de superfície apresentadas pelo filme de β -Ta₂O₅ depositado por pulverização catódica sobre a superfície do Ticp foi capaz de não aumentar a colonização bacteriana inicial e ainda, melhorar o processo de adesão e espalhamento de células da linhagem MC3T3-E1.

Ainda, levando-se em consideração que nenhum estudo avaliou a interação proteínas/filme de β -Ta₂O₅ em tempo real e que a literatura carece de estudos que avaliaram a degradação eletroquímica de filmes de β -Ta₂O₅ em ambiente oral simulado, o Capítulo 2 da referida tese apresenta os resultados dos ensaios eletroquímicos e demais testes biológicos do filme de óxido de Ta cristalino. No que diz respeito à caracterização eletroquímica, os ensaios revelaram que o tratamento de superfície proposto foi capaz de melhorar a estabilidade eletroquímica do Ticp. Nos testes de adsorção de fibrinogênio, o grupo tratado com filme de β -Ta₂O₅ levou menos tempo para atingir o valor máximo de variação de massa (ΔM) quando comparado ao grupo recoberto somente com Ti, indicando uma resposta mais rápida do grupo tratado com β -Ta₂O₅ para a adsorção de fibrinogênio. Além disso, os achados do presente capítulo demonstraram que a superfície tratada com filme de β -Ta₂O₅ tem potencial para antecipar a diferenciação de células osteoblásticas precursoras e, assim, suportar a hipótese de que o filme de β -Ta₂O₅ afeta funcionalmente marcadores de diferenciação osteoblástica, levando ao aumento da mineralização *in vitro*.

Apesar dos resultados do presente estudo mostrarem que o filme cristalino de Ta₂O₅ pode ser considerado uma alternativa viável e promissora para melhorar as propriedades de superfície do Ticp, sua estabilidade eletroquímica e performance biológica, futuros estudos *in vivo* são encorajados para avaliar a bio-interação do tratamento de superfície proposto.

4 CONCLUSÃO

Este trabalho desenvolveu filmes de óxido de tântalo por meio da técnica de pulverização catódica. Através da modificação dos parâmetros de deposição, foi possível a criação de filmes com diferentes propriedades estruturais (amorfa e cristalina) e morfológicas. Tais filmes não aumentaram a colonização bacteriana quando comparados ao Ticp polido. Além disso, este trabalho mostrou que o filme de Ta₂O₅ cristalino foi capaz de prover proteção à corrosão e, ao mesmo tempo, aumentar a biocompatibilidade e bioatividade do Ticp.

REFERÊNCIAS*

Alami J, Bolz S, Sarakinos K. High power pulsed magnetron sputtering: Fundamentals and applications. *J Alloys Compd.* 2009;483:530–4.

Baía I, Quintela M, Mendes L, Nunes P, Martins R. Performances exhibited by large area ITO layers produced by r.f. magnetron sputtering. *Thin Solid Films.* 1999;337:171–5.

Balla VK, Banerjee S, Bose S, Bandyopadhyay A. Direct laser processing of a tantalum coating on titanium for bone replacement structures. *Acta Biomater.* 2010;6:2329–34.

Barao VA, Mathew MT, Assunção WG, Yuan JC, Wimmer MA, Sukotjo C. The role of lipopolysaccharide on the electrochemical behavior of titanium. *J Dent Res.* 2011;90(5):613–8.

Beline T, Garcia CS, Ogawa ES, Marques ISV, Matos AO, Sukotjo C, et al. Surface treatment influences electrochemical stability of cpTi exposed to mouthwashes. *Mater Sci Eng C.* 2016 Feb;59:1079–88.

Beline T, Marques I da SV, Matos AO, Ogawa ES, Ricomini-Filho AP, Rangel EC, et al. Production of a biofunctional titanium surface using plasma electrolytic oxidation and glow-discharge plasma for biomedical applications. *Biointerphases.* 2016;11(1):011013. doi: 10.1116/1.4944061.

Bencharit S, Byrd WC, Altarawneh S, Hosseini B, Leong A, Reside G, et al. Development and applications of porous tantalum trabecular metal-enhanced titanium dental implants. *Clin Implant Dent Relat Res.* 2014 Dec;16(6):817–26. doi: 10.1111/cid.12059.

Bermúdez MD, Carrión FJ, Martínez-Nicolás G, López R. Erosion-corrosion of stainless steels, titanium, tantalum and zirconium. *Wear.* 2005; 258 (1-4): 696-700.

*De acordo com as normas da UNICAMP/FOP, baseadas na padronização do International Committee of Medical Journal Editors - Vancouver Group. Abreviatura dos periódicos em conformidade com o PubMed.

- Bhola R, Bhola SM, Mishra B, Olson DL. Corrosion in titanium dental implants/prostheses - A review. *Trends Biomater Artif Organs*. 2011;25(1):34–46.
- Bouchet-Fabre B, Fadjié-Djomkam A, Fernandez-Pacheco R, Delmas M, Pinault M, Jegou P, et al. Effect of tantalum nitride supporting layer on growth and morphology of carbon nanotubes by thermal chemical vapor deposition. *Diam Relat Mater*. 2011;20(7):999–1004.
- Casado PL, Quinelato V, Cataldo P, Prazeres J, Campello M, Bonato LL, et al. Dental genetics in Brazil: Where we are. *Mol Genet Genomic Med*. 2018 Sep;6(5):689–701.
- Chang YY, Huang HL, Chen HJ, Lai CH, Wen CY. Antibacterial properties and cytocompatibility of tantalum oxide coatings. *Surf Coatings Technol*. 2014;259:193–8.
- Chrcanovic BR, Kisch J, Albrektsson T, Wennerberg A. A retrospective study on clinical and radiological outcomes of oral implants in patients followed up for a minimum of 20 years. *Clin Implant Dent Relat Res*. 2018 Apr;20(2):199–207.
- Cohen J. Current concepts review. Corrosion of metal orthopaedic implants. *J Bone Joint Surg Am*. 1998;80(10):1554.
- Ellis EAI, Chmielus M, Baker SP. Effect of sputter pressure on Ta thin films: Beta phase formation, texture, and stresses. *Acta Mater*. 2018;150:317–26.
- Fairbrother F. The chemistry of niobium and tantalum. Amsterdam: Elsevier Pub. Co; 1967. 20–36 p.
- He G, Chen X, Sun Z. Interface engineering and chemistry of Hf-based high-k dielectrics on III-V substrates. *Surf Sci Rep*. 2013;68(1):68–107.
- He G, Deng B, Chen H, Chen X, Lv J, Ma Y, et al. Effect of dimethylaluminumhydride-derived aluminum oxynitride passivation layer on the interface chemistry and band alignment of HfTiO-InGaAs gate stacks. *APL Mater*. 2013;1:012104.

He G, Gao J, Chen H, Cui J, Sun Z, Chen X. Modulating the interface quality and electrical properties of HfTiO/InGaAs gate stack by atomic-layer-deposition-derived Al₂O₃ passivation layer. *ACS Appl Mater Interfaces*. 2014;6(24):22013–25.

He G, Liu J, Chen H, Liu Y, Sun Z, Chen X, et al. Interface control and modification of band alignment and electrical properties of HfTiO/GaAs gate stacks by nitrogen incorporation. *J Mater Chem C*. 2014;2:5299–5308.

Kester DJ, Messier R. Macro-effects of resputtering due to negative ion bombardment of growing thin films. *J Mater Res*. 1993;8:1928–37.

Kim N, Stebbins JF. Structure of amorphous tantalum oxide and titania-doped tantalum: 17O NMR results for sol-gel and ion-beam-sputtered materials. *Chem Mater*. 2011;23:3460–5.

Mathew MT, Barão VA, Yuan JCC, Assunção WG, Sukotjo C, Wimmer MA. What is the role of lipopolysaccharide on the tribocorrosive behavior of titanium? *J Mech Behav Biomed Mater*. 2012;8:71–85.

Nakagawa M, Matsuya S, Shiraishi T, Ohta M. Effect of fluoride concentration and pH on corrosion behavior of titanium for dental use. *J Dent Res*. 1999;78(9):1568–72.

Olmedo DG, Duffó G, Cabrini RL, Guglielmotti MB. Local effect of titanium implant corrosion: an experimental study in rats. *Int J Oral Maxillofac Surg*. 2008;37(11):1032–8.

Pelletier H, Muller D, Mille P, Grob JJ. Structural and mechanical characterisation of boron and nitrogen implanted NiTi shape memory alloy. *Surf Coatings Technol*. 2002;158–159:309–17.

Pereira ALJ, Gracia L, Beltrán A, Lisboa-Filho PN, Da Silva JHD, Andrés J. Structural and electronic effects of incorporating Mn in TiO₂ films grown by sputtering: Anatase versus Rutile. *J Phys Chem C*. 2012;116(15):8753–8762.

Pham VH, Lee SH, Li Y, Kim HE, Shin KH, Koh YH. Utility of tantalum (Ta) coating to improve surface hardness in vitro bioactivity and biocompatibility of Co-Cr. *Thin Solid Films*. 2013;536:269–74.

Prasad S, Ehrensberger M, Gibson MP, Kim H, Monaco EA. Biomaterial properties of titanium in dentistry. *J Oral Biosci*. 2015;57:192–9.

Royhman D, Dominguez-Benetton X, Yuan JCC, Shokuhfar T, Takoudis C, Mathew MT, et al. The role of nicotine in the corrosive behavior of a Ti-6Al-4V dental implant. *Clin Implant Dent Relat Res*. 2015;17:352–63.

Safioti LM, Kotsakis GA, Pozhitkov AE, Chung WO, Daubert DM. Increased levels of dissolved titanium are associated with peri-implantitis – A case-control study. *J Periodonto*. 2016;1–12.

Sagomyants KB, Hakim-Zargar M, Jhaveri A, Aronow MS, Gronowicz G. Porous tantalum stimulates the proliferation and osteogenesis of osteoblasts from elderly female patients. *J Orthop Res*. 2011 Apr;29(4):609–16.

Sarakinos K, Alami J, Konstantinidis S. High power pulsed magnetron sputtering: A review on scientific and engineering state of the art. *Surf Coat Technol*. 2010;204(11):1661-1684.

Sridhar S, Wilson TG, Palmer KL, Valderrama P, Mathew MT, Prasad S, et al. In Vitro Investigation of the Effect of Oral Bacteria in the Surface Oxidation of Dental Implants. *Clin Implant Dent Relat Res*. 2015;17(2):e562-575.

Strnad G, Chirila N. Corrosion Rate of Sand Blasted and Acid Etched Ti6Al4V for Dental Implants. *Procedia Technol*. 2015;19:909–15.

Sun YS, Chang JH, Huang HH. Corrosion resistance and biocompatibility of titanium surface coated with amorphous tantalum pentoxide. *Thin Solid Films*. 2013;528:130–5.

Tagger Green N, Machtei EE, Horwitz J, Peled M. Fracture of dental implants: literature review and report of a case. *Implant Dent*. 2002;11(2):137–43.

Turzo K. Surface Aspects of Titanium Dental Implants. In: *Biotechnology - Molecular Studies and Novel Applications for Improved Quality of Human Life*. InTech; 2012. Available from: <http://www.intechopen.com/books/biotechnology-molecular-studies-and-novel-applications-for-improved-quality-of-human-life/surface-aspects-of-titanium-dental-implants>

Wauthle R, van der Stok J, Amin Yavari S, Van Humbeeck J, Kruth J-P, Zadpoor AA, et al. Additively manufactured porous tantalum implants. *Acta Biomater*. 2015;14:217–25.

Welldon KJ, Atkins GJ, Howie DW, Findlay DM. Primary human osteoblasts grow into porous tantalum and maintain an osteoblastic phenotype. *J Biomed Mater Res Part A*. 2008;84A(3):691–701.

Zein-El-Abedin S, Welz-Biermann U, Endres F. A study on the electrodeposition of tantalum on NiTi alloy in an ionic liquid and corrosion behaviour of the coated alloy. *Electrochem Commun*. 2005;7(9):941–6.

Zhang JW, He G, Zhou L, Chen HS, Chen XS, Chen XF, et al. Microstructure optimization and optical and interfacial properties modulation of sputtering-derived HfO₂ thin films by TiO₂ incorporation. *J Alloys Compd*. 2014;611:253–9.

Zhang SM, Qiu J, Tian F, Guo XK, Zhang FQ, Huang QF. Corrosion behavior of pure titanium in the presence of *Actinomyces naeslundii*. *J Mater Sci Mater Med*. 2013;24(5):1229–37.

ANEXOS

Anexo 1 – Comprovante de que não é necessária licença para uso do Artigo 1 na tese



RightsLink®

Home

Create Account

Help



Title: Tailoring the synthesis of tantalum-based thin films for biomedical application: Characterization and biological response

Author: Thamara Beline, José H.D. da Silva, Adaias O. Matos, Nilton F. Azevedo Neto, Amanda B. de Almeida, Francisco H. Nociti Júnior, Douglas M.G. Leite, Elidiane Cipriano Rangel, Valentim A.R. Barão

Publication: Materials Science and Engineering: C

Publisher: Elsevier

Date: August 2019

© 2019 Elsevier B.V. All rights reserved.

LOGIN

If you're a [copyright.com](#) user, you can login to RightsLink using your copyright.com credentials. Already a RightsLink user or want to [learn more?](#)

Please note that, as the author of this Elsevier article, you retain the right to include it in a thesis or dissertation, provided it is not published commercially. Permission is not required, but please ensure that you reference the journal as the original source. For more information on this and on your other retained rights, please visit: <https://www.elsevier.com/about/our-business/policies/copyright#Author-rights>

BACK

CLOSE WINDOW

Copyright © 2019 [Copyright Clearance Center, Inc.](#) All Rights Reserved. [Privacy statement](#). [Terms and Conditions](#). Comments? We would like to hear from you. E-mail us at customercare@copyright.com

Anexo 2 – Licença para uso do Artigo 2 na tese

14/04/2020 <https://mail-attachment.googleusercontent.com/attachment/u/0/?ui=2&ik=ac66c27efd&attid=0.1&permmsgid=msg-f:166395118948...>

ELSEVIER

Rights and Access

-Ta2O5 thin film for implant surface modification triggers superior anti-corrosion performance and cytocompatibility of titanium

Corresponding author
Mr. Valentim A. R. Barão
E-mail address
ybarao@unicamp.br
Journal
Applied Surface Science
Article number
146326
Our reference
APSUSC_146326
PII
S0169-4332(20)31083-7

Order Confirmation

Thank you for taking the time to complete the Rights and Access form.

Order number
OACSRAPSUSC1463260
Order date
14 April 2020

Research Funders

Fundação de Amparo à Pesquisa do Estado de São Paulo
Grant numbers: 2016/07269-3, 2016/11470-6, 2017/18916-2
Coordenação de Aperfeiçoamento de Pessoal de Nível Superior
Grant numbers: Finance code 001

Publishing Option
Subscription

Data Protection & Privacy

I do not wish to receive news, promotions and special offers about products and services from Elsevier B.V. and its affiliated companies worldwide.

Publishing Agreement

- I am one author signing on behalf of all co-authors of the manuscript
- I am not a US Government employee but some of my co-authors are
- I am signing on behalf of the corresponding author.
 - **Name/Job title/Company:** Valentim Adelino Ricardo Barão, Associate Professor, University of Campinas (UNICAMP)
 - **E-mail address:** ybarao@unicamp.br

I may post the accepted manuscript in my institutional repository and make this public after an embargo period. To ensure the sustainability of peer-reviewed research in journal publications, I may

<https://mail-attachment.googleusercontent.com/attachment/u/0/?ui=2&ik=ac66c27efd&attid=0.1&permmsgid=msg-f:1663951189483689861&th=1...> 1/2

14/04/2020 <https://mail-attachment.googleusercontent.com/attachment/u/0/?ui=2&ik=ac66c27efd&attid=0.1&permmsgid=msg-f:166395118948...>

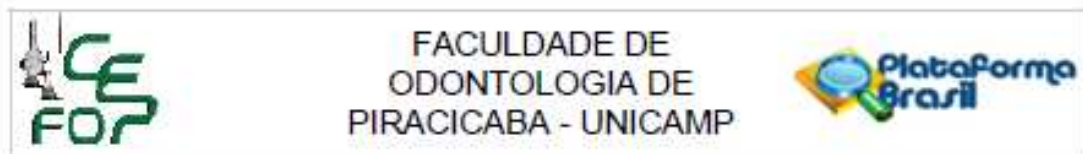
not share the final article publicly, for example on ResearchGate or Academia.edu.
Further details on [Elsevier Sharing Policy here](#).

Based on information provided the embargo period/end date is 24 months.

Copyright © 2020 Elsevier B.V. All rights reserved.



Anexo 3 – Certificado de aprovação do Comitê de Ética



PARECER CONSUBSTANCIADO DO CEP

DADOS DO PROJETO DE PESQUISA

Título da Pesquisa: Deposição por pulverização catódica de filmes de óxido de tântalo na superfície de titânio para aplicações biomédicas: comportamento eletroquímico, biocompatibilidade e análise microbiológica

Pesquisador: Thamara Beline

Área Temática:

Versão: 3

CAAE: 57496116.5.0000.5418

Instituição Proponente: Faculdade de Odontologia de Piracicaba - Unicamp

Patrocinador Principal: Financiamento Próprio

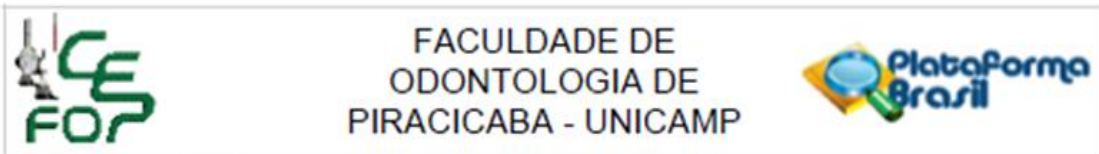
DADOS DO PARECER

Número do Parecer: 1.739.542

Apresentação do Projeto:

Trata-se de estudo laboratorial, com tratamento de amostras e utilizando dois produtos de origem humana, uma linhagem celular e amostras de saliva total não estimulada de dois voluntários. O projeto está detalhadamente descrito e envolve numerosas metodologias associadas aos seus objetivos. Resumidamente, discos de TiCp serão divididos em dois grupos: superfície I - usinada (controle) e superfície II (experimental) - tratada com filme de Ta₂O₅. Para o ensaio eletroquímico, testes padrões como potencial de circuito aberto, espectroscopia de impedância eletroquímica e teste potenciodinâmico serão conduzidos em solução de fluido corpóreo (pH 7,4). A capacitância (Cdl) e resistência de polarização (Rp) da camada de óxido serão determinados por meio do circuito elétrico mais apropriado. O método de Tafel será utilizado para determinar a densidade de corrente de corrosão (I_{corr}) e o potencial de corrosão (E_{corr}). A densidade de corrente de passivação (I_{pass}) corresponderá ao valor da corrente na transição entre a região ativa e passiva expressas na curva de polarização. A topografia dos discos será caracterizada através da microscopia eletrônica de varredura (MEV), espectroscopia de energia dispersiva (EDS), microscopia de força atômica (MFA), espectroscopia de fotoelétrons de raios X (XPS), difratografia de raios-x (DRX), perfilometria e energia livre de superfície. Para os testes biológicos, será utilizada a linhagem celular pré-osteoblásticas MC3T3E1. A estrutura e morfologia celular serão avaliadas por

Endereço: Av. Limeira 901 Caixa Postal 52
 Bairro: Areião CEP: 13.414-903
 UF: SP Município: PIRACICABA
 Telefone: (19)2106-5349 Fax: (19)2106-5349 E-mail: cep@fop.unicamp.br



Continuação do Parecer: 1.739.542

Declaração de Manuseio Material Biológico / Biorepositório / Biobanco	65Autarq.PDF	30/06/2016 15:42:28	Thamara Beline	Aceito
Declaração de Instituição e Infraestrutura	64Decinfra.PDF	30/06/2016 15:42:00	Thamara Beline	Aceito
Declaração de Instituição e Infraestrutura	62DecInst.PDF	30/06/2016 15:41:49	Thamara Beline	Aceito
Declaração de Pesquisadores	61DecPesq.PDF	30/06/2016 15:41:33	Thamara Beline	Aceito
TCLE / Termos de Assentimento / Justificativa de Ausência	5TCLE.pdf	30/06/2016 15:41:20	Thamara Beline	Aceito
TCLE / Termos de Assentimento / Justificativa de Ausência	4comentarios.pdf	30/06/2016 15:41:10	Thamara Beline	Aceito
Projeto Detalhado / Brochura Investigador	3Projeto.pdf	30/06/2016 15:40:49	Thamara Beline	Aceito
Outros	2Cartadeenvio.PDF	30/06/2016 15:40:36	Thamara Beline	Aceito
Folha de Rosto	1Folhaderosto.pdf	30/06/2016 15:39:06	Thamara Beline	Aceito

Situação do Parecer:

Aprovado

Necessita Apreciação da CONEP:

Não

PIRACICABA, 22 de Setembro de 2016

Assinado por:
jacks jorge junior
(Coordenador)

Anexo 4 – Relatório de verificação de originalidade e prevenção de plágio

Tese			
ORIGINALITY REPORT			
20%	12%	15%	9%
SIMILARITY INDEX	INTERNET SOURCES	PUBLICATIONS	STUDENT PAPERS
PRIMARY SOURCES			
1	repositorio.unicamp.br Internet Source		4%
2	Thamara Beline, José H.D. da Silva, Adaias O. Matos, Nilton F. Azevedo Neto et al. "Tailoring the synthesis of tantalum-based thin films for biomedical application: Characterization and biological response", Materials Science and Engineering: C, 2019 Publication		3%
3	Isabella da Silva Vieira Marques, Maria Fernanda Alfaro, Miki Taketomi Saito, Nilson Cristino da Cruz et al. "Biomimetic coatings enhance tribocorrosion behavior and cell responses of commercially pure titanium surfaces", Biointerphases, 2016 Publication		1%
4	Thamara Beline, Aljomar José Vechiato Filho, Alvin G. Wee, Cortino Sukotjo et al. "Initial investigation of the corrosion stability of craniofacial implants", The Journal of Prosthetic		1%